SIMULATION OF SOLAR CEREAL DRYER USING TRNSYS

BY

Habtamu Tkubet Ebuy

Advisor: Dr.-Ing. Abebayehu Assefa

A thesis submitted to the School of Graduate Studies of Addis Ababa University in partial fulfillment of the requirements for the Degree of Masters of Science in Mechanical Engineering.

Addis Ababa University
Addis Ababa, Ethiopia
January, 2007

Addis Ababa University

School of Graduate Studies

Mechanical Engineering Program

SIMULATION OF SOLAR CEREAL DRYER USING TRNSYS

BY

Habtamu Tkubet Ebuy

Approved by the Examining Board:

____________________ ________________

Chairman, Department's Graduate Committee

__________________ _________________

Advisor

______________________ _________________

External Examiner

______________________ _________________

Internal Examiner

ACKNOWLEDGMENT

This project would be impossible with out the help of God and his Mother. I would like to express my sincere gratitude to my advisor Dr.-Ing Abebayehu Assefa for giving me the opportunity to work on this project and for his guidance and encouragement without which this work could have not been completed. He has been a constant source of inspiration through out my study period.

I am also grateful to Dr. Bradley David and the Solar Energy Lab at the University of Wisconsin, Madison for the kind support rendered to me on different occasions.

Last but not list, I would like to thank my family, my lovely friend Aychesh Mengistu and friends who are always beside me and played part a great role in the completion of my work.

Table of contents

List of Tables

List of Figures

ABSTRACT

In many countries of the world, the use of solar thermal systems in the agricultural area to conserve vegetables, fruits, coffee and other crops has shown to be practical, economical and responsible approach environmentally. Solar heating systems to dry food and other crops can improve the quality of the product, while reducing wastes produce and traditional fuels - thus improving the quality of life. However the availability of good information is lacking in many of the countries where solar food processing systems are most needed. This work presents the performance of several individual, medium and large-scale food processing systems, which incorporate solar drying.

A general purpose of solar crop dryer for drying of various agricultural products such as coffee, fruits, Vegetables, cereals, etc, is simulated. The simulated solar dyer consists of the solar air heater (solar collector) which uses low emissivity glass cover, weather data, and an integrated dryer chamber attached to the collector where the products to be dried are placed.

A thermal solar collector model is developed to determine the available useful energy for heating the ambient air with the available solar radiation.

Basic heat transfer equations for single-plate and double glass glazing are drived and techniques for the solution of these questions are presented.

A computer program is written to predict the collector outlet temperature, mass flow rate and other engineering variables from the input of the meteorological data and collector parameters and also done for the dryer chamber by using the input from the collector out put and the properties like initial moisture content, initial temperature of cereals and other engineering properties.

Results of the system simulation are presented in graphical form suitable for system performance determination. From the incident flux, ambient air temperature and solar collector parameters, the useful energy, collector output temperatures of the out put air are determined.

The output properties of the collector are the input parameters for the drying chamber. These parameters are used to determine the moisture content, the relative humidity, the mass of water vapor and the output temperature of the air at the out put of the drying chamber.

ACRONYMS

TRNSYS TRaNsient SYstem Simulation program

ASAE American Society of Agricultural Engineers

M_{f1} Final moisture content of the cereals in the first bed in the drying bed

M_{f2} Final moisture content of the cereals in the second bed in the drying bed

M_{f3} Final moisture content of the cereals in the third bed in the drying bed

M_{f4} Final moisture content of the cereals in the fourth bed in the drying bed

T_1 Exit temperature of the air from the collector

T_2 Exit temperature from the first bed in the drying bed

T_3 Exit temperature from the second bed in the drying bed

T_4 Exit temperature from the third bed in the drying bed

T_5 Exit temperature from the fourth bed in the drying bed

T_{g1} Exit temperature of the grain from the collector

T_{g2} Exit temperature of the grain from the first bed in the drying bed

T_{g3} Exit temperature of the grain from the second bed in the drying bed

T_{g4} Exit temperature of the grain from the third bed in the drying bed

T_a Ambient temperature

M_{w1} Water vapor removed from cereals in the first bed in the drying bed

M_{w2} Water vapor removed from cereals in the second bed in the drying bed

M_{w3} Water vapor removed from cereals in the third bed in the drying bed

M_{w4} Water vapor removed from cereals in the fourth bed in the drying bed

DR_1 Drying rate for the first bed in the drying bed

DR_2 Drying rate for the second bed in the drying bed

DR_3 Drying rate for the third bed in the drying bed

DR_4 Drying rate for the forth bed in the drying be

Chapter 1

1.1 Background

Reduction of post harvest losses in developing countries can significantly contribute to the availability of food. Estimations of these losses are generally cited to be of the order of 40% but they can, under very adverse conditions, be nearly as high as 100%. A significant percentage of these losses are related to improper and/or untimely drying of foodstuffs such as cereal grains, pulses, tubers, meat, fish, etc [8].

Traditional drying, which is frequently done on the ground in the open air, is the most widespread method used in developing countries because it is the simplest and cheapest method of conserving foodstuffs. Some disadvantages of open air drying are: exposure of the foodstuff to rain and dust; uncontrolled drying; exposure to direct sunlight which is undesirable for some foodstuffs; infestation by insects, attack by animals, etc.

In order to improve traditional drying, solar dryers which have the potential of substantially reducing the above-mentioned disadvantages of open air drying have received considerable attention over the past 20 years. There has unfortunately not been any significant use of solar dryers in developing countries for various reasons described by Bassey. These can be attributed to: poor problem definition which makes the developed dryers technically inadequate and economically unviable; inappropriate dryer designs due to the choice of construction materials and the use of electrically operated fans; inadequate understanding of the operation of solar dryers and lack of design procedures [6].

Solar dryers of the forced convection type can be effectively used. They however need electricity, which unfortunately is non-existent in many rural areas, to operate the fans. Even when electricity exists, the potential users of the dryers are unable to pay for it due to their very low income. Forced convection dryers are for this reason not going to be readily applicable on a wide scale in many developing countries.

Natural convection dryers circulate the drying air without the aid of a fan. They therefore have low air flow rates which tend to give them slower drying rates, compared to traditional open air methods. Despite this disadvantage, experience with these dyers has indicated that they can be of significant use in many rural areas in developing countries [10].

Designs of natural flow dryers have, for the most part, been done by trial and error. Most of the developed dryers have not performed satisfactorily. There is a need to understand the overall operation of the dryer, the interaction between its component parts, the influence of various design and operating parameters on its performance, and the development of systematic design procedures and guidelines. These technical constraints have been partially responsible for the lack of use of natural convection solar dryers.

1.2 Literature Review

A substantial number of studies have been reported in the literature on solar drying. Forced convection solar dryers can be effectively designed using available standard design procedures for solar collectors, calculation of air flow rates, and the determination of moisture removal from the commodity to be dried. These dyers, because of their inappropriateness in the rural setting of many developing countries, are not treated in this report [6].

Indirect natural convection solar dryers can be used for drying various commodities. Although the literature on these dryers is vast, there is little information on studies which have used rigorous engineering analysis to develop design procedures, investigate the effect of changing key parameters on the operation of the dryers, and obtain reliable experimental data on dryer performance. This study gives a brief review of some recent and relevant work, in the above-mentioned neglected areas. Excel has outlined the basic factors to be considered in the design of natural convection solar rice dryer. The method outlined is very approximate, due to the simplified formulations used to calculate the air flow rates and collector area, which did not take into account heat transfer rates, properties of construction materials, etc. The dryer which was built from this design was effectively a mixed mode dryer making it difficult to evaluate the accuracy of the design procedure [8].

Bassey outlined a detailed experimental study aimed at understanding the performance of indirect natural convection solar dryers under various outdoor conditions. The dryers used had the collector area equal to that of the rice bed which was 30 cm above the exit of the collector.

Two types of collectors were used. Results indicated that the dryers gave lower drying rates than traditional open air drying due to the low air flow rates through the dryer. Efforts were made to improve the air flow by painting the 38 cm diameter chimney (1m and 2m high) black and covering it with a transparent plastic material (effectively making it a solar collector), but no significant improvements on dryer performance were observed (Bassey, 1982b). The complicated nature of the interaction between the various parameters were noted and it was suggested that more detailed work was needed to understand the heat transfer and air flow through the various components of the dryer [11].

Based on the work of Bassey, Whitfield carried out work on natural convection solar dryers to determine the effect of chimney sizes and insulating the dryer cabinet. Though the results were not conclusive, mainly due to limitations in the accuracy of experimental measurements, it was shown that the insulated dryer would improve the airflow through the dryer. In collaboration with Whitfield, Koroma carried out limited experiments on indirect natural convection solar dryers made from mud bricks.

Results indicated that the insulating and energy storage effects of the mud walls improved drying rates even during the night, resulting in the dryer giving better drying performance compared to ground drying for the same bed thickness. Preston used the experimental results of Bassey to develop a simulation model for an indirect natural convection solar dryer. The overall agreement between the predictions and experiments were good for the empty dryer but not very good for the dryer loaded with rice. This indicated that the modeling of the rice bed and the formulations used for the drying rates were inadequate. Despite these shortcomings, the model gave useful information on the effects of various design changes on the performance of the dryers [12].

Extensive work has been reported by Oasthuizen on indirect natural convection solar rice dryers. It consisted of an experimental study and the development of a computer model capable of predicting outdoor results. The experiments (Oosthuizen and Sheriff) consisted of indoor lab testing of dryers in which the solar collectors were simulated by electrically heated plates maintained at temperatures of actual solar dryers. The effect of parameters such as chimneys, depth of rice bed, insulation of the drying chamber, height of the rice bed above the collector exit, on the performance of the dryer were studied. Concrete recommendations were given for these parameters in the design of solar dryers and a "standardized drying rate" was developed to enable comparison to be made between results obtained under different ambient conditions. The computer modeling study (Oosthuizen, Oosthuizen) involved the use of field measurements of solar radiation, assumptions for heat transfer in the collector, calculation of flow through the dying chamber and the rice bed, to predict the field drying rates. Results agreed very well with field experiments obtained by Bassey, Whitfield and Koroma [13].

Recent work has been reported by Koroma on the effect of the length of solar collectors on the performance of indirect natural convection dyers. Although the experimental data could only be considered preliminary, the results indicated that collectors with shorter lengths give faster dying rates provided their total surface area remains constant. More work is needed to determine the applicability of such findings.

1.3 Objectives

The objective of this thesis is to develop a mathematical model to evaluate the performance of solar cereal dryer (SCD) systems. The new design tool will allow engineers to make design changes and determine their effects on the thermal performance at a reasonable cost. The program will be arranged so that very detailed information can be specified. It will allow a company specializing in solar cereal dryer systems to investigate the impact of design changes on the thermal performance of the systems. For the task to be useful to the solar cereal dryer industry, the design program will have to provide performance equations and data that can use system simulation programs like TRNSYS.

The specific objectives of this thesis are:

- Developing a model;
- Analysis and simulating of the model using TRNSYS; and
- Study the effect of varying system parameters for the evaluation of the performance of the SCD system.

1.4 Methodology

The methods to be employed to achieve the objectives of the research are:

- Literature review;
- Collection of solar data for selected areas in Ethiopia;
- Collection of the properties of the cereal;
- Analysis of solar cereal dryer using TRNSYS; and
- Analyzing and interpretation of the output results.

Chapter 2

2.1 Definitions and Basic Concepts

Some very important terms frequently used in crop drying calculations and their relationships are described below. Most of these terms can be represented on a psychometric chart [15].

2.1.1 Vapor Pressure

The vapor pressure, P_V**,** is the partial pressure exerted by the water vapor molecules in moist air. When air is fully saturated with water vapor, its vapor pressure is called the saturated vapor pressure P_{vs}. The natural tendency for pressures to equalize will cause moisture to migrate from an area of high vapor pressure to an area of low vapor pressure.

2.1.2 Relative Humidity

Relative humidity, ϕ is defined as the ratio of the mole fraction of water vapor in a given moist air sample to the mole fraction in a saturated air sample at the same temperature and pressure. By use of the perfect gas law, this can be expressed as the ratio of the actual vapor pressure to the vapor pressure of saturated air at the same temperature that is [20]:

$$\phi = \frac{P_V}{P_{VS}} \qquad \textbf{(2-1)}$$

where: $P_V = 6.11 * 10.0 ** (7.5 * T_{dc} / (237.7 + T_{dc}))$

$P_{VS} = 6.11 * 10.0 ** (7.5 * T_c / (237.7 + T_c))$

ϕ = Relative Humidity, [decimal]

A close approximation in ordinary terms is the ratio of vapor present in the air to the maximum amount of vapor that the air can hold at a given temperature. Relative humidity is expressed as a percentage. ϕ-can be defined as the ratio of the mass of water vapor to the mass of water vapor required to produce a saturated mixture at the same temperature:

$$\phi = \frac{m_V}{m_{sat}} \qquad \textbf{(2-2)}$$

2.1.3 Humidity Ratio

The amount of water vapor in the air can be specified in various ways; probably the most logical way is to specify directly the mass of water vapor presented in a unit mass of dry air. This is called absolute or specific humidity (also called humidity ratio) and is denoted by ω, that is:

$$\omega = \frac{m_v}{m_a} \quad \textbf{(2-3)}$$

This may also be called the moisture content or mixing ratio**.** The humidity ratio is not affected by a temperature change unless it drops below the saturation temperature. The humidity ratio can be related to relative humidity using as follows:

$$\omega = \phi\omega_{sat} \quad \textbf{(2-4)}$$

2.1.4 Dry-Bulb Temperature

The term dry-bulb temperature, T_{db}**,** refers simply to the temperature as registered by an ordinary thermometer placed in a gas mixture.

2.1.5 Wet-Bulb Temperature

The psychometric wet -bulb temperature, T_{wb}**,** is basically measured by placing a thermometer, with a water-moistened wick covered bulb, into a fast moving stream of ambient air. If the air surrounding the wet-bulb thermometer is not saturated, evaporation of water from the wick will occur; cooling the bulb, the amount of cooling is proportional to the evaporation rate, which in turn is inversely proportional to the amount of water in the air. Eventually, a steady-state is reached in which the change in temperature of the thermometer is zero with respect to time. This final equilibrium temperature is called the wet-bulb temperature of the moist air [20].

It should be noted that the psychometric wet-bulb temperature is not the same as the adiabatic or thermodynamic wet-bulb temperature which is the temperature reached by moist air and water-if the air is adiabatically saturated by the evaporating water. However**,** the adiabatic and psychometric wet-bulb temperatures are nearly equal for moist air [15].

2.1.6 Wet-Bulb Depression

The wet-bulb depression is the difference between the dry-bulb and wet-bulb temperatures. The temperature is depressed by evaporative cooling of the wet bulb. The greater the differences between the amounts of water in the air and the saturation water capacity the greater the temperature depression.

2.1.7 Dew-Point Temperature

The dew-point temperature, T_{dp}**,** is the temperature at which water vapor, being cooled at a constant mixture pressure and humidity ratio, begins to condense**.**

2.1.8 Enthalpy

The enthalpy, h, is the heat content of the moist air per unit mass of dry air above a certain datum temperature. The enthalpy of moist air per unit mass is the sum of the enthalpies per unit mass of dry air and of superheated water vapor that is [20]:

$$h = h_a + \omega h_v \quad \textbf{(2-5)}$$

where: ω is the humidity ratio of air, kg of water per kg of dry air

The enthalpy of dry air per unit mass can be expressed as:

$$h_a = C_a (T - T_{dat}) \quad \textbf{(2-6)}$$

where: C_a is the specific heat of dry air at constant pressure, [J, Kg^{-1}, K^{-1}]

The enthalpy of the superheated water vapor can be expressed as the sum of the enthalpy of the superheated vapor, the latent heat of evaporation at the dew point temperature and the enthalpy of the water at dew point temperature. Thus:

$$h_v = C_v \left(T - T_{dp} \right) + h_{fg} + C_w \left(T_{bp} - T_{dat} \right) \quad \textbf{(2-7)}$$

where: T_{dp} = dew point temperature, [^{0}C]

C_V = specific heat of vapor. [J, Kg^{-1}, K^{-1}]

C_w = specific heat of water, [J, Kg^{-1}, K^{-1}]

h_{fg} = latent heat of vaporization at $T_{dp,}$ [J, Kg^{-1}]

Enthalpy is expressed in joule per kilogram of dry air [J, Kg^{-1}] measurement of enthalpy is relative, that is, the actual heat content is dependent on the datum or zero point chosen.

2.1.9 Specific Heat Capacity

The specific heat capacity, C, is the quantity of heat needed to increase the temperature of a unit mass of a material by one degree. (ASAE Standards 1996) gives the following equation for the average value of specific heat of cereals:

$$C_G = 1.110 + 0.0448 \times M_{cw} \quad \textbf{(2-8)}$$

Wratten et al, give the following relation for the specific heat capacity of cereals: Suministrado as quoted by Jindal the following equation [20]:

$$C_G = 0.3153 + 0.0073 M_{cw} + 0.0009 \times T_i \quad \textbf{(2-9)}$$

where: M_{cw}= the percentage moisture content, wet basis,

T_i= the initial grain temperature, [^OC], and

C_G = the specific heat of grain, [kJ, kg^{-1}, $^0C^{-1}$]

2.1.10 Sensible Heat

The sensible heat, Q_s, is the heat energy absorbed or released when a body changes temperature.

$$Q_S = m \times C \times \Delta T \quad \textbf{(2-10)}$$

where: m = mass, [kg]

C = specific heat capacity, [J, kg^{-1}, $^0C^{-1}$]

ΔT = Change in temperature, [^{0}C]

2.1.11 Latent Heat of Vaporization

The latent heat of vaporization, h_{fg}**,** is the quantity of heat required to change a substance from a liquid to a vapor at constant temperature. Slightly higher energy is required to evaporate water from grains than that is required to evaporate free water because water is partially bound in grains. The actual amount needed is a function of the temperature at which the vaporization occurs and the moisture content of grains. It decreases as the temperature increases and increases as the moisture content decreases [20].

Wang gives the latent heat vaporization of water in cereals as a function of the moisture content, % dry bases, and air temperature as:

$$h_{fg} = (1795.44 - 0.811 \times T) \times M_{cd}^{-0.346} \quad \textbf{2-11)}$$

$$h_{fg} = 2502535.259 - 2385.76424 \times T \quad \textbf{(2-12)}$$

where: h_{fg}; is in J/kg**,** and T in ^{0}C**.**

2.1.12 Moisture Content

The moisture content, M_c, is a measure of wetness or dryness of material. It can be calculated on either a wet or dry basis. The wet basis moisture is the ratio of mass of water in a sample to wet mass of the sample that is [18]:

$$M_{cw} = \frac{M_w - M_d}{M_w} \quad \textbf{(2-13)}$$

The dry basis moisture is the ratio of the mass of water in a sample to the mass of the dry matter, that is:

$$M_{cd} = \frac{M_w - M_d}{M_d} \quad \textbf{(2-14)}$$

where: M_w = mass of wet sample, [kg]

W_d = mass of dry matter in the sample, [kg]

Conversion from one base to another can be made using one of the following relations:

$$\%M_{cw} = \frac{100 \times (\%M_{cd})}{100 + (\%M_{cd})} \quad \textbf{(2-15)}$$

$$\%M_{cd} = \frac{100 \times (\%M_{cw})}{100 + (\%M_{cw})} \quad \textbf{(2-16)}$$

where: $\%M_{cw}$= percentage moisture content wet basis

$\%M_{cd}$ = percentage moisture content dry basis

Although the wet basis moisture is used for trading, all calculations of mass of cereal in drying and trading should be made on a dry basis because percentage point of mass change on a dry basis is always the same; but a percentage point of mass change on a wet basis changes with basis Unless otherwise noted, moisture contents in the following chapters are on dry basis.

2.1.13 The Equilibrium Moisture Content

The equilibrium moisture content, E_{Mc}**,** is the moisture content of a product that is in equilibrium with air at a particular mean dry-bulb temperature and relative humidity that would be attained by the grain over infinite time, at a constant value of air relative humidity and temperature. The equilibrium moisture content is expressed as a decimal on a dry basis. Several models, theoretical as well as empirical, have been suggested for the calculation of the E_{Mc}**.** The following Chung-Pfost and the modified Henderson equilibrium equation apply well to cereal [15]:

$$E_{Mc} = E - F \times \ln\{-(T_E + c) \times \ln\varphi\} \quad \textbf{(2-17)}$$

where: E_{Mc} **=** drying air equilibrium moisture content, dry basis, [decimal]

T_E = the equilibrium temperature of drying air, [0C]

ϕ = relative humidity of drying air, [decimal]

The equilibrium moisture content can also be expressed by the modified Henderson Equation:

$$E_{Mc} = \frac{\left[\dfrac{\ln(1-\phi)}{-1.9187\times10^{-5}\left(T_E + 51.161\right)}\right]^{0.40898}}{100} \qquad \textbf{(2-18)}$$

2.1.14 Equilibrium Temperature of Drying Air

The drying process takes place at a temperature that is between the temperature of the air entering the crop bed and that of the air exiting the dryer. The equilibrium temperature of drying air can be calculated by establishing a heat balance between the initial conditions and the equilibrium conditions and assuming that the temperature of the equilibrium equals that of the grains and the humidity ratio at equilibrium equals that of drying air.

$$C_a T_i + \omega_i\left(h_{fg} + C_v T_i\right) + C_G T_{Gi}\left(\frac{m_{rd}}{m}\right) = C_a T_E + \omega_i\left(h_{fg} + C_v T_E\right) + C_G T_E\left(\frac{m_{rd}}{m}\right)$$

This gives:

$$T_E = \frac{C_a T_i + C_v T_{Gi}\omega_i + C_G T_{Gi}\left(\dfrac{m_{rd}}{m}\right)}{C_a + C_v\omega_i + C_G\left(\dfrac{m_{rd}}{m}\right)} \qquad \textbf{(2-19)}$$

where: C_a= specific heat capacity of air, [kJ, Kg^{-1},K^{-1}]

C_G= specific heat capacity of grain, [kJ**,** Kg^{-1}, K^{-1}]

C_V= specific heat capacity of water vapor = 1.884 [kJ**,** Kg^{-1}, K^{-1}]

T_E= the equilibrium temperature, [K]

T_{Gi}= the initial temperature of grains, [K]

T_i= the initial temperature of drying air, [K]

ω_i = the initial humidity ratio, [kg of water / kg of air]

m_{rd}= the mass of dry cereal, [kg]

m = the mass of drying air passing through the cereal bed during the time increment the quantity $\frac{m}{m_{rd}}$ is termed air-to-grain ratio.

Chapter 3

3.1 Drying

Drying is a mass transfer process resulting in the removal of water or moisture from another solvent, by evaporation from a solid, semi-solid or liquid (hereafter product) to end in a solid state. To achieve this, there must be a source of heat, and a sink for the vapor produced.

In the most common case, a gas stream (example air) applies the heat by convection and carries away the vapor as humidity. Other possibilities are vacuum drying, where heat is supplied by contact conduction or radiation (or microwaves) while the produced vapor is removed by the vacuum system. Another indirect technique is drum drying, where a heated surface is used to provide the energy and aspirators draw the vapor outside the room [6].

Freeze drying is a drying method where the solvent is frozen prior to drying and is then sublimed, that is, passed to the gas phase directly from the solid phase, below the melting point of the solvent. Freeze drying is often carried out under high vacuum to allow drying to proceed at a reasonable rate. This process avoids collapse of the solid structure, leading to a low density, highly porous product, able to regain the solvent quickly. In biological materials or foods, freeze drying is regarded as one of the best, if not the best method to retain the initial properties. It was first used industrially to produce dehydrated vaccines, and to bring dehydrated blood to assist war casualties. Now freeze drying is increasingly used to preserve some foods, especially for backpackers going to remote areas. The method may keep protein quality intact, the same as the activity of vitamins and bioactive compounds [15].

In turn, the mechanical extraction of the solvent, e.g., water, by centrifugation, is not considered "drying". The ubiquitous term dehydration may mean drying of water-containing products as foods, but its meaning is vaguer, as it is also applied for water removal by osmotic drive from a salt or sugar solution. In medicine, dehydration is the situation by which a person loses water by respiration, sweating and evaporation and does not incorporate, for whatever reason, the "make-up" water required to keep the normal physiological behavior of the body.

Drying may be either a natural or an intentional process. The process of extreme drying is called desiccation.

General drying is dividing in so many branches as shown in Figure 3-1.

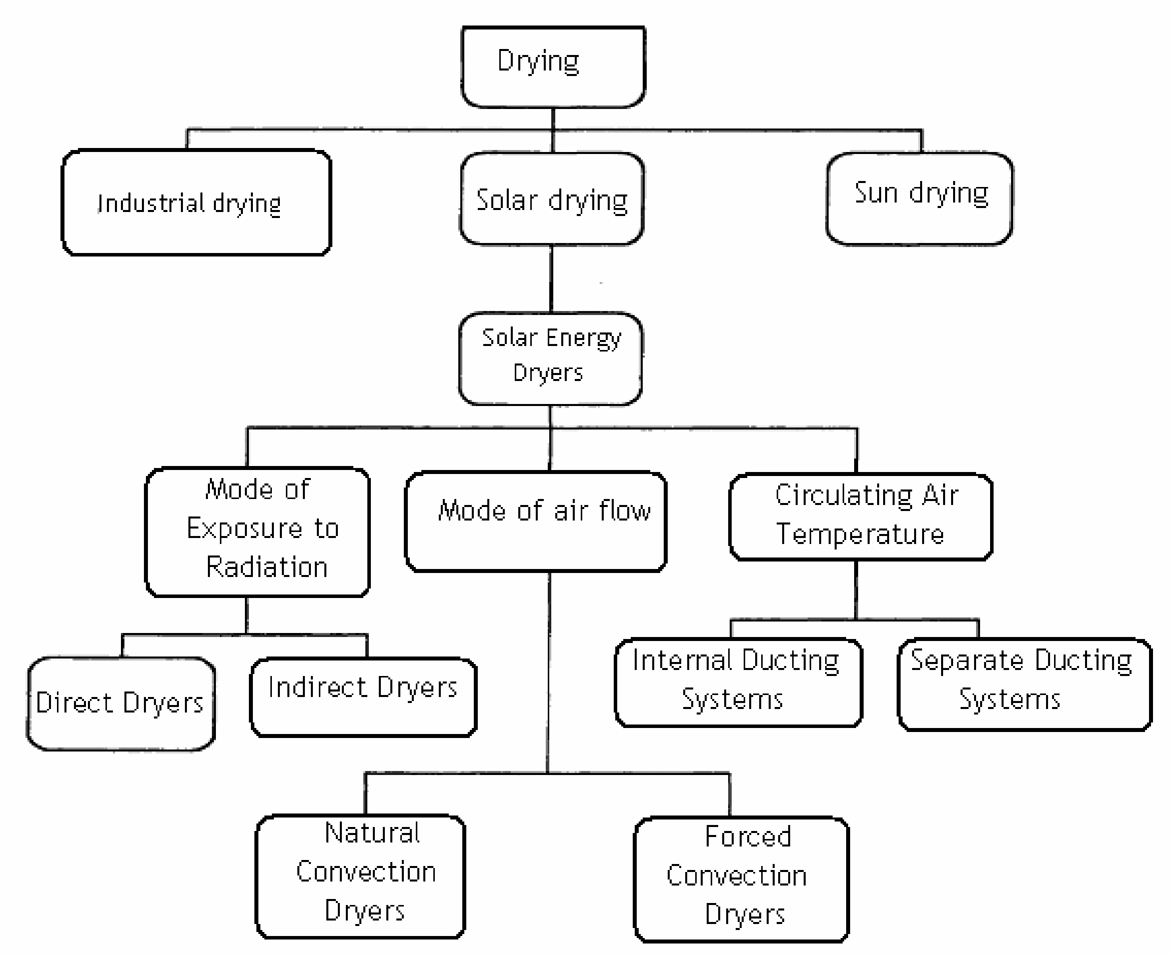

Figure 3-1: Flowchart Depicting General Classification of Solar Dryers

3.1.1 Mode of Exposure to Solar Radiation

3.1.1.1 Direct Dryers

Dryers in which crops are directly exposed to solar radiation are termed direct solar dryers. They consist essentially of an enclosure with a transparent cover or side panels. To further enhance the efficiency, the internal surfaces of the enclosure are painted black. The heat generated from the absorption of the solar radiation within the crops as well as the surfaces of the enclosure causes the removal of moisture. Direct dryers are simple to construct, and more hygienic than open-air Sun drying. They can heat the crops to temperatures higher than those achieved by sun drying. However, they are known to suffer from many problems some of which are slow drying, overheating, and changes in crop color and flavor due to the direct exposure to Sun. Unless they are built in large sizes, direct dryers can only dry small quantities of crops, because they use the same ground area as that which the traditional Sun drying requires. Another major disadvantage of direct dryers is the difficulty in controlling the rate of moisture removal. At the start of the drying process, it is often necessary to close the outlet air holes to allow the temperature of air in the dryer to rise. Water evaporates from the crop and condenses on the inside of the transparent cover and thus reducing the amount of solar radiation transmitted to the dryer interior. This condition is subsequently improved by opening the outlet vents, but in turn it causes temperature inside the dryer to fall. A sketch of a direct solar dryer is shown on Figure 3-2 [15].

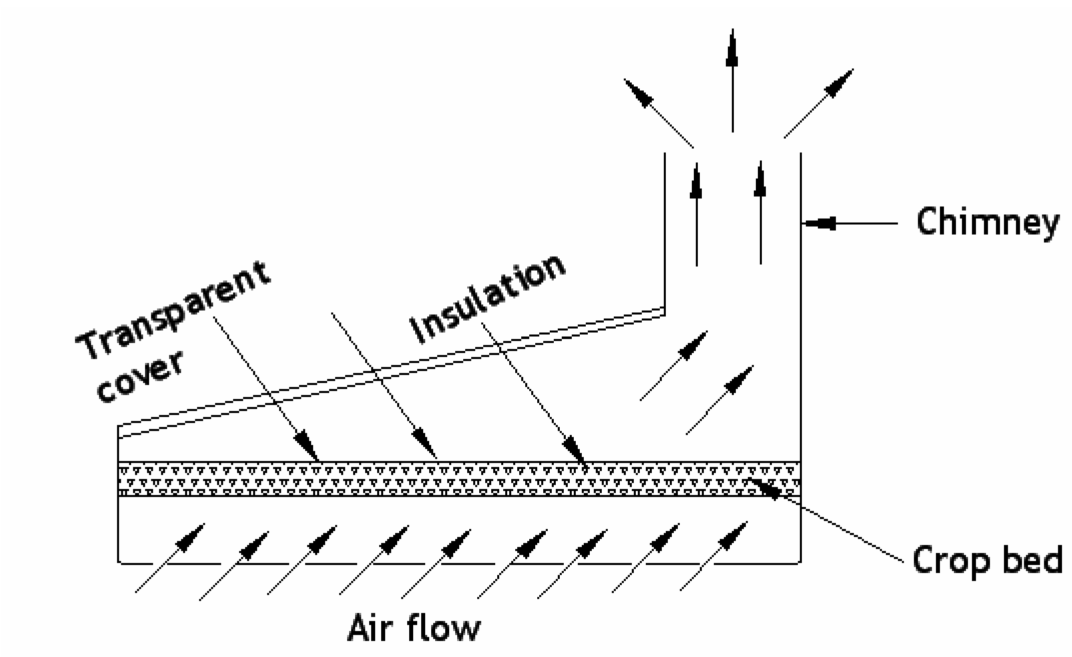

Figure 3-2: Typical Arrangement of a Direct Dryer

3.1.1.2 Indirect Dryers

Indirect solar dryers are those in which the crops are placed in an enclosed drying cabinet there by being shielded from direct exposure to solar radiation. An indirect solar dryer basically consists of two major components: an air heater, which is used to raise the temperature of the drying air and a drying chamber which is the enclosure that accommodates the crops. A chimney is usually incorporated in natural convection indirect dryers to increase the air-flow through the crop bed Figure 3-3.

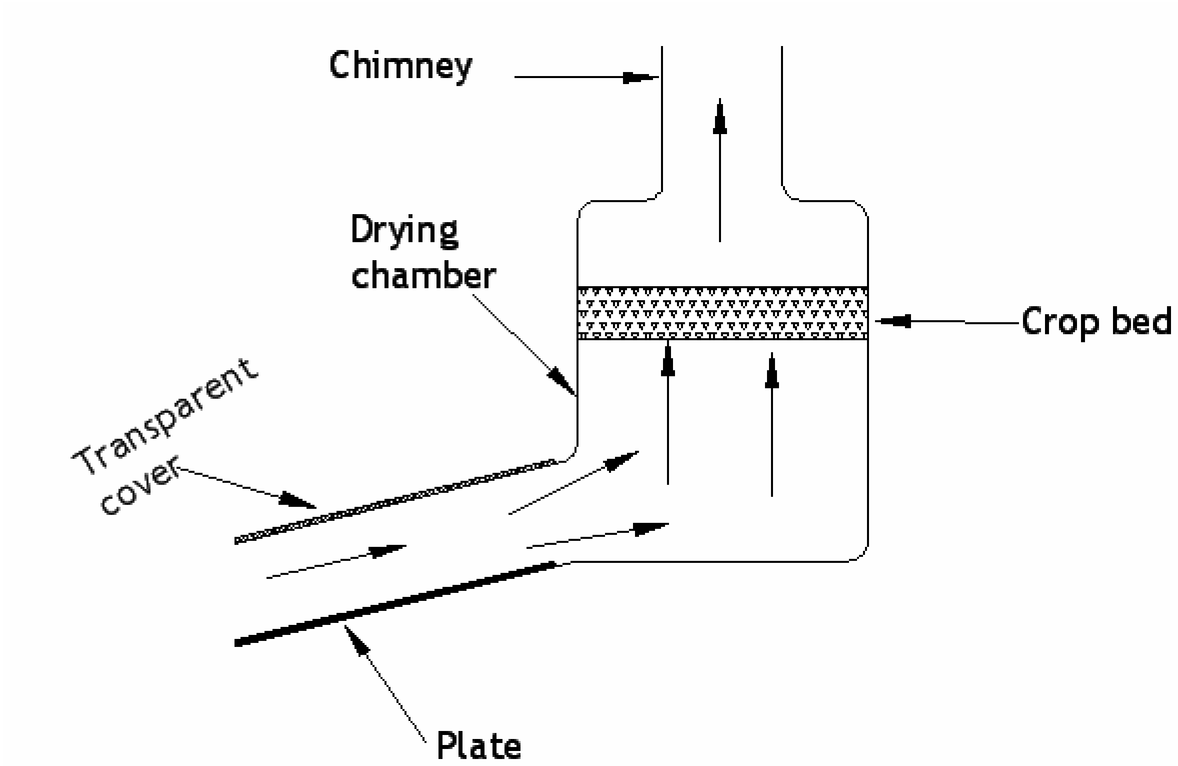

Figure 3-3: Typical Natural Convection Indirect Solar Dryer with Chimney

Air heated in the collector passes through the drying chamber where the crop to be dried is placed on one or more porous trays. The air passes through the wet crop bed and becomes nearly saturated, thus lowering its temperature to nearly that of the ambient air, before it exits via a chimney. This type of dryer is used when the crop being dried can be damaged if it is exposed to the Sun direct rays. Crops can be dried in deeper layers, therefore saving ground space. However, natural convection indirect solar dryers are prone to poor performance. Since the air above the crop bed is not substantially different in temperature from that of the ambient air, which is also damp in humid regions, the resulting buoyancy forces, which are proportional to the temperature difference, are very small, and in turn produce very low air-flow rates. A combination of direct and indirect solar dryers is termed mixed mode dryers. They normally are indirect dryers with transparent drying chamber tops and/ or sides. Mixed mode dryers are best suited to drying crops to which the exposure to sunlight is considered essential for the required color or flavor development in the dried product. Arabic coffee dates, and certain varieties of raisin grapes are examples of such crops. A ketch of a mixed mode dryer is shown on Figure 3-4.

3.1.2 Mode of Air-Flow

According to the mode of air-flow through the dryer, a solar dryer is said to be either a natural or forced convection dryer.

3.1.2.1 Natural or Free Convection Dryers

In this type of dryer, the flow through the dryer is generated by thermally induced density gradients or as a result of wind pressure caused by a wind powered fan fitted at the top of the chimney. Natural convection solar dryers are sometimes termed passive dryers. The major short comings of natural convectional dryers are: the dryer performance depends on the ambient climatic conditions, and the low flow rates observed through the dryer. To overcome these disadvantages, thermal storages are sometimes incorporated into the dryer design. Storage is placed either inside the drying chamber beneath or above the crop bed or outside it around the chimney or beneath the collector. Figure 3-4 depicts one of these variations [15].

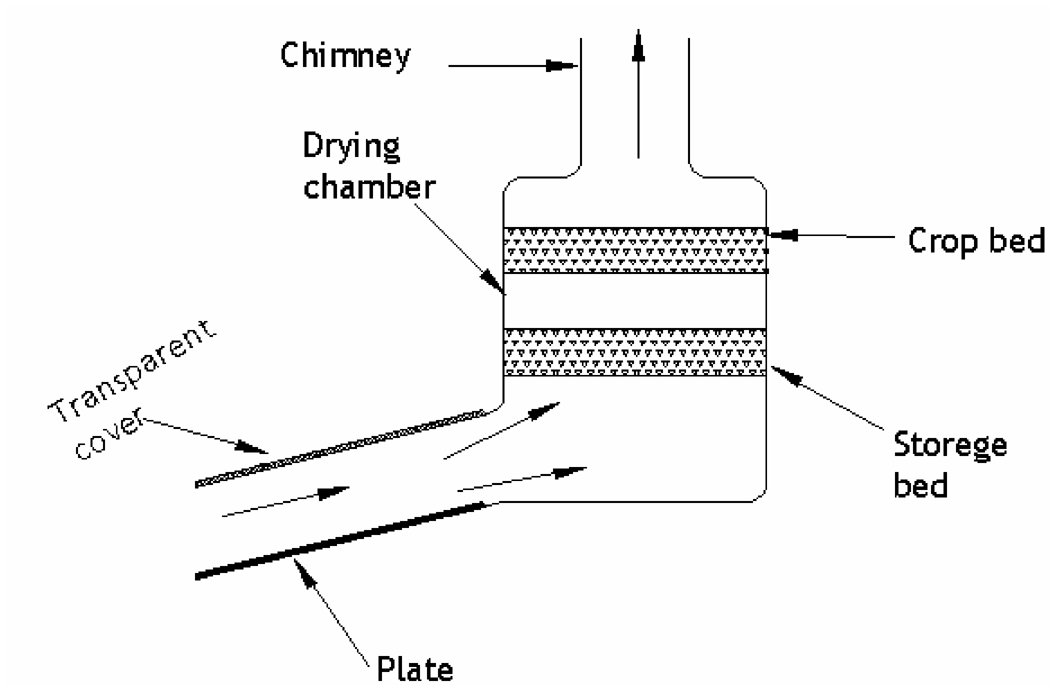

Figure 3-4: Indirect Natural Convection Solar Dryer with Storage Bed beneath the Crop Bed

3.1.2.2 Forced Convection Dryers

A dryer is said to be a forced convection dryer if the air circulation is dependent on pressure differentials generated by a fan.

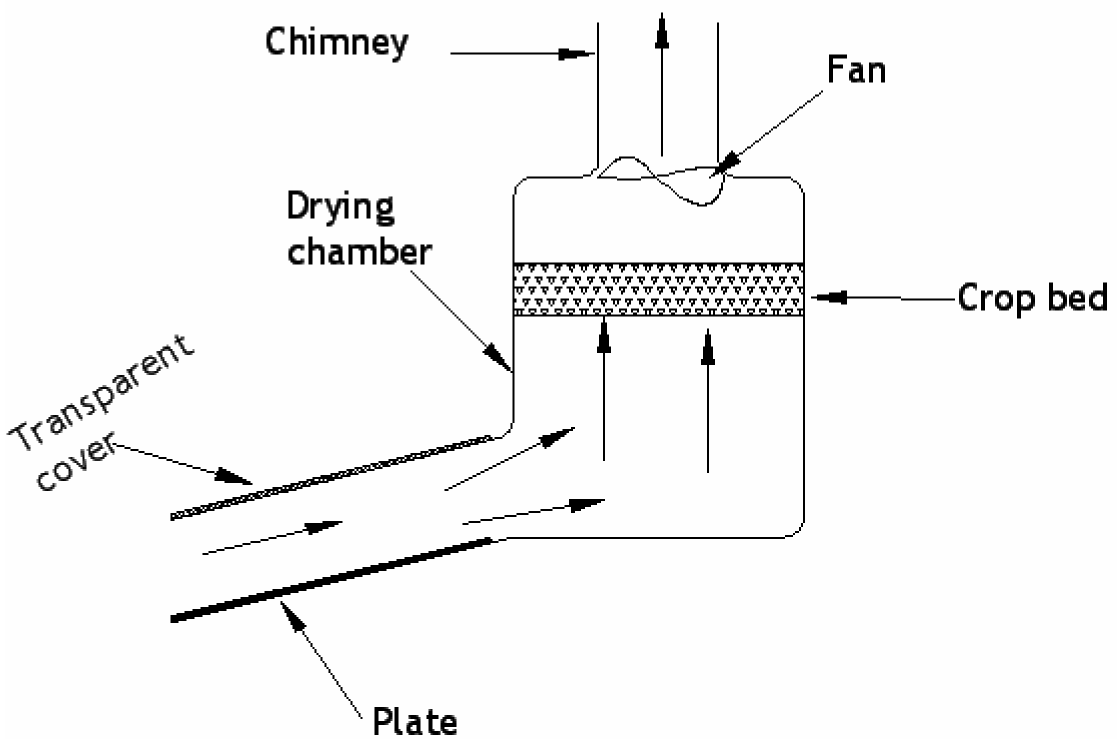

Figure 3-5: Sketch of an Indirect Forced Convection Solar Dryer

Forced Convection solar dryers obviously generate much higher air-flow than that generated by natural convection dryers and this makes them suitable for drying large loads of crops. High air-flows are required to overcome pressure drops through the crop bed, as well as, through internal thermal storage beds if such storage beds are incorporated in the dryer design. Furthermore, greater collector efficiency results from the higher air velocities in the solar collector. Forced Convection dryers require a source of power to operate the fan, be it electricity or fossil fuel, and this is the most significant obstacle to their deployment in rural areas where they are needed the most. In many rural areas, in the developing world, such sources of power are either rarely available or at best unreliable and expensive.

3.1.3 Circulated Air Temperature Mode

The air entering the drying chamber of a solar dryer can be either at the ambient temperature or at higher temperature. The air temperature rise is achieved by the passage of air through a solar collector prior to the drying chamber. If the collector and the drying chamber are combined, the dryer is termed integral ducting dryer. Dryers that employ a separate solar collector and drying chamber are termed separate ducting dryers. Separate ducting dryers tend to be more efficient as both the collector and the drying chamber can be designed for the optimum efficiency of their respective functions. However, separate ducting dryers can require relatively elaborate structures while the integral ducting dryers can be relatively simple and compact. Despite the vast variations in solar dryers studied and tested, solar dryers are still far from being a widely used technology due to their unsatisfactory performance. A good solar dryer must both reduce the relative humidity of drying air and produce a high air flow. While passive solar dryers can produce significant reductions in relative humidity through heating, many of them can not produce satisfactory flow rates. Their low drying rates, which are in some cases lower than those achieved with sun-drying, has made their adoption very limited. Forced convection dryers also have not achieved success in rural areas due to the high cost involved, both capital and operational [15].

3.2 Solar Dryer Theory

A solar dryer with transparent or translucent walls is designed to transmit the largest practical percentage of the incident solar energy into the dryer. Surfaces inside the dryer are painted dull or flat black so that as much of the transmitted energy as possible is then absorbed. When this energy is absorbed, the absorbing surfaces are heated. Energy is then transferred from the heated surfaces to the air in the dryer, primarily by convection. The air, circulated by natural convection, then transfers energy to the cereal where it evaporates and moves water from the cereal to the air.

Drying preserves foods by removing enough moisture from food to prevent decay and spoilage. Water content of properly dried food varies from 5 to 25 percent depending on the food.

Successful drying depends on:

- Enough heat to draw out moisture, without cooking the food;
- Dry air to absorb the released moisture; and
- Adequate air circulation to carry off the moisture.

When drying foods, the key is to remove moisture as quickly as possible at a temperature that does not seriously affect the flavor, texture and color of the food. If the temperature is too low at the beginning, microorganisms may grow before the food is adequately dried. If the temperature is too high and the humidity too low the food may harden on the surface. This makes it more difficult for moisture to escape and the food does not dry properly.

They agree that solar food drying can be used in most areas but clarify that how quickly the food dries is affected by many variables, especially the amount of sunlight and relative humidity. They provide some basic guidelines to drying food. Most of the resources researched recommend pre-treatment of the food, such as blanching, (boiling/steaming). Wash fresh fruits and ripe vegetables thoroughly [15].

The properties of solar dryings are

- Effective drying is accomplished with a combination of heat and air movement;
- Remove 80 to 90% of moisture from the food;
- Typical drying times range from 1 to 3 days, again depending on sun, air movement, humidity, quantity, and type of food;
- Once the drying process has started it should not be interrupted, do not allow freezing;
- Direct sunlight is not recommended;
- Temperature ranges of 37 to 71 ^{0}C will effectively kill bacteria and inactivate enzymes, although temperatures around 43 ^{0}C are recommended for solar dryers;
- Too much heat especially early in the process will prevent complete drying;

- Food should be cut into thin slices, less than 1/2" thick (1.25cm) and spread out on trays to allow free air movement;
- Rotate trays 180 degrees daily for uniform drying. Move dryer food to bottom racks;
- Allow food to cool completely before storing;
- Store food in airtight jars or plastic containers, and do not expose dried food to air, light or moisture;
- Most fruits taste great dried including apples, apricots bananas, grapes etc.

Unlike water heating and electricity generation, drying crops is a direct use of solar energy. The use of solar energy to dry crops is nothing new in the tropics but the sun heats the products and the air around them, which allows the water to evaporate. Direct solar dryers are cheap to make and easy to use, but allow almost no way to control the temperature. It is hard to protect the product that drying from external factors. Also, many vegetables and fruits change color, many vitamins are lost if they are exposed to sunlight for too long. With indirect drying it is possible to control the temperature better. The product is not exposed to ultraviolet radiation, and therefore would not change color. However, indirect dryer are more expensive to make and harder to use. Thus, drying of agricultural product permits

1. Early harvest;
2. Planning of the harvest season;
3. Long-term storage without deterioration;
4. Taking advantage of a higher price a few months after harvest;
5. Maintenance of the availability of seeds; and finally
6. Selling a better quality product.

3.2.1 Methods of Drying

- Application of heated air (convective or direct drying). Air heating reduces air relative humidity, which is the driving force for drying. Besides, higher temperatures speed up diffusion of water inside the solids, so drying is faster. However, product quality considerations limit the applicable rise to air temperature. Too hot air almost completely dehydrates the solid surface because pores to shrink and almost close, leading to crust formation or "case hardening" [6].

- Indirect or contact drying (heating through a hot wall), as drum drying, vacuum drying.

- Dielectric drying (radiofrequency or microwaves being absorbed inside the material). It is the focus of intense research nowadays. It may be used to assist air drying or vacuum drying.

- Freeze drying is increasingly applied to dry foods, beyond its already classical pharmaceutical or medical applications. It keeps biological properties of proteins, and retains vitamins and bioactive compounds. Pressure may be reduced by a vacuum pump or steam nozzle. If using a vacuum pump, the vapor produced by sublimation is removed from the system by converting it into ice in a condenser, operating at very low temperatures, outside the freeze drying chamber.

- Supercritical drying, example superheated steam drying Steam dry products with water. Strange as it seems, this is possible because the water in the product is boiled off, and joined with the drying medium, increasing its flow. It is usually employed in closed circuit and allows a proportion of latent heat to be recovered by recompression, a feature which is not possible with conventional air drying, for instance. May have potential for foods if carried out at reduced pressure, to lower the boiling point [6].

3.2.2 Applications of Drying

Hundreds of millions of tones of wheat, corn, soybean, rice and other grains as sorghum, sunflower seeds, rapeseed/canola, barley, oats, etc., are dried in Grain dryers. In the main agricultural countries, drying comprises the reduction of moisture from about 17-30%w/w to values between 8 and 15%w/w, depending of the grain. The final moisture content for drying must be adequate for storage. The more oil the grain has, the lower its storage moisture content will be (though its initial moisture for drying will also be lower). Cereals are often dried to 14% w/w, while oilseeds, to 12.5% (soybeans), 8-9% (sunflower) and 9% (peanuts). Drying is carried out as a requisite for safe storage, in order to inhibit microbial growth. However, low temperatures in storage are also highly recommended to avoid degradative reactions and, especially, the growth of insects and mites. A good maximum storage temperature is about 18°C. The largest dryers are normally used "Off-farm", in elevators, and are of the continuous type: Mixed-flow dryers are preferred in Europe, while Cross-flow dryers in the USA. In Argentina, both types are usually found. Continuous flow dryers may produce up to 100 metric tones of dried grain per hour. The path of grain the air must traverse in continuous dryers range from some 0.15 m in mixed flow dryers to some 0.30 m in Cross-Flow. Batch dryers are mainly used "on-farm", particularly in the USA and Europe. They normally consist of a bin, with heated air flowing horizontally from a narrow-diameter cylinder through a perforated metal sheet, placed in the center of the bin. Air passes through a path of grain some 0.50 m deep in radial direction and leaves the system through another perforated sheet. The usual drying times range from 1 h to 4 h depending on how much water must be removed, the air temperature, and the grain depth. In the USA, continuous counter flow dryers may be found on-farm, adapting a bin to slowly drying the grain, and removing the dried product using an auger. Grain drying is an active area of manufacturing and research. Now it is possible to "simulate" the performance of a dryer with computer programs based on equations that represent the physics and physical chemistry of drying [8].

3.3 Drying Mechanism

In the process of drying, heat is necessary to evaporate moisture from the material and a flow of air helps in carrying away the evaporated moisture. There are two basic mechanisms involved in the drying process: the migration of moisture from the interior of an individual material to the surface, and the evaporation of moisture from the surface to the surrounding air. The drying of a product is a complex heat and mass transfer process which depends on external variables such as temperature, humidity and velocity of the air stream and internal variables which depend on parameters like surface characteristics (rough or smooth surface), chemical composition (sugars, starches, etc.), physical structure (porosity, density, etc.), and size and shape of products. The rate of moisture movement from the product inside to the air outside differs from one product to another and depends very much on whether the material is hygroscopic or non-hygroscopic. Non-hygroscopic materials can be dried to zero moisture level while the hygroscopic materials like most of the food products will always have residual moisture content. This moisture, in hygroscopic material, may be bound moisture which remained in the material due to closed capillaries or due to surface forces and unbound moisture which remained in the material due to the surface tension of water as shown in Figure 3-6 [22].

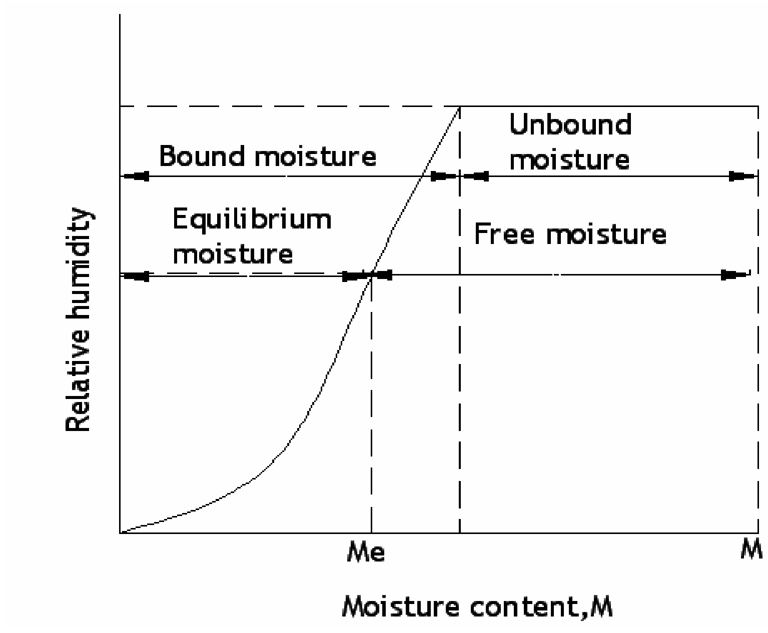

Figure 3-6: Moisture in the Drying Material.

When the hygroscopic material is exposed to air, it will absorb either moisture or desorbs moisture depending on the relative humidity of the air. The equilibrium moisture content (EMC = Me) will soon reach when the vapor pressure of water in the material becomes equal to the partial pressure of water in the surrounding air. The equilibrium moisture content in drying is therefore important since this is the minimum moisture to which the material can be dried under a given set of drying conditions. A series of drying characteristic curves can be plotted. The best is if the average moisture content M of the material is plotted versus time as shown in Figure **3-7** [22].

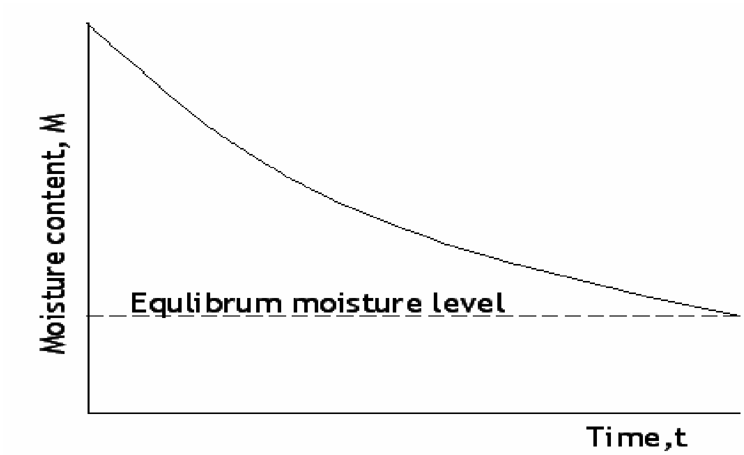

Figure 3-7: Rate of Moisture Loss

Another curve can be plotted between drying rate dM/dt versus time t as shown in Figure **3-8**. But more information can be obtained if a curve is plotted between drying rate dM/dt versus moisture content M as shown in Figure **3-9**.

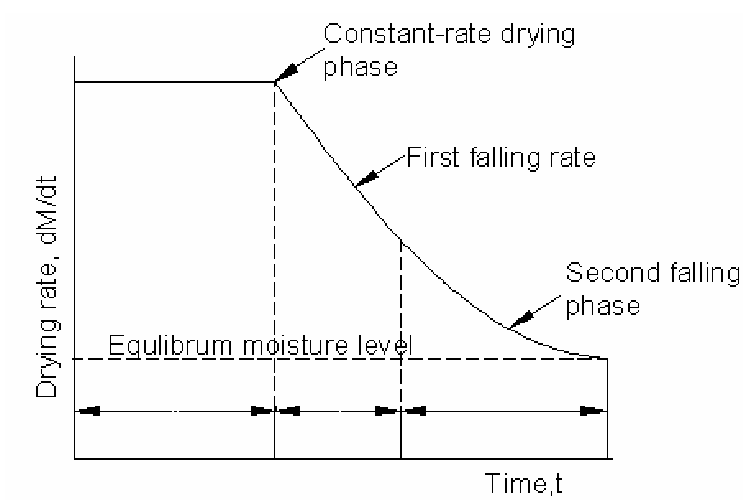

Figure 3-8: Drying Rate with Time Curve

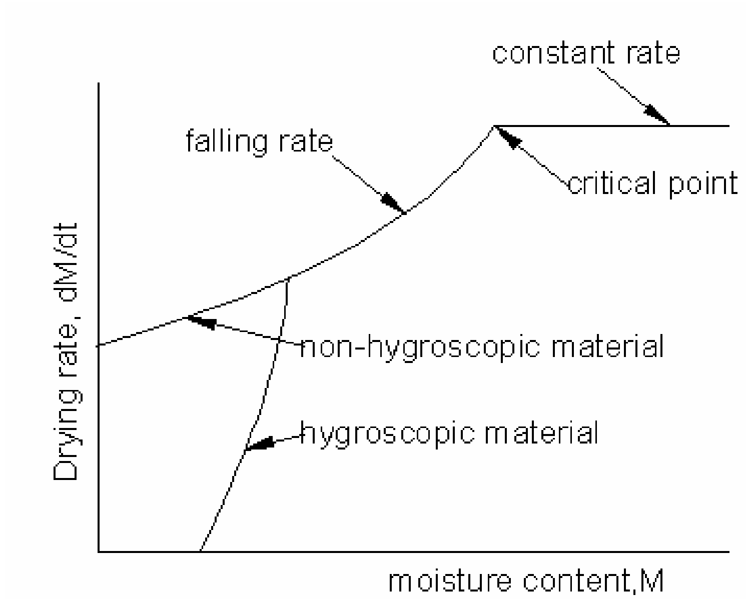

Figure 3-9: Typical Drying Rate Curve

As can be seen from Figure 3-8 for both non-hygroscopic and hygroscopic materials, there is a constant drying rate terminating at the critical moisture content followed by falling drying rate. The constant drying rate for both non-hygroscopic and hygroscopic materials is the same while the period of falling rate is little different. For non-hygroscopic materials, in the period of falling rate, the drying rate goes on decreasing till the moisture content becomes zero. While in the hygroscopic materials, the period of falling rate is similar until the unbound moisture content is completely removed, then the drying rate further decreases and some bound moisture is removed and continues till the vapor pressure of the material becomes equal to the vapor pressure of the drying air. When this equilibrium reaches then the drying rate becomes zero [22].

The period of constant drying for most of the organic materials like fruits, vegetables, timber, etc. is short and it is the falling rate period in which is of more interest and which depends on the rate at which the moisture is removed. In the falling rate regime moisture is migrated by diffusion and in the products with high moisture content, the diffusion of moisture is comparatively slower due to turgid cells and filled interstices. In most agricultural products, there is sugar and mineral of water in the liquid phase which also migrates to the surfaces, increase the viscosity, reduces the surface vapor pressure and hence reduce the moisture evaporation rate.

Drying is done either in thin layer drying or deep layer drying. In thin layer drying; which is done in case of most of fruits and vegetables, the product is spread in thin layers with entire surface exposed to the air moving through the product and the Newton's law of cooling is applicable in the falling rate region. Most of the grains are dried in deep layer which can be considered as a series of thin layers and the temperature and the humidity varies from layer to layer.

3.4 The Quantity of Air Needed for Drying

The drying of any material involves migration of water from the interior of the material to its surface, followed by removal of the water from the surface. The rate of movement differs from one substance to another. These differences are greatest between hygroscopic and non-hygroscopic materials. For non-hygroscopic materials, drying can be carried out to zero moisture content, as for example, the textile materials being dried in a laundry. Hygroscopic material, such as grains, fruits, and foodstuffs in general, will have residual moisture content. There is then equilibrium between the vapor pressure of the air and that of the material being dried and the drying rate becomes zero. It may be necessary in drying to reduce the rate of drying to prevent cracking of the surface. In most drying operations, the heat comes from the air itself, which is cooled by the evaporation; this relationship (latent for evaporation heat given up by air) can be expressed by the following [22]:

$$m_w h_{fg} = m_a C_p (T_2 - T_1) \quad \textbf{(3-1)}$$

where: m_w= water removed per kg of the air, [kg]

h_{fg}=latent heat of vaporization, [J, kg^{-1}]

m_a = mass flow rate of the air, [kg, sec^{-1}]

C_p=specific heat, [J, kg^{-1}, $^0C^{-1}$]

T_1, T_2= the initial and final temperature of the given parameter, [^{0}C]

The quantity of water is calculated from the initial and desired final moisture content with the help of the following Equation (3-2) [27]:

$$m_w = m_g\left(\frac{M_o - M_f}{1 - M_f}\right) \quad \textbf{(3-2)}$$

where: m_w = water removed per kg of the air, [kg]

m_g = mass of grain in the dryer chamber, [kg]

M_0 = initial moisture content, [decimal]

M_f = final moisture content, [decimal]

3.5 Air Properties

The properties of the air flowing around the product are major factors in determining the rate of removal of moisture. The capacity of air to remove moisture is principally dependent upon its initial temperature and humidity; the greater the temperature and lower the humidity the greater the moisture removal capacity of the air. The relationship between temperature, humidity and other thermodynamic properties is represented by the psychrometric chart. It is important to appreciate the difference between the absolute humidity and relative humidity of air. The absolute humidity is the moisture content of the air (mass of water per unit mass of air) whereas the relative humidity is the ratio, expressed as a percentage, of the moisture content of the air at a specified temperature to the moisture content of air if it were saturated at that temperature.

The changes in condition of air when it is heated using the solar energy and then passed through a bed of moist product are shown in Figure 3-10. The heating of air from temperature T_A to T_B is represented by the line AB. During heating the absolute humidity remains constant at ω_A whereas the relative humidity falls from Φ_A to Φ_B. As air moves through the material to be dried, it absorbs moisture. Under (hypothetical) adiabatic drying; sensible heat in the air is converted to latent heat and the change in the condition of air is represented along a line of constant enthalpy, BC. Both absolute humidity and relative humidity increase from ω_B and ω_C and from Φ_B to Φ_C, respectively, but air temperature decreases to, T_C. The absorption of moisture by the air would be the difference between the absolute humidities at C and B. (ω_B- ω_A). If unheated air is passed through the bed, the drying process would be represented by the line AD. Assuming that the air at D to be at the same relative humidity, Φ_C, as the heated air at C, then the absorbed moisture would be (ω_D- ω_A), considerably less than that absorbed by the heated air (ω_C- ω_A) [3].

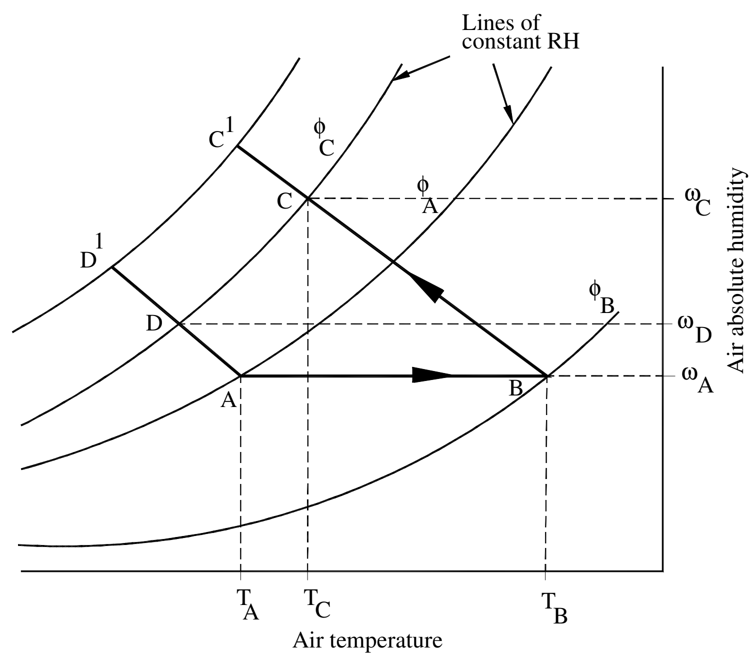

Figure 3-10: Representation of Drying Process

Chapter 4

4.1 An Introduction to TRNSYS

TRNSYS is a transient system simulation program with a modular structure. The program is well suited to simulate the performance of systems, the behavior of which is a function of the passage of time. This is the case if outside conditions that influence the system behavior change, such as weather conditions, or if the system components themselves go through conditions that vary with time.

Modular simulation of a system requires the identification of components whose collective performance describes the performance of the system. Each component is formulated by mathematical equations that describe its physical behavior. The mathematical models for each component are formulated in FORTRAN code, so that they can be used within the TRNSYS program. Formulation of the components has to be in accordance with the required TRNSYS format. A basic principle in this format is the specification of parameters, inputs and outputs for each component. Parameters are constant values that are used to model a component; these can be for example, the geometric parameters of the solar dryer such as length, depth and width. Inputs are time-dependent variables that can come from a user supplied data source such as weather data or from outputs of other components [6].

There can be several components of the same type specified in one simulation. The way this identification is accomplished is that each component is assigned an identifying type number that is component specific. A second number, the unit number is unique; one can only be used once in a simulation.

Different unit numbers can be associated with the same type number, although there are limitations on how many types of one kind can be used in one simulation. A system is set up in TRNSYS by means of an input file, called a TRNSYS deck. This deck contains all the information that specifies the components and how the components interact. The system is set up by connecting all inputs and outputs in an appropriate way to simulate the real system. For example the cooling demand for the building unit is the evaporator energy of the air conditioner unit. Once a system is set up in a TRNSYS deck, the program can be run over a user defined time interval. The time interval is divided into equal number of time steps. At each time step the program calls each component and solves all the mathematical equations that specify the component performance. The program iteratively calls the system component until a stationary state is reached. The stationary state is reached when all the calculated inputs to the components remain constant between two iterations. Naturally, in a numerical solution such as calculated by TRNSYS, there will always be a difference in results between two iterations. Therefore the user has to specify tolerances that define a stationary state.

Aside from the components that simulate actual physical parts of the system, there are predefined utility components that can be used in the simulation. One of them is the data reader. The data reader is able to read data from a user supplied data file that has to be assigned in the TRNSYS deck. At every time step of the simulation the data file then reads the desired values from the file and makes them accessible to the components.

Another kind of utility component is a printer that stores output data in a file. Several printers can be defined in one deck. These output files can be imported into a spreadsheet program and the results further examined. The online plotter can be used to make the progress of the simulation visible on the screen, so that the user can immediately decide whether a run was useful or not. Additionally, a quantity integrator is available to integrate values over time.

A special feature of the TRNSYS program package is the possibility to create a user-friendly input file called a TRNSED file. When the TRNSED program is started, the user only has to supply the important parameters and can change these easily for different simulations. In this way the program is accessible to users who are not experienced in using TRNSYS but are only interested in examining a particular system.

4.2 Creating a New Component

This section will briefly illustrate how to generate new components using the Simulation Studio.

Create the component Performa

- Launch the Simulation Studio and open File/New

- Select “New Component" (see Figure 4-1)
- In the component "General" tab, type in the component's object and its Type number. It is important to assign a Type number different from zero. The selected number should be in the [201-300] range in order to avoid conflicts with existing libraries.

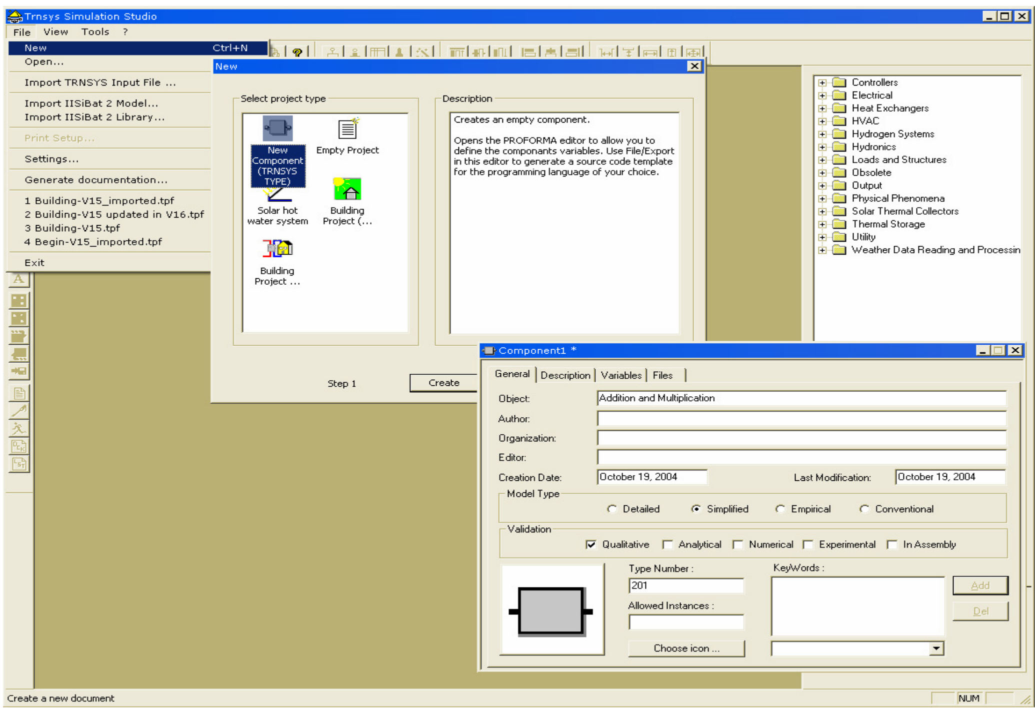

Figure 4-1: Creating a New Component Proforma (1)

- Variables can then be added to the Performa in the "Variables" tab. Click on "variables” select the "Parameters or input or output" tab and click on "Add". Parameter information can be entered in the row that has been created or "Modify" is clicked on to have a more detailed view (see Figure 4-2).

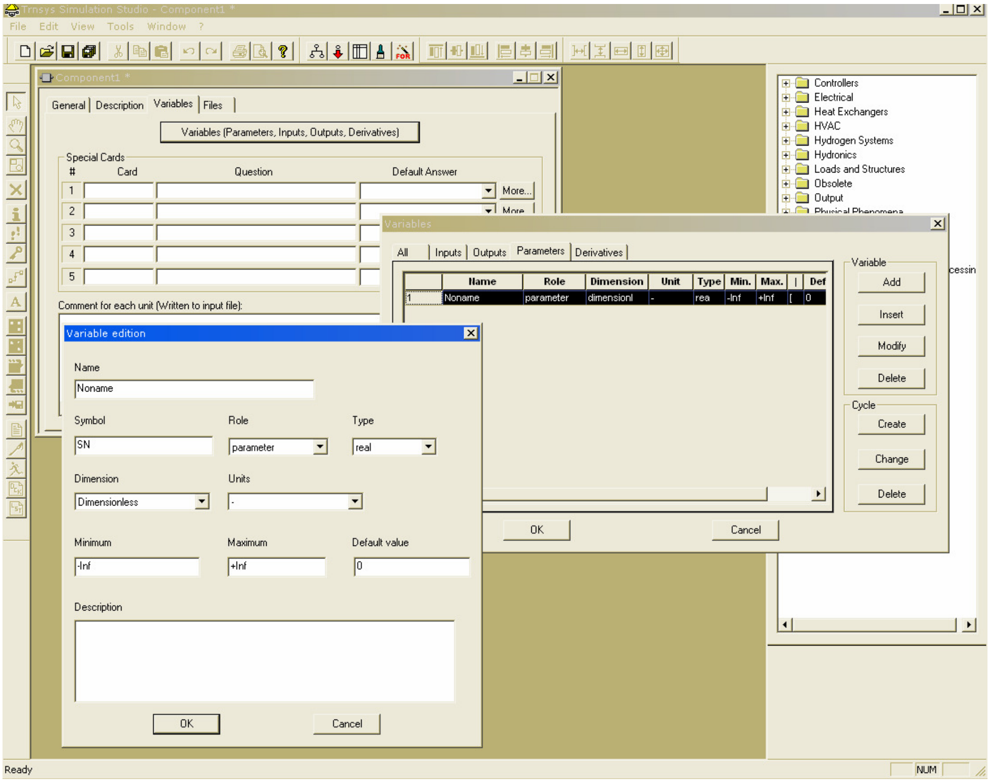

Figure 4-2: Creating a New Component (2)

- Save the Performa. To be accessible in the Studio, the Performa needs to be in "%TRNSYS16%\Studio\Proformas". A folder, for example, called "My Components" is created and saved as "Type200.tmf".

- Open "File/Export as/Fortran" and create a "Type200" folder anywhere on the disk, (e.g. in "My Projects"). Save the component as Type200.for there (see Figure 4-3).

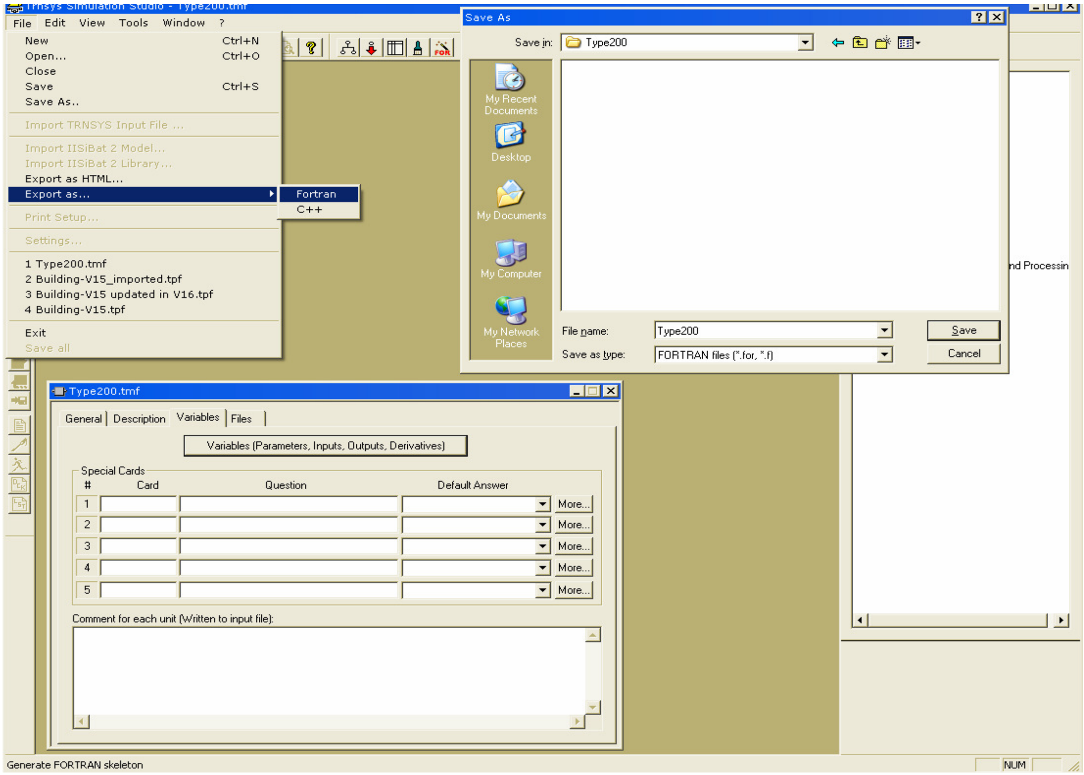

Figure 4-3: Exporting as FORTRAN

The Studio will then do several things for the user (see the dialog box in Figure 4-4):

- Create a FORTRAN skeleton for the created Type (Type200.for)
- Generate a project that you can open in the Compaq Visual FORTRAN 6.6 compiler or in the Intel Visual Fortran compiler. That project includes all the settings you need in order to generate an external DLL that will be placed in the \UserLib\ReleaseDLLs or \UserLib\DebugDLLs folder, where TRNSYS will be able to load the created Type.
- Open the project in the compiler that is setup in File/Settings/Directories/Fortran environment (by default the settings are correct for CVF 6.6, if it has been installed, in the default location.

The following will assume that Compaq Visual FORTRAN 6.6 is installed on the machine.

- The skeleton includes all basic TRNSYS manipulations. At the minimum, the question marks in the lines that calculate outputs from inputs need to replaced, (see Figure 4-4).

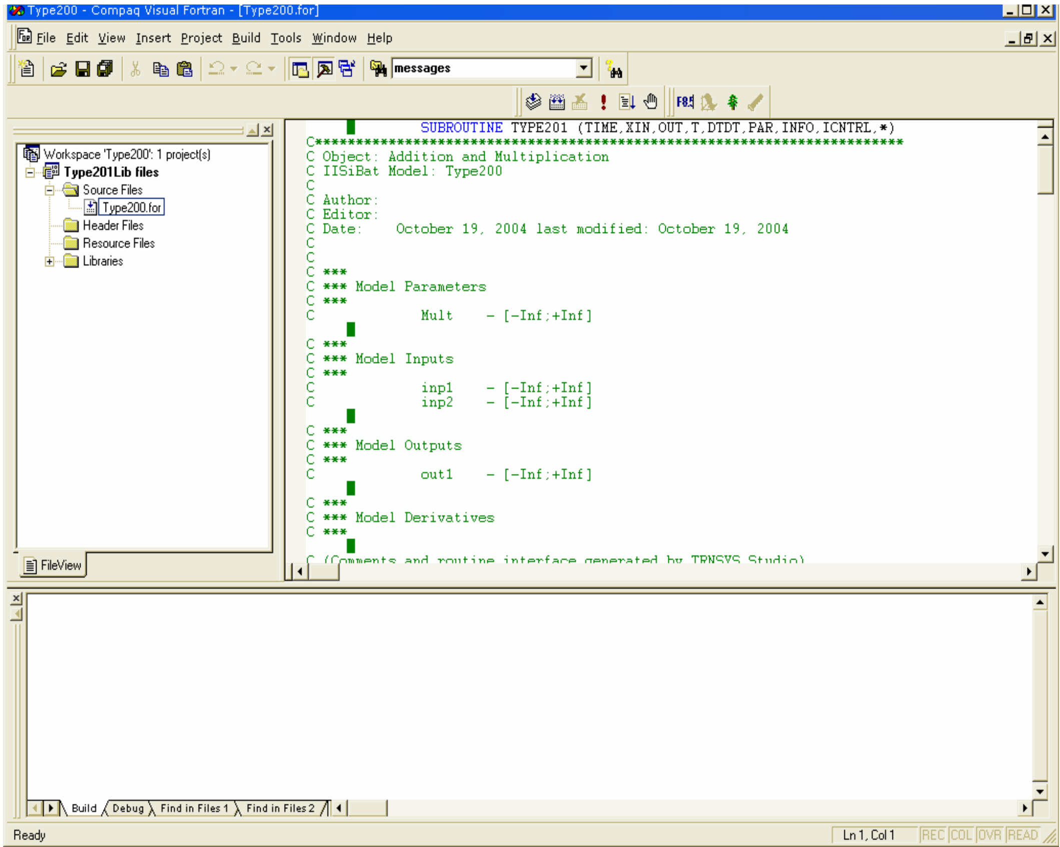

Figure 4-4: Setting the Component Outputs

- Equation(s) of the out put are written in the line in place of the question mark (?). After writing the equation(s) F7 is pressed to build the .DLL file. This will generate "Type200.dll" in the 'UserLib\ DebugDLLs directory if there is no error (see Figure 4-5).

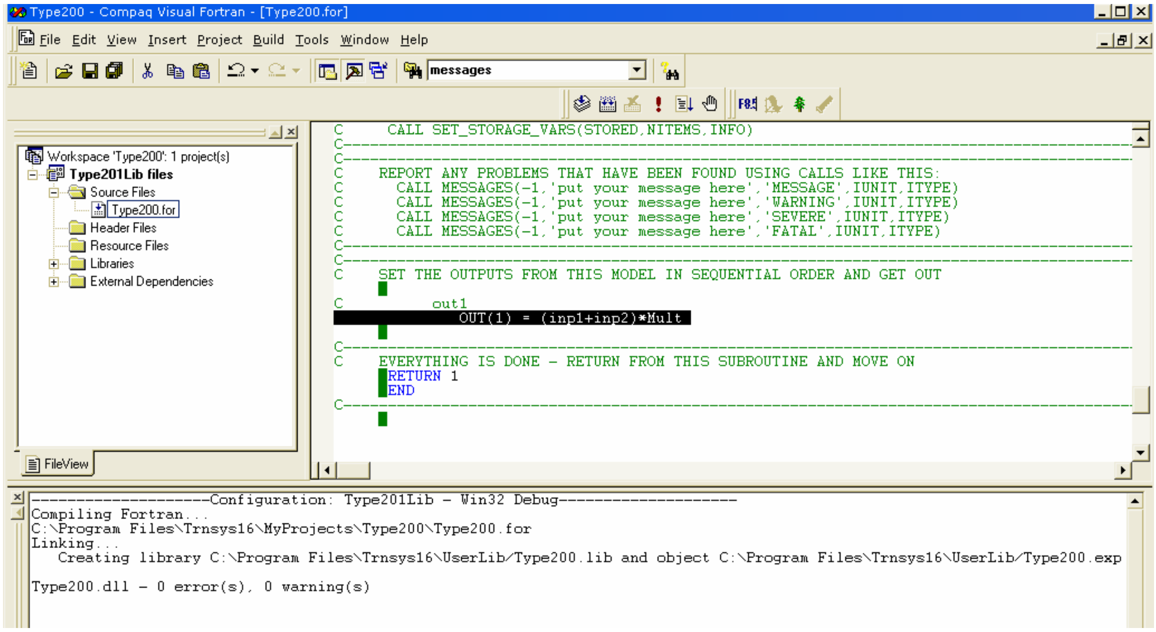

Figure 4-5: Compiling the Component and Building the DLL

- Open 'Build/Set Active Configuration', and select the 'Release' project configuration and select "Ok". Press F7 to build the DLL. This will generate "Type200.dll" in the 'UserLib\ReleaseDLLs' directory. TRNSYS loads external libraries depending on the mode in which the main DLL was compiled: 'UserLib\ReleaseDLLs' and 'UserLib\DebugDLLs'. In this case, it will use the Release directory.

- Activate the Simulation Studio and create a project to use the new component. Go to "File/New/Empty Projects". In order for the newly created Performa to appear in the direct access tool (component list on the right of the screen), it is refreshed using "Direct Access/Refresh tree" (see Figure 4-6).

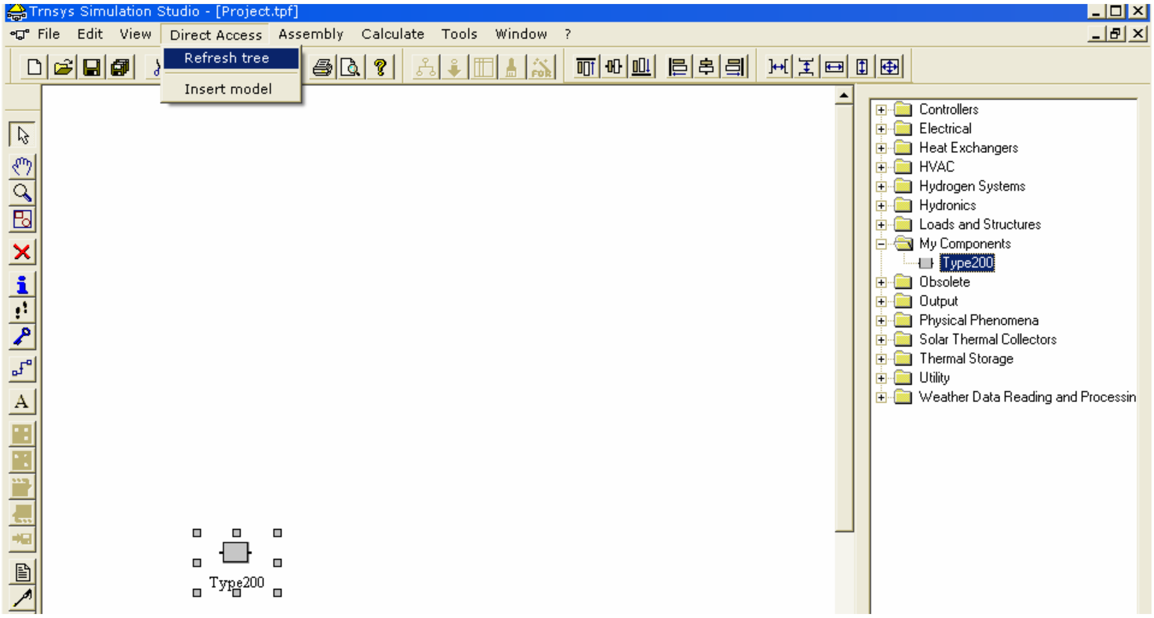

Figure 4-6: Using the New Component in a Project

In this thesis, one of the components added is the dying bed. Below is given an illustration of the inclusion of the dryer into the TRNSYS component Types.

- From the simulation studio, click on File-New and then click on New Component-and finally on create(see Figure 4-7)

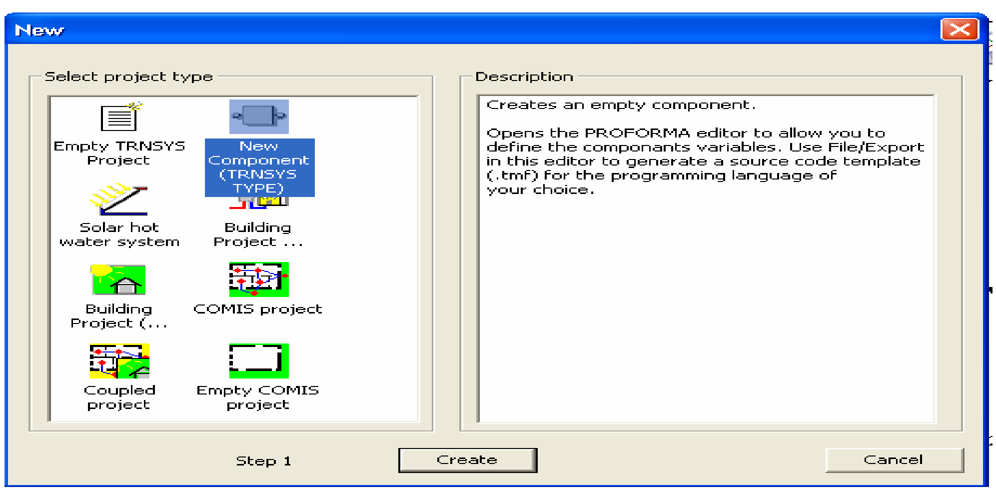

Figure 4-7: Creating a New Component Proforma (1a)

- On the Component1 window select General and enter the Object name and Type Number, (see Figure 4-8).

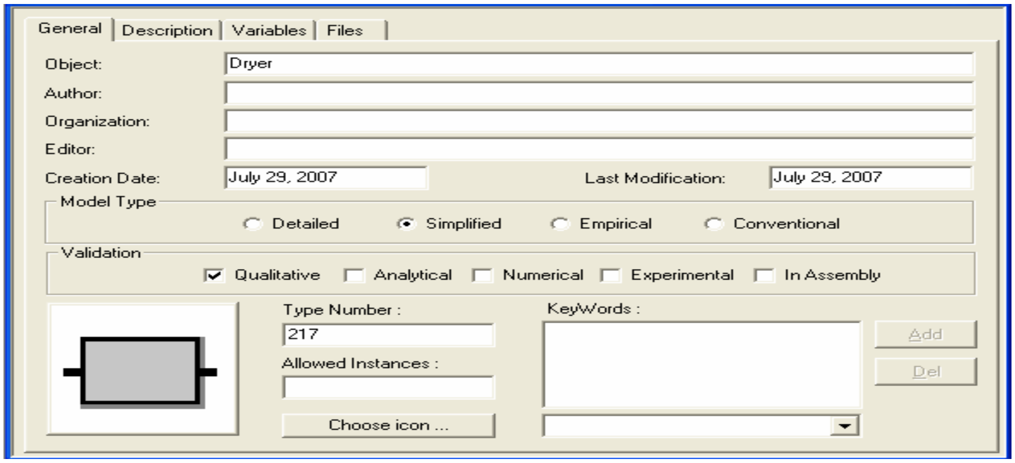

Figure 4-8: Entering Object Name and Type Number for the New Component

- Pick on the Variables menu and then click on Variables (Parameters, Inputs, Outputs, and Derivatives) button. The rows under Name, Role, Dimension, Unit, etc. are filled appropriately for the Inputs, the Outputs, the Parameters and Derivatives by clicking on the Add button. After all the required Inputs, Outputs, Parameters, etc. are entered click on OK, see Figure 4-9.

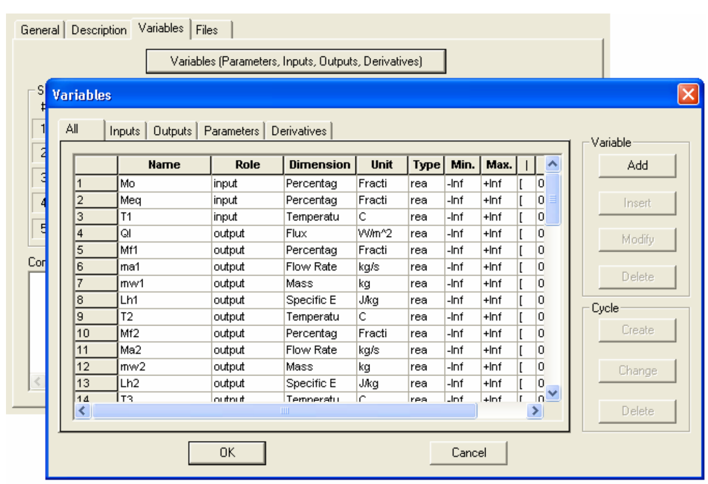

Figure 4-9: Entering Variables for the New Component

- Then click on File-Save and save the new component in the directory of Trnsys16 - Studio-Performa- in the folder ”My Components” then click on the Save button, see Figure 4-10.

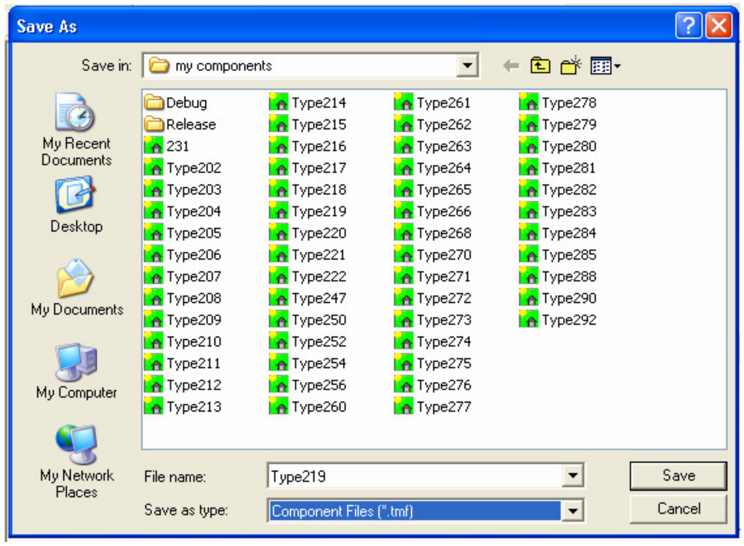

Figure 4-10: Saving the New Component

- Then click on File-Export as… and pick on FORTRAN and save the component type”Type N” in a new folder that has been created.

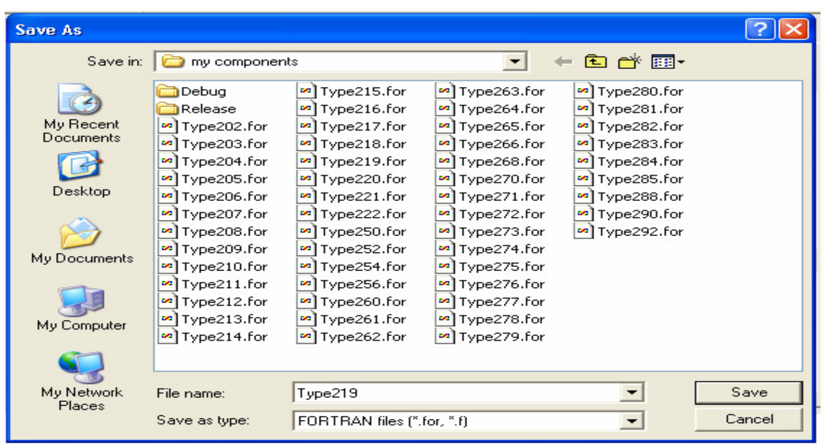

Figure 4-11: Saving the Generated FORTRAN Subroutine of the New Component

- Finally, the equation(s) for the component are entered in place of the question mark (?), Out (1) **=?** as shown in Figure 4-12**.**

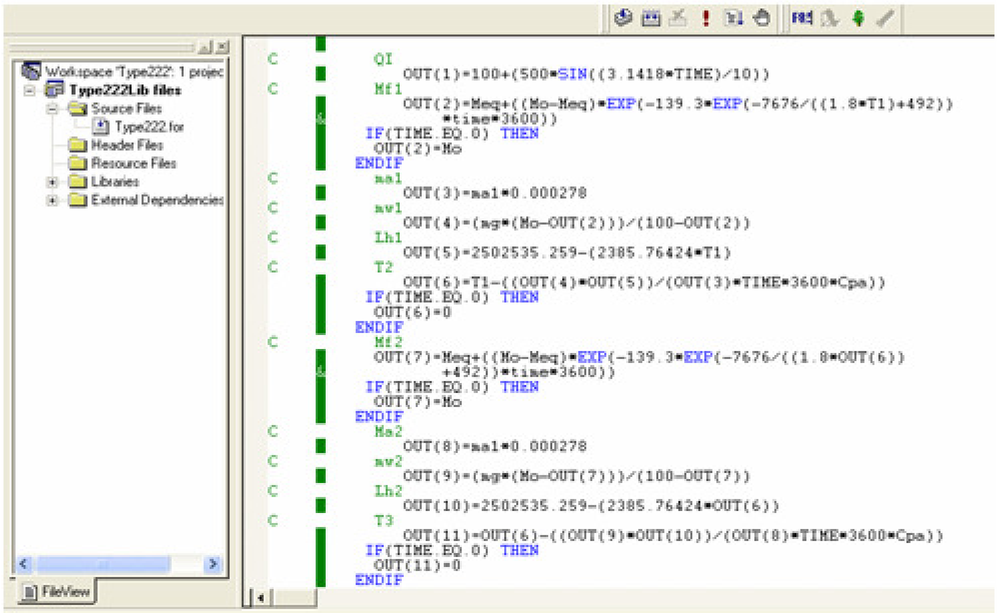

Figure 4-12: Entering Equation(s) into the Subroutine of the New Component

- Then the component's inputs are connected to the component's output its output is connected to an online plotter (see Figure 4-13).

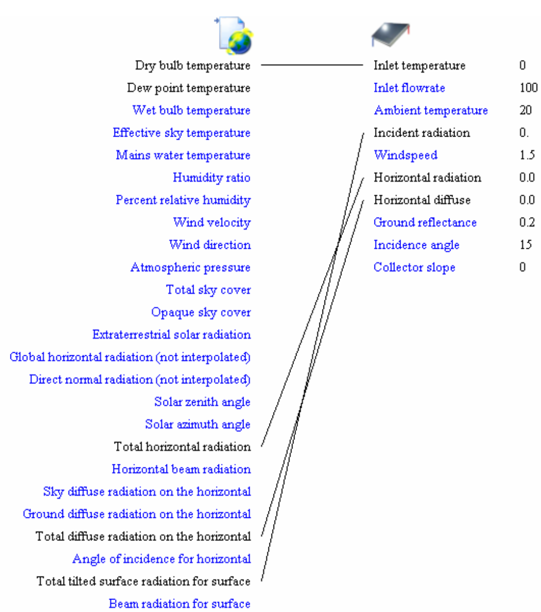

Figure 4-13: Shows the TRNSYS input file with the components placed in position.

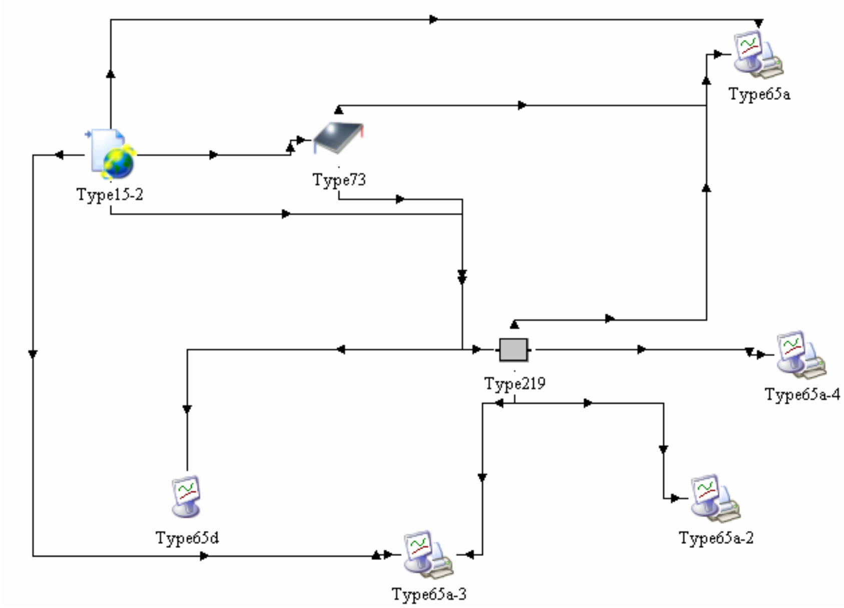

Figure 4-14: Sample Assemble Panel

- Run the project (F8). The output should be equal to: You can check the values in the online plotter by pressing CTRL+SHIFT and moving the mouse over the plot (see Figure 4-15).

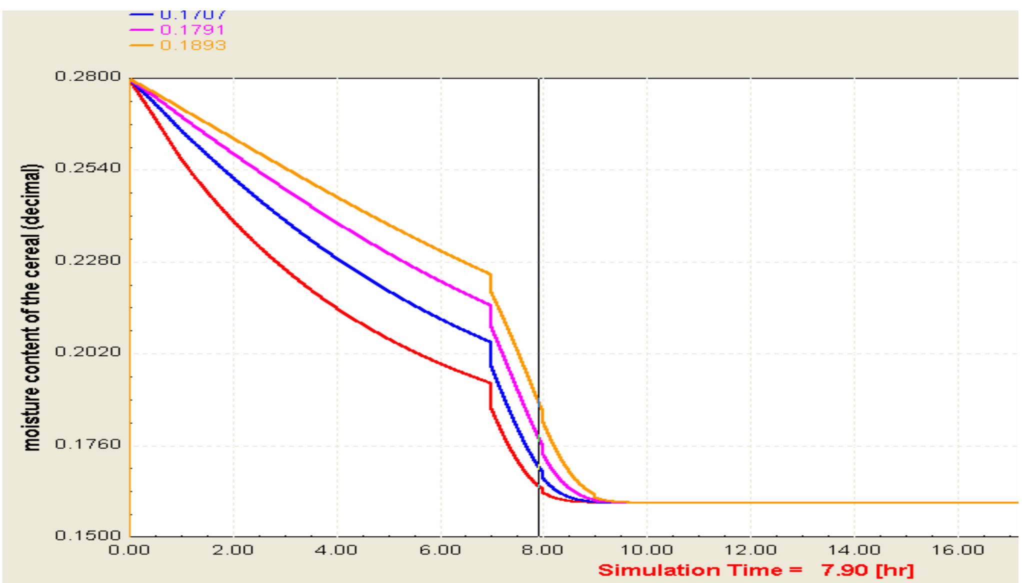

Figure 4-15: Checking the Components Output

4.3 Weather Data for Addis Ababa

The design of a solar energy conversion system requires precise knowledge regarding the availability of global solar radiation and its components at the location of interest. Since the solar radiation reaching the earth's surface depends upon climatic conditions of the place, a study of solar radiation under local climatic conditions is essential. In developing countries such as Ethiopia, due to absence or malfunction of measuring instruments, reliable solar radiation data is not available. In Ethiopia, Global Solar Radiation data on horizontal surface is recorded at Addis Ababa at only two stations: (Bole airport and Tikur Ambesa hospital).

In the absence and scarcity of trustworthy solar radiation data, the need for an empirical model to predict and estimate global solar radiation seems inevitable. These models use climatological parameters of the location under study. Among all such parameters, sunshine hours are the most widely and commonly used. The models employing this common and important parameter are called sunshine-based models.

Sunshine-based models use only bright sunshine hours as input parameter while others use additional climatological data together with bright sunshine hours. In some of the models geographical and seasonal parameters are also taken into account to reflect the latitudinal and seasonal variation of the air mass.

The first empirical correlation using the idea of employing sunshine hours for the estimation of global solar radiation was proposed by Angstrom. The Angstrom correlation was modified by Prescott and Page. Many researchers have employed hours of bright sunshine to estimate solar radiation. Other workers, e.g. Reddy, Sayyigh, Glover and McCullouch, derived their equations by using sunshine duration, relative humidity, temperature and latitude of the locations under study. Reddy suggested the use of the number of rainy days, sunshine hours and a factor which depends on the geographical location of the place along with the latitude. Barbaro related daily total solar radiation to the sunshine duration and the noon height of the sun on the 15^{th} of the given month.

The simplest model used to estimate hourly average daily solar radiation on horizontal surface is the well-known Angstrom equation.

4.3.1 Climatic Classification

Classification of climate with respect of Solar drying means zoning the country into regions in such a way that the difference of climate from region to region is reflected in the Solar Drying, warranting some special provision for each region. Based on this criteria, there are five major climatic zones, hot-dry; warm-humid, cold, temperate, composite.

Table 1: Climatic Zones of Area

Climatic Zone	Mean Monthly Maximum Temperature, ^{o}C	Mean Monthly Relative Humidity, %
Hot-Dry	Above 30	Below 55
Warm-Humid	Above 30 Above 25	Above 55 Above 75
Temperate	25-30	Below 75
Cold	Below 25	All values

According to Table **1** most hot areas of Ethiopia are classified as hot and dry. For example for Addis Ababa the average mean monthly maximum temperature for all months of the year is greater than 25-30^{0}C and the mean monthly relative humidity is less than 55-75%.

4.3.2 Temperatures and Relative Humidity

TRNSYS needs hourly dry bulb temperatures, dew point temperature, and relative humidity in its weather file; however in Ethiopia it is difficult to get hourly data for most cities. Hence estimation of hourly dry-bulb temperature from the daily mean maximum and daily mean minimum temperatures will give a reasonable result. It is then good assumption to take a sinusoidal variation of the dry-bulb temperature through the day.

If the outside temperature is T (t) at any time t, then:

$$T(t)=T(\max)-\frac{T_{\max}-T_{\min}}{2}\left[1-\sin\frac{(t\pi-9\pi)}{12}\right] \quad \textbf{(4-1)}$$

where: T (t) = the temperature at any time t, [^{0}C]

T_{max} = mean daily maximum temperature, [^{0}C]

T_{min} = men daily minimum temperature, [^{0}C]

t = sun time in hours, [sec]

The relative humidity is also assumed to vary sinusoidal with time where it's minimum value and maximum value of the place. By rearranging in the form of equation (4-2) it can be used to estimate the hourly relative humidity of any place.

$$RH(t)=RH(\min)+\frac{RH(\max)-RH(\min)}{2}\left(1-\sin\left(\frac{\pi t-9\pi}{12}\right)\right) \quad \textbf{(4-2)}$$

where: RH (t) = relative humidity at any time t, [%]

RH (min) = minimum relative humidity, [%]

RH (max) = Maximum relative humidity, [%]

t = time in hours, [sec]

4.3.3 Solar Radiation

The Ethiopian Meteorological Service collects only the average sunshine hours as solar radiation data for some cities of the country. Hence the solar radiations used in TRNSYS are estimated from the average monthly sunshine hours available.

4.3.3.1 Extraterrestrial Radiation

The extraterrestrial radiation which is the radiation value on a plane normal to the radiation on the n^{th} day of the year is given by [12]**:**

$$I_{on} = I_{sc}\left[1 + 0.033\cos\left(\frac{360n}{365}\right)\right] \qquad \textbf{(4-3)}$$

where: I_{on} = Extraterrestrials radiation normal to the radiation, [W/m^2]

I_{sc} = solar constant, given by I_{sc} = 1367 W/m^2

n = day of the year, 1 for 1st January, 2 for 2nd January,

The extraterrestrial radiation incident on a horizontal plane outside the atmosphere is given by:

$$I_{on} = I_{sc}\left[1 + 0.033\cos\left(\frac{360n}{365}\right)\right]\cos\theta_Z \qquad \textbf{(4-4)}$$

where: θ_z is the **zenith angle** and is given by:

$$\mathrm{Cos}\theta_Z = \mathrm{Cos}\varphi\,\mathrm{Cos}\delta\,\mathrm{Cos}\omega + \mathrm{Sin}\varphi\,\mathrm{Sin}\delta \qquad \textbf{(4-5)}$$

Φ, **latitude**, is the angular location of the area north or south of the equator, north positive.

δ, **declination**, is the angular position of the sun at solar noon given by:

$$\delta = 23.45\sin\left(360\frac{284+n}{365}\right) \qquad \textbf{(4-6)}$$

ω, **hour angle**, the angular displacement of the sun east or west of the local meridian due to rotation of the earth on its axis at 15^0 per hour, morning negative, afternoon positive. It is [12]:

$$\omega = (h - 12)\times 15^0, \quad \text{h is the sun time in hours}$$

By integrating equation (4-4) from sunrise to sunset we can obtain the daily extraterrestrial radiation on a horizontal surface, $H_{0:}$

$$H_0 = \frac{24 \times 3600 G_{sc}}{\pi}\left[1 + 0.033\cos\frac{360n}{365}\right]\left(\cos\varphi\cos\delta\sin\omega_s + \frac{\pi\omega_s}{180}\sin\varphi\sin\delta\right) \quad \textbf{(4-7)}$$

where: ω_s is the sunset hour angle given by:

$$\omega_s = \mathrm{Cos}^{-1}(-\tan\phi\tan\delta) \quad \textbf{(4-8)}$$

The monthly mean daily extraterrestrial radiation $\bar{H}_0$ can be calculated using equation (4-7) with n and δ for the mean day of the month. Integrating equation (4-8) for an hour period between hour angles ω_1 and ω_2 will give the hourly extraterrestrial radiation incident on a horizontal surface, I_0, which is given by [12]:

$$I_0 = \frac{12 \times 3600}{\pi} G_{sc}\left(1 + 0.033\cos\frac{360n}{365}\right)\left[\cos\varphi\cos\delta(\sin\omega_2 - \sin\omega_1) + \frac{\pi(\omega_2 - \omega_1)}{180}\sin\varphi\sin\delta\right] \quad \textbf{(4-9)}$$

The I_0 is in MJ/m^2, and dividing by 3600seconds/hour will give in Wh/m^2.

4.3.3.2 Solar Radiation on a Horizontal Surface

The original Angstrom regression equation related monthly average daily radiation to clear day radiation at the location in question and average fraction of possible sunshine hours**:**

$$\frac{\bar{H}}{\bar{H}_c} = a' + b'\frac{\bar{n}}{N} \quad \textbf{(4-10)}$$

where: H= monthly average daily radiation on a horizontal surface

H_c= average clear sky daily radiation for the location and month on question.

a' , b' = empirical constants

n = monthly average daily sunshine hours

N = monthly average of the maximum possible daily hours of bright Sunshine (i.e. the day length of the average day of the month)

The difficulty in using equation (4-10) is in defining a clear sky; hence it is modified by the method to base it on extraterrestrial radiation on a horizontal surface rather than on clear day radiation [12]:

$$\frac{\bar{H}}{\bar{H}_0} = a + b\frac{\bar{n}}{N} \qquad \textbf{(4-11)}$$

where: $\bar{H}_0$ is the extraterrestrial radiation for the location, averaged over the time period in question, and a and b are constants depending on location.

$$a = -0.11 + 0.235\cos\varphi + 0.323\left(\frac{\overline{n_S}}{\overline{N_S}}\right)$$

$$b = 1.449 - 0.553\cos\varphi - 0.649\left(\frac{\overline{n_S}}{\overline{N_S}}\right)$$

The monthly average of the maximum possible daily hours of bright sunshine, N, can be calculated as:

$$N_S = \frac{2}{15}\mathrm{Cos}^{-1}(-\tan\phi\tan\delta) \qquad \textbf{(4-12)}$$

By assuming the monthly daily average sunshine hours to be the same for all days of the month can be rewrite equation (4-11) in terms of the daily total radiation:

$$\frac{H}{H_0} = a + b\frac{\bar{n}}{N} \qquad \textbf{(4-13)}$$

The hourly solar radiation can be estimated now from the daily solar radiation given by equation(4-13) but the method best estimates for clear days, as there is no way to estimate from the daily total the effect of circumstances such as intermittent heavy clouds, continuous light clouds, or heavy cloud cover for part of the day. Statistical studies of the time distribution of total radiation on a horizontal surface through the day, using monthly average data for a number of stations, have lead to generalized chart of r_t, the ratio of hourly total to daily total radiation as a function of day length and the hours in question [12]:

$$r_t = \frac{I}{H} \qquad \textbf{(4-14)}$$

The hours are designed by the time for the midpoint of the hour, and days are assumed to by symmetrical about solar noon. r_t can be estimated as**:**

$$r_t = \frac{\pi}{24}(C + D\cos\omega)\frac{\cos\omega - \cos\omega_S}{\sin\omega_S - \frac{\pi\omega_S}{180}\cos\omega_S} \qquad \textbf{(4-15)}$$

The coefficients C and D are given by:

$$C = 0.409 + 0.5016\sin(\omega_S - 60)$$
$$D = 0.6609 - 0.4767\sin(\omega_S - 60)$$

4.3.3.3 Beam and Diffuse Components

The beam and diffuse radiation components can now be calculated from the hourly clearness index, $k_T = I/I_0$.

The diffuse solar radiation on a horizontal surface is then given as:

$$\frac{I_d}{I_0}=\begin{cases}1-0.249k_T & \text{for } k_T \le 0.35\\ 1.557-1.84k_T & \text{for } 0.35<k_T<0.75\\ 0.177 & \text{for } k_T \ge 0.75\end{cases} \quad \textbf{(4-16)}$$

Hence, the beam or direct radiation on a horizontal surface is given by:

$$I_b = I - I_d \quad \textbf{(4-17)}$$

The beam radiation normal to the solar rays can be calculated as:

$$I_{bn}=\frac{I_b}{\cos\theta_z} \quad \textbf{(4-18)}$$

Variation of the total, beam and diffuse solar radiation incident on inclined collector with the time of the year for Addis Ababa using the measured data is shown in Figure 4-16

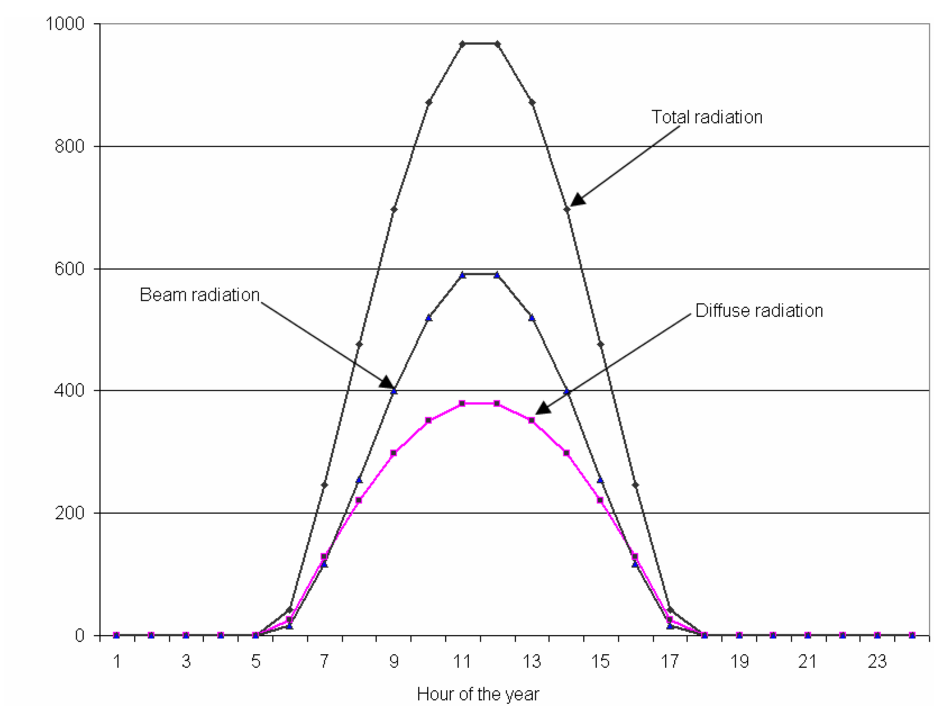

Figure 4-16: Daily Total (Beam Plus Diffuse) Solar Radiation Profile of January

Chapter 5

5.1 Solar Collectors

In the solar-energy industry great emphasis has been placed on the development of "active" solar energy systems which involve the integration of several subsystems: solar energy collectors, heat transfer beds, fluid transport and distribution systems, and control systems. The major component unique to active systems is the solar collector. This device absorbs the incoming solar radiation, converting it into heat at the absorbing surface, and transfers this heat to a fluid (usually air or water) flowing through the collector. The warmed fluid carries the heat either directly to the hot water or space conditioning equipment or to a storage subsystem from which can be drawn for use at night and on cloudy days. A large number of solar collector designs have been shown to be functional; these have fallen into two general classes:

• **Flat plate collectors**, in which the absorbing surface is approximately as large as the overall collector area that intercepts sun’s rays.

• **Concentrating collectors**, in which large areas of mirrors or lenses focus the sunlight onto a smaller absorber.

5.1.1 Flat-Plate Solar Collectors

Flat-plate solar collectors have potential applications in many space-heating situations, air conditioning, industrial process heat, and also for drying of agricultural products. These collectors use both beam and diffuse radiation. They are usually fixed in position permanently, have fairly simple construction, and require little maintenance. To keep costs at a level low enough to make solar heating more attractive than other sources of heat, the materials, dimensions, and method of fabrication must be chosen with care. A flat-plate solar collector consists of a radiation-absorbing flat plate beneath chosen with care.

A flat-plate solar collector consists of a radiation-absorbing flat plate beneath one or more transparent covers, and back and edge insulation to reduce heat loss. Heated air are circulates through the collector by natural convection to remove the absorbed heat.

Even though the theory of flat-plate solar collectors is well established, accurate design programs, which have an easy-to-use graphic interface and include all the design factors, are not available. In this thesis a detailed model is developed that includes all of the design features of the collector such as: plate material and thickness, number of covers and cover material, back and edge insulation dimensions, etc. The program is useful for collector design and for detailed understanding of how collectors function. For system simulation programs such as TRNSYS, simple models such as instantaneous efficiency and incident angle modifier are usually adequate.

A solar collector is a very special kind of heat exchanger that uses solar radiation to heat the working fluid. While conventional heat exchangers accomplish a fluid-to fluid heat exchange with radiation as a negligible factor, the solar collector transfers the energy from an incoming solar radiation to a fluid. The wavelength range of importance for flat-plate solar collectors is from the visible to the infrared. The radiation heat transfer should be considered thoroughly in the calculation of absorbed solar radiation and heat loss. While the equations for collector performance are reduced to relatively simple forms in many practical cases of design calculations, they are developed in detail in this thesis to obtain a thorough understanding of the performance of flat-plate solar collectors. Important parts are the cover system with one or more glass or plastic covers, a plate for absorbing incident solar energy, and edge and back insulation. The detailed configuration may be different from one collector to the other. However, the basic geometry is similar for almost flat-plate solar collectors.

Some assumptions made to model the flat-plate solar collectors are:

1. The collector operates in steady state;
2. Temperature gradient through the covers is negligible;
3. There is one-dimensional heat flow through the back and side insulation and through the cover system;
4. The temperature gradient through the absorber plate is negligible;
5. The collector may have zero to two covers;
6. In calculating instantaneous efficiency, the radiation is incident on the solar

Collector with fixed incident angle;

7. The collector is free-standing;

8. The area of absorber is assumed to be the same as the frontal transparent area.

5.2 Air Collectors

Air collectors have the advantage of eliminating the freezing and boiling problems associated with liquid systems. Although leaks are harder to detect and plug in an air system, they are also less troublesome than leaks in a liquid system. Air systems can often use less expensive materials, such as plastic glazing, because their operating temperatures are usually lower than those of liquid collectors.

Air collectors are simple, flat-plate collectors used primarily for space heating and drying crops. The absorber plates in air collectors can be metal sheets, layers of screen, or non-metallic materials. The air flows through the absorber by natural convection or when forced by a fan. Because air conducts heat much less readily than liquid does, less heat is transferred between the air and the absorber than in a liquid collector. In some solar air-heating systems, fans on the absorber are used to increase air turbulence and improve heat transfer. The disadvantage of this strategy is that it can also increase the amount of power needed for fans and, thus, increase the costs of operating the system. In colder climates, the air is routed between the absorber plate and the back insulation to reduce heat loss through the glazing. However, if the air will not be heated more than 17°C above the outdoor temperature, the air can flow on both sides of the absorber plate without sacrificing efficiency [6].

The best features of air collector systems are simplicity and reliability. The collectors are relatively simple devices. A well-made blower can be expected to have a 10 to 20 year life span if properly maintained, and the controls are extremely reliable. Since air will not freeze, no heat exchanger is required.

However, the use of solar air heating collectors is still limited to supply hot air for space heating and for drying of agricultural products mainly in developing countries. The major limitations for the wide adoption of solar air heaters are the high cost for commercially produced solar air heaters, the large collector area required due to the low density and the low specific heat capacity of the air compared to liquid heat transfer fluids, the extended air duct system required, the high power requirement for forcing the air through the collector, and the difficulty of heat storage. In countries with comparatively low insolation and extended periods of adverse weather, supplementary heat is required which increases investment costs to a level which limits its competitiveness to conventional heating systems. Promising ways to reduce the collector cost are the integration of the collector into the walls or roofs of buildings and the development of collectors which can be constructed using prefabricated components [6].

5.2.1 Transient Analysis of Solar Collector (on Single Plate and Single Glass)

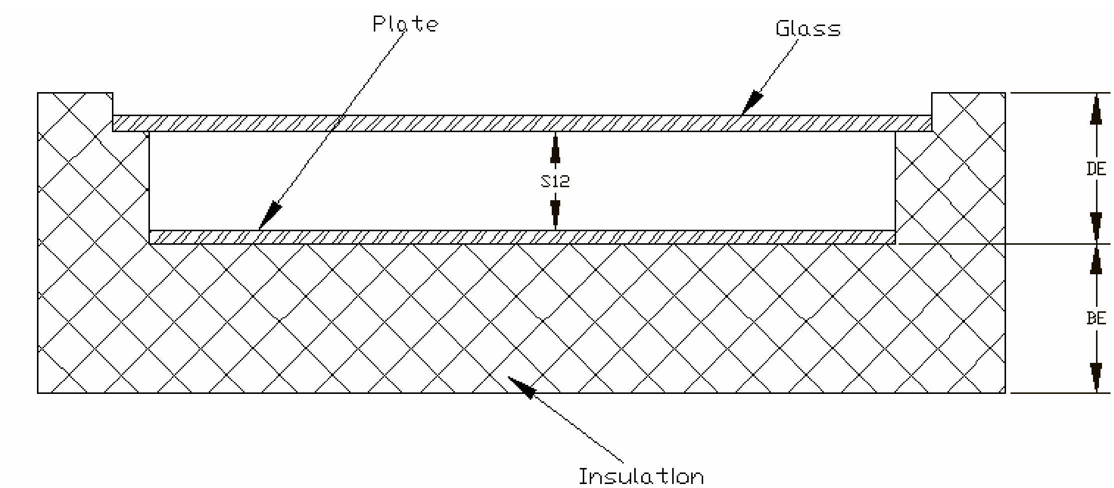

Figure 5-1: Solar Collector with Single Glass and Plate

The transient thermal performance of the solar collector is evaluated by applying energy balance on its components [2].

The solar radiation energy incident on the collector surface which is inclined at an angle θ to the horizontal, defined in terms of the global radiation G_r, the diffuse radiation D_r, the beam radiation factor R_b and the ground reflectivity factor =0.2 is given by:

$$I_N = R_b(G_r - D_r) + 0.5(1.0 + \cos\theta)D_r + 0.5\rho(1.0 - \cos\theta)G_r \quad \textbf{(5-1)}$$

$$R_b = \frac{\cos(\phi + \beta)\cos\delta\cos\omega + \sin(\phi - \beta)\sin\delta}{\cos\phi\cos\delta\cos\omega + \sin\phi\sin\delta} \quad \textbf{(5-2)}$$

The flux collected per unit time is given by:

$$I_c = I_N(\tau_g \alpha_p) \quad \textbf{(5-3)}$$

Energy balance on the absorber plate, the air stream and the glass cover are performed based on the thermal circuit indicated in Figure 5-1.

Absorber plate

Energy balance on the absorber plate is expressed as:

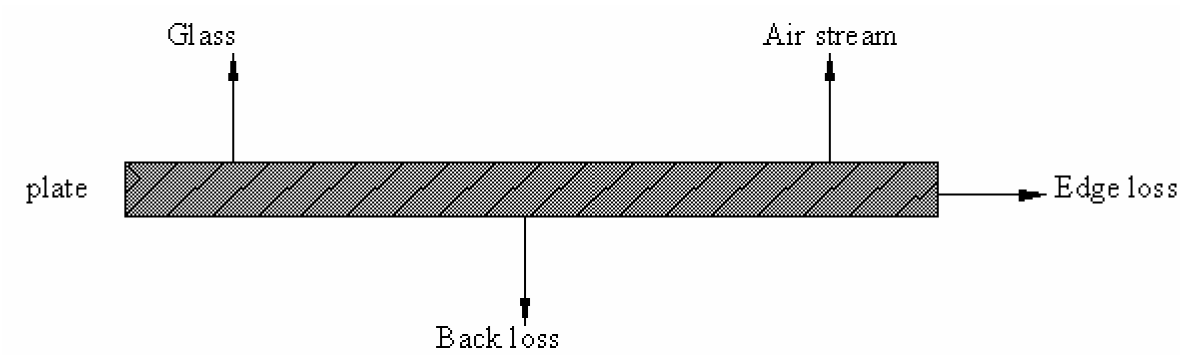

From first law of thermodynamics:

- Conservation of mass:

$$\frac{\partial}{\partial t}\oiiint_V \rho dv + \oiint_S \rho V \cdot ds$$

$$\frac{\partial \rho}{\partial t} + \nabla \cdot (\rho V) = 0 \quad \textbf{(5-4)}$$

- Conservation of energy:

$$\frac{\partial}{\partial t}\left[\rho\left(e + \frac{V^2}{2}\right)\right] + \nabla \cdot \left[\rho\left(e + \frac{V^2}{2}\right)V\right] = \rho \dot{q} - \nabla \cdot (pV) + \rho(f \cdot V) + \dot{W}_{viscous} + \dot{Q}_{viscous} \quad \textbf{(5-5)}$$

Or
$$\rho \frac{D(e + V^2/2)}{Dt} = \rho \dot{q}$$

where: $\frac{D}{Dt} = \frac{\partial}{\partial t} + (V \cdot \nabla)$

The fluid is assumed to be incompressible (density is constant) and inviscid, then equation (5-5) and equation (5-4) will be respectively:

$$\frac{\partial e}{\partial t} + \nabla \cdot V = \dot{q}$$

$$\frac{\partial e}{\partial t} + \left[\frac{\partial U}{\partial x} + \frac{\partial v}{\partial y} + \frac{\partial w}{\partial z}\right] = \dot{q} \qquad \textbf{(5-6)}$$

$$\nabla \cdot V = 0$$

$$\frac{\partial U}{\partial x} + \frac{\partial v}{\partial y} + \frac{\partial w}{\partial z} = 0 \qquad \textbf{(5-7)}$$

From equation (5-6) and equation (5-7):

$$\frac{\partial e}{\partial t} = \dot{q} \qquad \textbf{(5-8)}$$

where e is the change of internal energy.

q is the heat added to the system by the surrounding (the region outside the system).

Therefore, from equation (5-8) energy equations for the plate, glass and the air stream can be derived as:

$$\left(mc_p\right)_p \frac{dT_p}{dt} = A_c I_c - A_c U_{pg}\left[T_p - T_g\right] - A_c U_a\left[T_p - \frac{T_{ai} + T_{ao}}{2}\right] - A_c U_{pab}\left[T_p - T_a\right] - A_1 U_{pae}\left[\frac{Tp + Ta}{2} - Ta\right] \qquad \textbf{(5-9)}$$

Where: $$U_{pg} = \left[0.06 - 0.017\frac{\theta}{90}\right]\frac{K_a}{S_{12}} G_{rl}^{\ 1/3} + \varepsilon_{pg}\sigma(T_p^{\ 2} + T_g^{\ 2})(T_p + T_g) \qquad \textbf{(5-10)}$$

The Grashof number and the volume expansion are given by:

$$G_{rl} = \frac{g\beta(T_p - T_g)L^3}{\vartheta^2} \qquad \textbf{(5-11)}$$

$$\frac{1}{\beta} = \frac{(T_{ai} + T_{ao})}{2} \qquad \textbf{(5-12)}$$

The overall emittance factor for the absorber plate and the glass cover is obtained from the relation:

$$\varepsilon_{pg} = \frac{1}{\left[\frac{1}{\varepsilon_p} + \frac{1}{\varepsilon_g} - 1\right]} \quad \textbf{(5-13)}$$

The heat transfer coefficient of the air is given by:

$$U_a = 0.664 \frac{K_a}{L} \left[\frac{P_r G_{rl} \cos\theta}{P_r + 0.9524} \right]^{0.25} \quad \textbf{(5-14)}$$

$$P_r = \frac{v_a}{\alpha_a} = \frac{c_p v}{K_a} \quad \textbf{(5-15)}$$

Therefore

$$T_{p1} = T_{p0} + \frac{A_c I_c}{\left(mc_p\right)_p} \Delta t - \frac{A_c U_{pg}}{\left(mc_p\right)_p} \left(T_{p0} - T_{g0}\right) \Delta t - \frac{A_c U_a}{\left(mc_p\right)_p} \left(T_{p0} - \frac{T_{ai0} + T_{ao0}}{2}\right) \Delta t$$
$$\frac{A_c U_{pab}}{\left(mc_p\right)_p} \left(T_{p0} - T_{a0}\right) \Delta t - \frac{A_1 U_{pae}}{\left(mc_p\right)_p} \left(\frac{T_{p0} + T_{a0}}{2} - T_{a0}\right) \Delta t \quad \textbf{(5-16)}$$

Air stream

Consider heat transfer from the collector plate to the air steam, heat transfer from the air-stream to the glazing and heat transfer to the air entering the collector, energy balance on the stream yields:

$$\left(mc_p\right)_a \frac{dT_{ao}}{dt} = A_c U_a \left[T_p - \frac{T_{ai} + T_{ao}}{2} \right] - A_c U_a \left[\frac{T_{ai} + T_{ao}}{2} - T_g \right]$$
$$- \left(\dot{m} c_p\right)_a \left[T_{ao} - T_{ai}\right] \quad \textbf{(5-17)}$$

$$\dot{m} = 1.7 \times \rho \times \mu \times L \times \left(\frac{Gr}{\left(Pr^2 + (Pr + 0.9524) \right)} \right)^{0.25} \qquad \textbf{(5-18)}$$

$$T_{a01} = \left\{ 1 - \frac{\Delta t}{(mc_p)_a} \left[A_c U_a + (\dot{m} c_p)_a \right] \right\} T_{ao0} + \frac{\Delta t}{(mc_p)_a} \left[-A_c U_a + (\dot{m} c_p)_a \right] T_{aio} + \frac{A_c U_a \Delta t}{(mc_p)_a} \left(T_{p0} + T_{g0} \right) \qquad \textbf{(5-19)}$$

Glass cover

Energy balance on the glass cover yields:

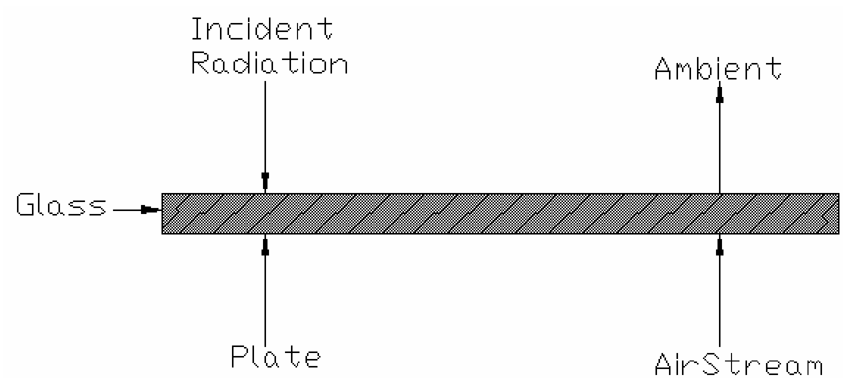

$$(mc_p)_g \frac{dT_g}{dt} = A_c I_N (1 - \tau_g) + A_c U_{pg} [T_p - T_g] - A_c U_{ga} [T_g - T_a] \qquad \textbf{(5-20)}$$

$$T_{g1} = \frac{A_c I_N (1 - \tau_g)}{(mc_p)_g} \Delta t + \left(1 - \frac{\Delta t}{(mc_p)_g} \left(A_c U_{pg} + A_c U_{ga} \right) \right) T_{g0} + \frac{A_c U_{pg} \Delta t}{(mc_p)_g} T_{p0} + \frac{A_c U_{ga} \Delta t}{(mc_p)_g} T_{a0} \qquad \textbf{(5-21)}$$

5.2.2 Thermal analysis of Solar Collector (on Double Glass and Single Plate)

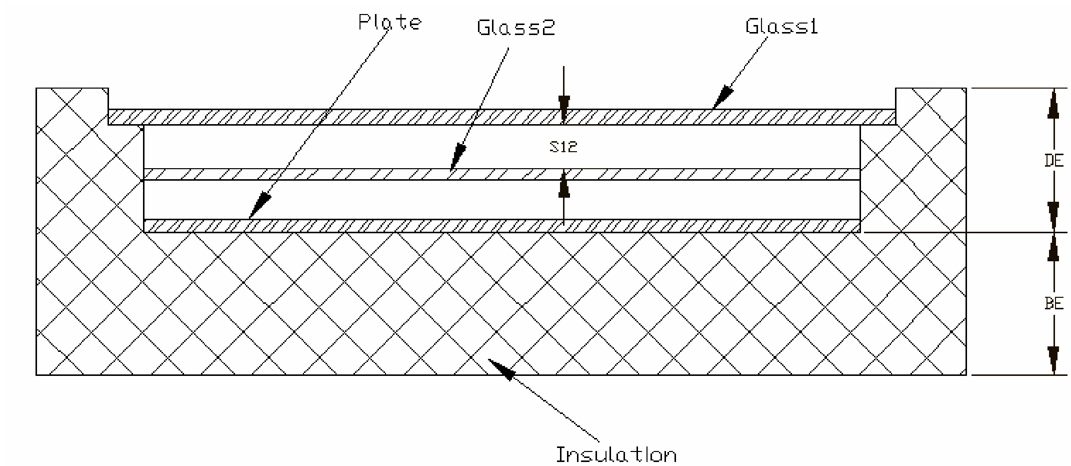

Figure 5-2: Solar Collector with Double Glass and Single Plate

Energy balanced on the absorber plate, the air stream and the glass cover are performed based on the thermal circuit indicated in Figure 5-2.

Energy balance for the **absorber plate:**

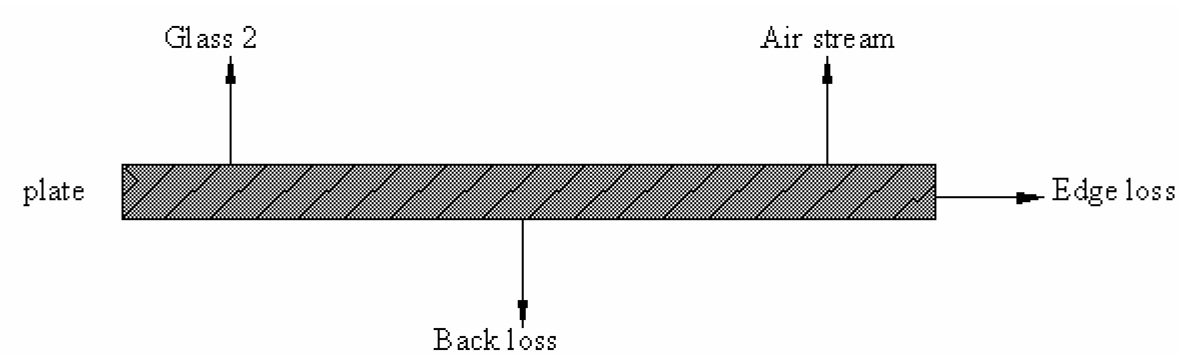

$$(mc_p)_p \frac{dT_p}{dt} = A_c I_c \tau_c - A_c U_{pg2}\left[T_p - T_{g2}\right] - A_c U_a \left[T_p - \frac{T_{ai} + T_{ao}}{2}\right] - A_c U_{pab}\left[T_p - T_a\right] -$$

$$A_1 U_{pae}\left[\frac{T_p + T_a}{2} - T_a\right]$$

$$T_{p1} = T_{p0} + \frac{A_c I_c \tau_c}{(mc_p)_p}\Delta t - \frac{A_C U_{pg2}}{(mc_p)_p}\left[T_{p0} - T_{g20}\right]\Delta t - \frac{A_c U_a}{(mc_p)_p}\left[T_{p0} - \frac{T_{ai0} + T_{ao0}}{2}\right]$$

$$\Delta t - \frac{A_c U_{pab}}{(mc_p)_p}\left[T_{p0} - T_{a0}\right]\Delta t - \frac{A_1 U_{pae}}{(mc_p)_p}\left[\frac{Tp0 + Ta0}{2} - Ta0\right]\Delta t \quad \textbf{(5-22)}$$

For the **trapped air**:

$$(mc_p)_a \frac{dT_{ao}}{dt} = A_c U_a \left[T_{g2} - \frac{T_{g1} + T_{g2}}{2}\right] - A_c U_a \left[\frac{T_{ai} + T_{ao}}{2} - T_{g1}\right]$$

$$T_{a1} = \left(1 - \frac{\Delta t}{(mc_p)_a}\left(A_c U_a + A_1 U_a\right)\right) T_{ao0} + \frac{\Delta t}{(mc_p)_a}\left(-A_c U_a - A_1 U_a\right) T_{ai0} +$$

$$\frac{A_c U_a}{(mc_p)_a} T_{g10}\Delta t + \frac{A_c U_a}{(mc_p)_a} T_{g20}\Delta t + \frac{A_1 U_a}{(mc_p)_a} T_{a0}\Delta t \quad \textbf{(5-23)}$$

Energy balance for **air stream:**

$$(mc_p)_a \frac{dT_{ao}}{dt} = A_c U_a \left[T_p - \frac{T_{ai} + T_{ao}}{2}\right] - A_c U_a \left[\frac{T_{ai} + T_{ao}}{2} - T_{g2}\right] - (\dot{m}c_p)_a \left[T_{ao} - T_{ai}\right]$$

$$T_{ao1} = Tao0 + \frac{A_c U_a}{(mc_p)_p}\left(T_{p0} - \frac{T_{ai0} + T_{ao0}}{2}\right)\Delta t - \frac{A_c U_a}{(mc_p)_a}\left(\frac{T_{ai0} + T_{ao0}}{2} - T_{g20}\right)\Delta t$$

$$- \frac{(\dot{m}c_p)_a}{(mc_p)_a}\left(T_{ao0} - T_{ai0}\right) \quad \textbf{(5-24)}$$

Energy balance for the **first Glass:**

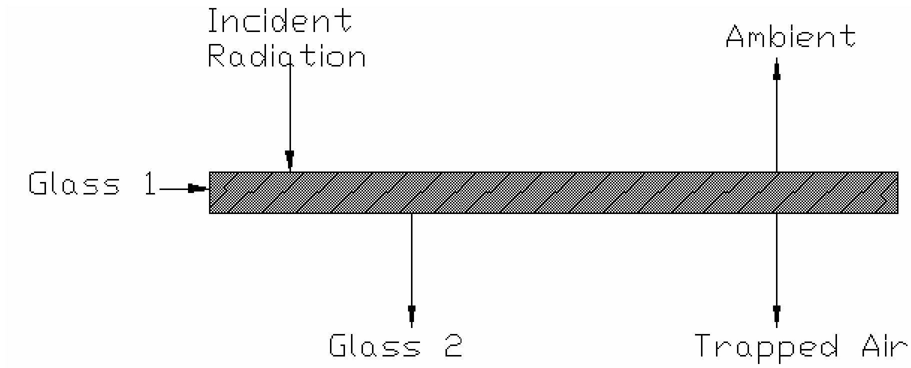

$$\left(mc_p\right)_g \frac{dT_{g1}}{dt} = A_c I_N \alpha_c - A_c U_{g1g2}\left(T_{g1} - T_{g2}\right) - A_c U_a \left(T_{g1} - T_a\right) - A_c U_{g1f1}\left(T_{g1} - \frac{T_{g1} + T_{g2}}{2}\right)$$

$$T_{g11} = T_{g10} + \frac{A_c I_c \alpha_c \Delta t}{\left(mc_p\right)_g} - \frac{A_c U_{g1g2}}{\left(mc_p\right)_g}\left(T_{g10} - T_{g20}\right)\Delta t - \frac{A_c U_{g1a}}{\left(mc_p\right)_g}\left(T_{g10} - T_{a0}\right)\Delta t - \frac{A_c U_a}{\left(mc_p\right)_g}\left(T_{g10} - \frac{T_{g10} + T_{g20}}{2}\right)\Delta t \qquad \textbf{(5-25)}$$

For Second **Glass cover**:

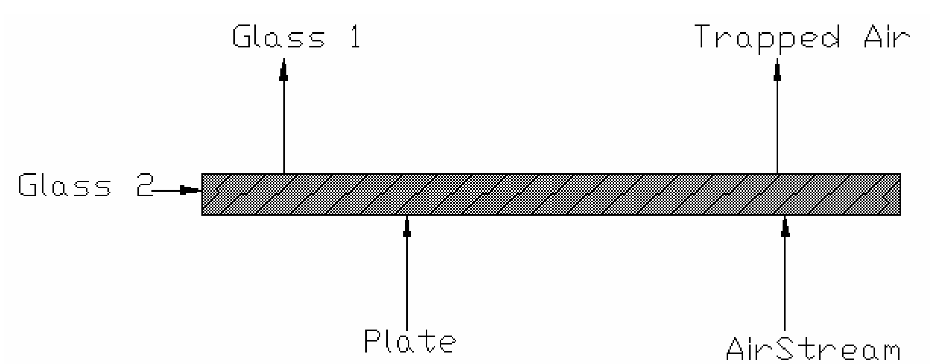

$$\left(mc_p\right)_g \frac{dT_{g2}}{dt} = A_c I_N \alpha_c \tau_c + A_c U_{pg2}\left[T_p - T_{g2}\right] - A_c U_{g2f1}\left[T_{g2} - \frac{T_{g1} + T_{g2}}{2}\right] - U_{g2f2} A_c \left(T_{g2} - \frac{T_{ao} + T_{ai}}{2}\right) - U_{g1g2} A_c \left(T_{g2} - T_{g1}\right)$$

$$T_{g21} = \frac{A_c I_N \alpha_c \tau_c \Delta t}{\left(mc_p\right)_g} + T_{g20} - \frac{A_c U_{pg2}}{\left(mc_p\right)_g}\left(T_{p0} - T_{g20}\right)\Delta t - \frac{A_c U_{g2f1}}{\left(mc_p\right)_g}\left(T_{g20} - \frac{T_{g10} + T_{g20}}{2}\right)\Delta t - \frac{U_{g2f2} A_c}{\left(mc_p\right)_g}\left(T_{g20} - \frac{T_{aoo} + T_{aio}}{2}\right)\Delta t - \frac{U_{g1g2} A_c}{\left(mc_p\right)_g}\left(T_{g20} - T_{g10}\right)\Delta t \qquad \textbf{(5-26)}$$

5.2.3 Energy Balance Equation

In steady state, the performance of a flat-plate solar collector can be described by the useful gain from the collector, Q_u which is defined as the difference between the absorbed solar radiation and the thermal loss or the useful energy output of a collector [12]:

$$Q_u = \left[A_p S - A_c U_L \left(T_p - T_a\right)\right]^+ \qquad \textbf{(5-27)}$$

where: A_c = the gross area of the collector, [m^2]

A_p = aperture area of the collector, [m^2]

The first term is the absorbed solar energy and the second term represents the heat loss from the collector. The solar radiation absorbed by a collector per unit area of absorber S can be calculated using the optical properties of covers and a plate. The thermal energy loss from the collector to the surroundings can be represented as the product of a heat transfer coefficient U_L times the difference between the mean absorber plate temperature T_p and the ambient temperature T_a. The + superscript indicates that only positive values of the terms in the square brackets are to be used. Thus, to produce useful gain greater than zero the absorbed radiation must be greater than the thermal losses. Two collector areas appear in Equation (5-27); gross collector area A_c is defined as the total area occupied by a collector and the aperture collector area A_p is the transparent frontal area. ASHRAE Standard employs the gross area as a reference collector area in the definition of thermal efficiency of the collector. The useful gain from the collector based on the gross collector area becomes:

$$Q_u = A_c\left[S_c - U_L\left(T_p - T_a\right)\right]^+ \quad \textbf{(5-28)}$$

S_c is the absorbed solar radiation per unit area based on the gross collector area, defined as:

$$S_c = S\times\left(\frac{A_p}{A_c}\right) \quad \textbf{(5-29)}$$

Since the radiation absorption and heat loss at the absorber plate is considered based on the aperture area, it is convenient to make the aperture collector area the reference collector area of the useful gain. Then Equation (5-27) becomes:

$$Q_u = A_p\left[S - U'_L\left(T_p - T_a\right)\right]^+ \quad \textbf{(5-30)}$$

U'_L is the overall heat loss coefficient based on the aperture area given by:

$$U'_L = U_L \times\left(\frac{A_c}{A_p}\right) \quad \textbf{(5-31)}$$

5.2.4 Solar Radiation Absorption

The prediction of collector performance requires knowledge of the absorbed solar energy by the collector absorber plate. The solar energy incident on a tilted collector consists of three different distributions: beam radiation, diffuse radiation, and ground-reflected radiation. The details of the calculation depend on which diffuse-sky model is used. In this thesis the absorbed radiation on the absorber plate is calculated by isotropic sky model [12]:

$$I_N = I_b R_b (\tau\alpha)_b + I_d (\tau\alpha)_d \left(\frac{1+\cos\beta}{2}\right) + (I_b + I_d)(\tau\alpha)_g \rho_g \left(\frac{1+\cos\beta}{2}\right) \quad \textbf{(5-32)}$$

where: b, d, and g = beam, diffuse, and ground-reflected radiation, Respectively,

I = intensity of radiation on a horizontal surface,

$(\tau\alpha)$= the transmittance absorptance product that represents the effective absorptance of the cover-plate system,

β =the collector slope,

ρ_g = is the diffuse reflectance of ground and

The geometric factor R_b is the ratio of beam radiation on the tilted surface to that on a horizontal surface. This section treats the way to calculate the transmittance-absorptance product of beam, diffuse, ground-reflected radiation for a given collector configuration and specified test conditions.

5.2.5 Equivalent Angles of Incidence for Diffuse Radiation

In the present sky radiation model, the radiation incident on a collector consists of beam radiation from the sun, diffuse solar radiation that is scattered from the sky, and ground-reflected radiation that is diffusely reflected from the ground. While the preceding analysis can be applied directly to beam contribution, the transmittance of cover systems for diffuse and ground-reflected radiation must be calculated by integrating the transmittance over the appropriate incidence angles with an assumed sky model. The calculation can be simplified by defining equivalent angles that give the same transmittance as for diffuse and ground-reflected radiation. Brandemuehl and Beckman have performed the integration of the transmittance over the appropriate incident angle with an isotropic sky model and suggested the equivalent angle of incidence for diffuse radiation:

$$\theta_{d,e} = 59.7 - 0.1388\beta + 0.001497\beta^2 \quad \textbf{(5-33)}$$

where: β = the tilted angle of solar collector, [degree]

5.2.6 Heat Loss from the Collector

In solar collectors, the solar energy absorbed by the absorber plate is distributed to useful gain and to thermal losses through the top, bottom, and edges. In this section the equations for each loss coefficient are derived for a general configuration of the collector. The semi-gray model is employed for radiation heat transfer.

5.2.7 Collector Overall Heat Loss

Heat loss from a solar collector consists of top heat loss through cover systems and back and edge heat loss through back and edge insulation of the collector. With the assumption that all the losses are based on a common mean plate temperature T_p, the overall heat loss from the collector can be represented as [12]:

$$Q_{loss} = U_L A_c (T_p - T_a) \qquad \textbf{(5-34)}$$

where: U_L= the collector overall loss coefficient, [W, m^{-2}]

The overall heat loss is the sum of the top, back, and edge losses:

$$Q_{loss} = Q_t + Q_b + Q_e \qquad \textbf{(5-35)}$$

If the thickness of the edge neglected the Equation (5-35) will be:

$$Q_{loss} = Q_t + Q_b \qquad \textbf{(5-36)}$$

where the subscripts t, b, and e represent for the top, back, and edge contribution, respectively.

5.2.8 Top Heat Loss through the Cover System

To evaluate the heat loss through the cover systems, all of the convection and radiation heat transfer mechanisms between parallel plates and between the plate and the sky must be considered as shown in Figure 5-3. The collector model have up to two covers in case of plastic covers that are partially transparent to infrared radiation the direct radiation exchange between the plate and sky through the cover system must be considered while it is neglected for the glass covers since glass is opaque to infrared radiation. Whillier has developed equations for top loss coefficients for the collector cover system using radiation heat transfer coefficients. In this study the net radiation method is applied to obtain the expression for the heat loss for the general cover system of flat-plate solar collectors.

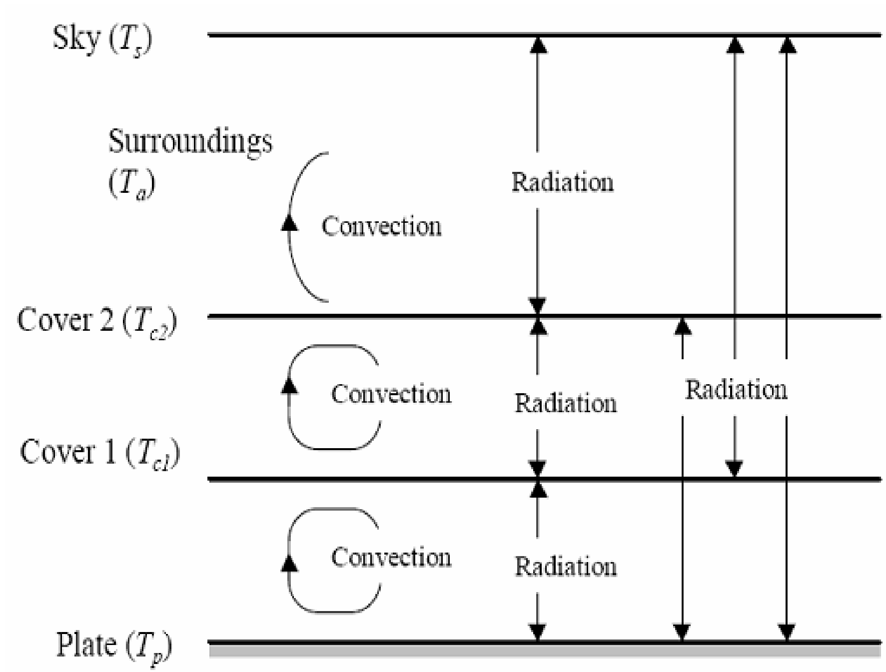

Figure 5-3: Heat Transfer Mechanisms through a Cover System with Two Covers.

5.2.9 Wind Convection Coefficient

Wind convection coefficient h_w represents the convection heat loss from a flat plate exposed to outside winds. It is related to three dimensionless parameters, the Nusselt number Nu, the Reynolds number Re, and the Prandtl number Pr, that are given by:

$$Nu = \frac{h_w L_e}{\kappa}, \qquad Re = \frac{V L_e}{\upsilon}, \qquad Pr = \frac{\upsilon}{\alpha} \qquad \textbf{(5-37)}$$

where: L_e =the characteristic length is four times the plate area divided by the plate perimeter, (m)

V= wind speed, [m, s^{-1}]

K= the thermal conductivity, [W, m^{-1}, ^0K]

υ = kinematic viscosity, [m^2, s^{-1}]

α=thermal diffusivity of air

For free standing collectors, Duffie and Beckman suggest that the wind convection coefficient be calculated using the correlation of Sparrow over the Reynolds number range of $2*10^4$ to $9*10^4$:

$$Nu = 0.86 Re^{0.5} Pr^{1/3} \qquad \left(2x10^4 < Re < 10^6\right) \qquad \textbf{(5-38)}$$

For laminar flow, the correlation of Pohlhausen is used:

$$Nu = 0.86 Re^{0.5} Pr^{1/3} \qquad \left(Re < 2x10^4\right) \qquad \textbf{(5-39)}$$

5.2.10 Natural Convection between Parallel Plates

For the prediction of the top loss coefficient, the evaluation of natural convection heat transfer between two parallel plates tilted at some angle to the horizontal is of obvious importance. The natural convection heat transfer coefficient hc is related to three dimensionless parameters, the Nusselt number Nu, the Rayleigh number Ra, and the Prandtl number Pr, that are given by:

$$Nu = \frac{h_c L}{\kappa}, \qquad Ra = \frac{g\beta_\upsilon \Delta T L^3}{\upsilon\alpha}, \qquad Pr = \frac{\upsilon}{\alpha} \qquad \textbf{(5-40)}$$

where: L=the plate spacing, [m]

g= the gravitational constant, [m, S^{-2}]

ΔT = the temperature difference between plates, [^0C] and

β_v = the volumetric coefficient of expansion of air.

The relationship between the Nusselt number and Rayleigh number for tilt angle β from 0 to 75^o as:

$$Nu = 1 + 1.44\left[1 - \frac{1708[\sin(1.8\beta)]^{1.6}}{Ra\cos\beta}\right]\left[1 - \frac{1708}{Ra\cos\beta}\right]^{+} + \left[\left(\frac{Ra\cos\beta}{5830}\right)^{1/3} - 1\right]^{+} \quad \textbf{(5-41)}$$

5.2.11 Back and Edge Heat Loss

The energy loss through the back of the collector is the result of the conduction through the back insulation and the convection and radiation heat transfer from back of the collector to surroundings. Since the magnitudes of the thermal resistance of convection and radiation heat transfer are much smaller than that of conduction, it can be assumed that all the thermal resistance from the back is due to the insulation. The back heat loss, Q_b, can be obtained from [12]:

$$Q_b = \frac{k_b}{L_b} A_c \left(T_p - T_a\right) \quad \textbf{(5-42)}$$

where: k_b = the back insulation thermal conductivity, [W, m^{-1},^{o}K^{-1}]

L_b= the back thickness, [m]

T_p=plate temperature, [^{0}C]

T_a=ambient temperature, [^{0}C]

While the evaluation of edge losses is complicated for most collectors, the edge loss in a well-constructed system is intended to be so small that it is not necessary to predict it with great accuracy. With the assumption of one-dimensional sideways heat flow around the perimeter of the collector, the edge losses can be estimated by [12]:

$$Q_e = \frac{k_e}{L_e} A_e \left(T_p - T_a\right) \quad \textbf{(5-43)}$$

where: k_e= the edge insulation thermal conductivity

L_e= the edge insulation thickness, [m]

A_e=the edge area of the collector, [m^2]

5.2.12 Overall Heat Loss Coefficient

The overall loss coefficient U_L based on the gross collector area can be calculated from Equation (5-35) with the known values of the overall heat loss Q_{loss} and the plate temperature T_p. To derive an expression for the mean temperature of the absorber plate, it is necessary to know the overall heat loss coefficient based on the absorber area. Since of heat transfer coefficient-area product is constant, it can be calculated from [12]:

$$U_t = \left[\frac{N}{\frac{C}{T_p}\left[\frac{T_p - T_a}{N+f}\right]^e} + \frac{1}{h_w} \right]^{-1} + \frac{\delta\left(T_p^2 - T_a^2\right)\left(T_p + T_a\right)}{\frac{1}{d} + \frac{2N + f - 1}{\varepsilon_g} - N} \quad \textbf{(5-44)}$$

where: N = number of glass covers $1 \le N \le 3$

$f = (1 + 0.04 h_w + 0.0005 h_w{}^2)(1 + 0.091 N)$

$C = 365.9(1 - 0.00883\beta + 0.0001298\beta^2) \quad 0^0 \le \beta \le 90^0$

β = collector tilt (degrees)

ε_g = emittance of glass

ε_p = emittance of plate $0.1 \le \varepsilon_p \le 0.95$

T_a = ambient temperature

T_p = plate temperature

h_w = wind heat transfer coefficient (W/m2 °C)

$0 \le h_w \le 10 m \sec^{-1}$

If the wind velocity is V (m/sec), then:

$$h_w = 5.7 + 3.8V \quad \textbf{(5-45)}$$

5.2.13 The Bottom Heat Loss Coefficient

Energy dissipation from the bottom of the collector is the collective effect of conduction from the absorbing surface to the insulator at the bottom and convection and radiation from the outside wall to the ambient surroundings. Thermal loss coefficient from the bottom could be calculated as follows [12]:

$$U_b = \frac{1}{\frac{x_i}{K_i} + \frac{X_w}{K_w} + \frac{1}{h_w}} \quad \textbf{(5-46)}$$

The magnitude of h_w is very large then the inverse of it will be negligible the equation (5-46):

$$U_b = \frac{K_i}{X_i} \quad \textbf{(5-47)}$$

where: K_i=thermal conductivity of the insulation, [W, m^{-1}, ^0K]

X_i=the thickness of the insulation, [m]

5.2.14 The Edge Heat Loss Coefficient

The edge loss coefficient depends on the area of the solar collector and this loss is very small if compared with the losses from top and bottom of the solar collector. The edge loss coefficient is given by the following equation:

$$U_e = 0.45(D \times P)\frac{A_e}{A_c} \qquad \textbf{(5-48)}$$

The total heat loss coefficient is given by the following:

$$U_L = U_t + U_b + U_e \qquad \textbf{(5-49)}$$

Assume the thickness of the insulation on the edge and back is the same the above equation becomes ($U_b = U_e$):

$$U_L = U_t + 2U_b \qquad \textbf{(5-50)}$$

5.2.15 Thermal Insulation

Flat-plate collectors must be insulated to reduce conduction and convection losses through the back and sides of the collector box. The insulation material should be dimensionally and chemically stable at high temperatures, and resistant to weathering and dampness from condensation. Usually, glass-wool insulation 10 cm thick is recommended. It would be between if the insulation also could contribute to the structural rigidity of the collector, but more rigid insulating materials are often less stable than glass-wool. Temperatures in flat-plate solar collectors can be high enough to melt some foam insulations, such as Styrofoam. And some foam give off corrosive frames at high temperatures which could damage the absorber plate [12].

Chapter 6

6.1 Drying Bed

Cereals are generally harvested at moisture level ranging from 16-30% wet basis (w.b) and must be dried to approximately 10-12% moisture level (w.b) to be suitable for storage. It is essential to minimize the development of fissures during drying which may from due to excessive moisture and temperature gradients. Fissures lead to broken grains during milling and reduce the milled cereal yield [6].

The efficiency of drying systems can be improved by the analysis of the drying process. Analysis of drying systems can be greatly expedited by using computer simulation.

Heat and mass transfer take place during drying of cereals. Heat is transferred from the drying air to the liquid water vapor in the grain. Mass is transferred in the form of internal moisture and evaporated liquid. Drying is a continuous process where the moisture content, air and cereal temperature and the humidity of the air all changes simultaneously [5].

The general equation of the moisture-time relation proposed by Newman can be represented by the first term:

$$M_r = Ae^{-akt} + Be^{-bkt} + Ce^{-ckt} \qquad \textbf{(6-1)}$$

where: M_r=moisture ratio, [decimal]

K= drying constant, [sec^{-1}]

t=time, [sec]

A, B, a, b, C, etc= characteristic constants of the drying product

Newman observed that the series converges rapidly and after a period of time represented by the first term

$$M_r = e^{-kt} \quad \textbf{(6-2)}$$

Lewis determined a relationship similar to equation above that is analogous to Newton's law of cooling. He suggested that the rate of removal of moisture from a product was proportional to the difference between the average moisture content (M) and the equilibrium moisture content (M_e) of the product and could be expressed as [27]:

$$\frac{dM}{dt} = k(M - M_e) \quad \textbf{(6-3)}$$

This equation is commonly known as the exponential or logarithmic model. If the constant "A" is equal to unity, the equation is reduced to the same form as the Newton's law of cooling model.

A single-term solution of the diffusion equation in spherical coordinate is a very common way to calculate the drying rate grains. This single term solution is good approximation of the diffusion series as it converges rapidly and is mathematically represented as [5]:

$$M_r = \left(\frac{6}{\Pi^2}\right) e^{-kt} \quad \textbf{(6-4)}$$

where: M_r=moisture ratio

M_f=moisture at time t, [%] (d.b.)

M_{eq}=equilibrium moisture content, [%] (d.b)

This single term solution is analogous to Newton's law of cooling, where it is assumed that the rate of moisture removal is proportional to the difference between the kernel moisture and equilibrium moisture content. Expressed mathematically as [27]:

$$\frac{dM}{dt} = -k\left(M - M_{eq}\right) \quad \textbf{(6-5)}$$

Integration gives $M_r = \dfrac{M_f - M_{eq}}{M_o - M_{eq}} = \exp^{-kt}$

$$M_f = \left(M_0 - M_{eq}\right)e^{-kt} + M_{eq} \tag{6-6}$$

$$K = 139.3\exp\left(\frac{-7676}{((1.8T)+492)}\right) \tag{6-7}$$

where: T is temperature of the air, [^oC]

The deep- bed of grain was assumed to consist of a series of thin layers positioned normal to the direction of air flow in the bed. No heat transfer was considered the bin wall. Drying air passed through a thin layer of grain for a drying time interval. During this interval the moisture evaporated from the grain in to the air increasing its absolute humidity. The grain temperature of the cereals and the evaporative cooling due to the temperature drop of the drying air.

6.1.1 Drying Air Temperature

This temperature is the equilibrium temperature of the drying air and the grains. Thompson et al. proposed a drying temperature based on sensible heat balance between the air and grain at each layer where the drying takes place to calculate this temperature. The heat balance equation is [5]:

$$\begin{aligned} &1.005T_0 + H_0\left(2467.4 + 1.884T_0\right) + Cp_G T_{G0} = 1.005T_e \\ &+ H_0\left(2467.4 + 1.884T_e\right) + Cp_G T_e \end{aligned} \tag{6-8}$$

From the equation (6-8)

$$T_e = \frac{\left(1.005 + 1.884H_0\right)T_0 + Cp_G T_{G0}}{1.005 + 1.884H_0 + Cp_G} \tag{6-9}$$

where: T_0=initial temperature, [^ok]

T_e=equilibrium temperature of cereals, [^ok]

H_0=initial humidity ratio of air, [decimal]

Cp_G=specific heat of cereals, [J, kg^{-1}, k^{-1}]

T_{G0}=initial grain temperature, [^ok]

6.1.2 Final Air Temperature and Grain Temperature

After calculating the moisture loss using Equation (6-6) for each layer during a time interval, the absolute humidity of the drying air was increased by an amount [5]:

$$\Delta H = H_f - H_0 = \frac{(M_0 - M_f)R}{100} \quad \textbf{(6-10)}$$

where: H_f =final air humidity ratio, [kg/kg]

M_0 = initial moisture content of cereals, [%] (d.b.)

M_f = final moisture content of cereals, [%] (d.b.)

R = cereal dry matter to air ratio

$$R = \frac{D_m}{m_a \times t} \quad \textbf{(6-11)}$$

where: D_m=cereal dry matter in each layer, [kg]

M_a=air mass flow rate, [kg, min^{-1}]

t=time step for simulation, [min]

The final temperature (T_f) of the air and grain respectively can be determined with the following heat balance based on the approach of Thompson et al:

$$m_a C_{pa}(T_i - T_{i+1}) = m_w h_{fg} \quad \textbf{(6-12)}$$

where: m_a = mass of the dry air through the drying bed, [kg]

C_{pa} = Specific heat of the drying air, [J, kg^{-1}, k^{-1}]

T_i = temperature of the air, [^oC] and i=1, 2, 3, 4

m_w = mass of water removed per kg of air, [kg]

h_{fg} = latent heat of vaporization, [KJ,kg^{-1}]

Therefore:

$$T_2 = T_1 - \left(\frac{m_w \times h_{fg}}{m_a C_{pa}} \right) \quad \textbf{(6-13)}$$

where: m_a = mass of the dry air through the drying bed, [kg]

C_{pa} = Specific heat of the drying air, [J, kg^{-1}, k^{-1}]

T_1 = temperature of the air entering to the bed or exit from the collector, [^{o}C]

T_2 = temperature of the air entering to the second chamber or exit from the first chamber, [^{o}C]

m_w = mass of water removed per kg of air, [kg]

h_{fg} = latent heat of vaporization, [KJ,kg^{-1}]

$$m_g C_{pg} \left(T_{i+1} - T_i \right) = m_w h_{fg} \quad \textbf{(6-14)}$$

where: m_a = mass of the grain in the drying bed, [kg]

C_{pg} = Specific heat of the drying grain, [J, kg^{-1}, k^{-1}]

T_i = temperature of the grain, [^{o}C] and i=1, 2, 3, 4

m_w = mass of water removed per kg of air, [kg]

h_{fg} = latent heat of vaporization, [KJ,kg^{-1}]

$$T_{2g} = T_{1g} + \left(\frac{m_w \times h_{fg}}{m_g C_{pg}} \right) \quad \textbf{(6-15)}$$

where: m_g = mass of grain in the drying bed, [kg]

C_{pg} = Specific heat of grain, [J, kg^{-1}, k^{-1}]

T_{1g} = temperature of grain in the first bed at time 1, [^oC]

T_{2g} = temperature of grain in the first bed at time i+1, [^oC]

m_w = mass of water removed per kg of air, [kg]

h_{fg} = latent heat of vaporization, [KJ,kg^{-1}]

$$m_w = m_g\left(\frac{M_0 - M_f}{100 - M_f}\right) \quad \textbf{(6-16)}$$

where: Mo=initial moisture content of grain, [%]

Mf=final moisture content of grain, [%]

mg=mass of grain in one layer of the bed, [%]

$$h_{fg} = 2502535.259 - 2385.76424T \quad \textbf{(6-17)}$$

where: hfg = latent heat of vaporization, [J,kg-1]

Ti = temperature of the air, [oC]

$$RH = \frac{P_{v_i}}{P_{vs}} x100 \quad \textbf{(6-18)}$$

where: $P_{v_i} = 6.11*10.0**(7.5*T_{dc}/(237.7 + T_{dc}))$

$P_{vs} = 6.11*10.0**(7.5*T_c/(237.7 + T_c))$

RH= relative humidity, [%]

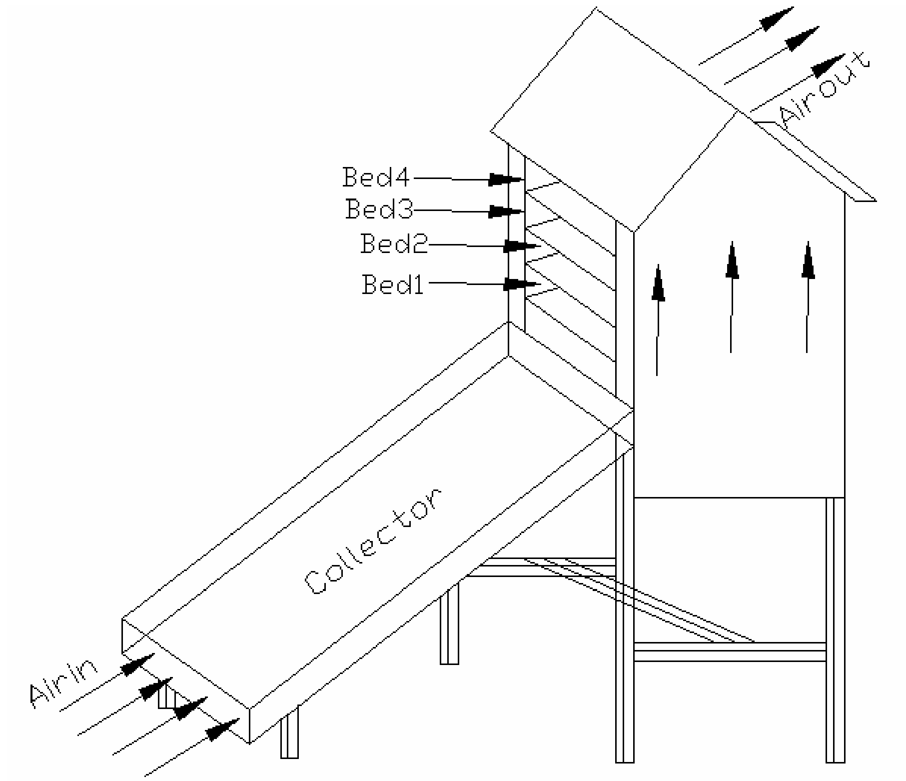

Figure 6-1: Illustration of a Deep Bed of the Thesis.

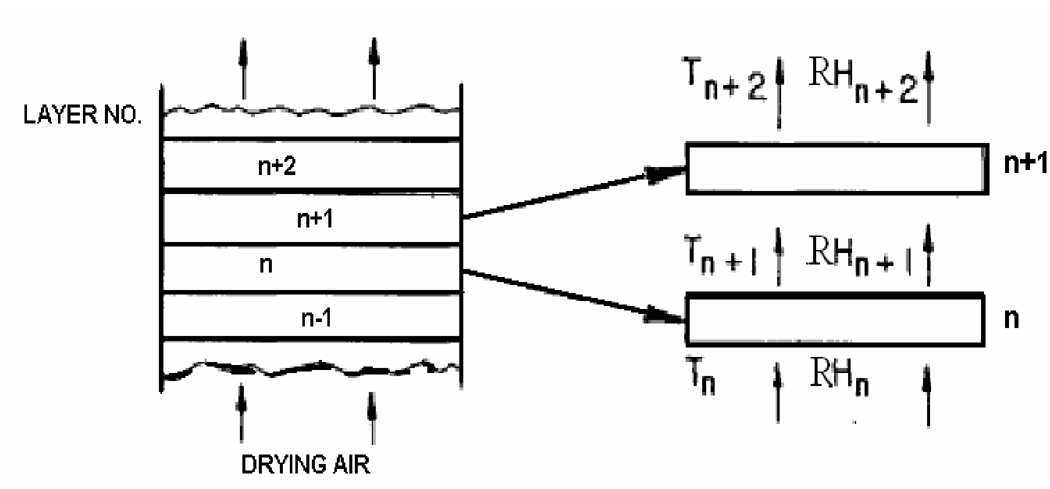

Figure 6-2: Illustration of a Deep Bed as a series of Thin Layers.

(T and H are temperature and humidity ratio of drying air, respectively. Subscripts n, n + 1, and n + 2 represent the corresponding grain layer.)

Table 2: Grain and Air Properties for Comparative Simulations

Parameters	Values	Units
Air inlet Temperature	Time dependent and out from the collector	^{o}C
Initial Grain Moisture content	0.28	decimal
Initial Grain temperature	Ambient temperature from metrology	^{o}C
Airflow rate	Output from collector(time dependant)	$Kg\ hr^{-1}$
Bulk density of grain	603	Kg/m^3
Specific heat capacity of dry air	1005	$J\ Kg^{-1}\ K^{-1}$
Specific heat capacity of dry grain	1298	$J\ Kg^{-1}\ K^{-1}$
Equilibrium moisture content	0.16	decimal
Volume of dryer bed	0.1	m^3
Collector area	2	m^2

7.1 Result and Discussion

Using the procedures discussed in the previous chapter and connections of the solar dryer project shown in Figure 6-3 to Figure 6-8, outputs of the TRNSYS simulation results are discussed in this chapter.

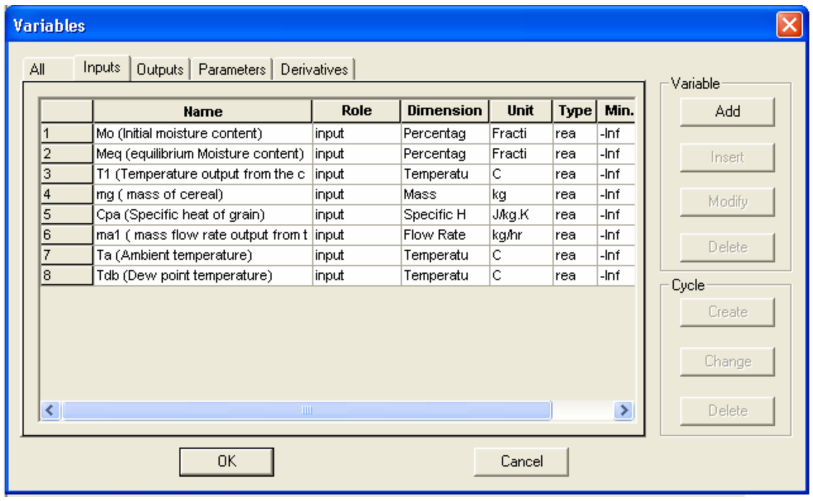

Figure 6-3: Input Parameters for the Drying Beds

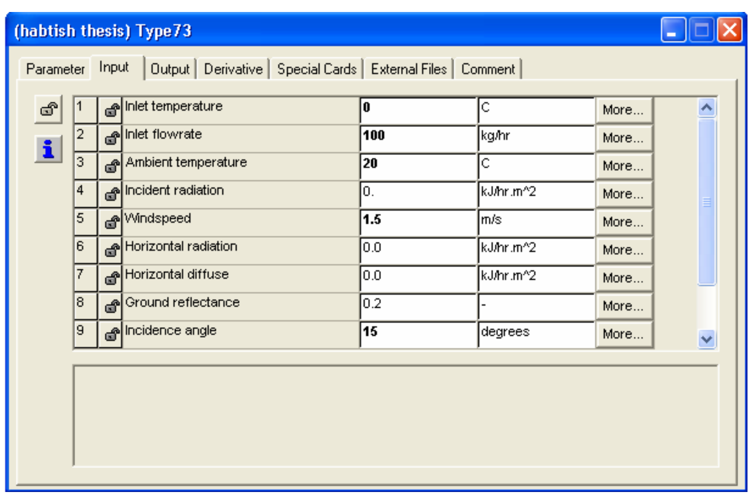

Figure 6-4: Input Parameters for the Collectors

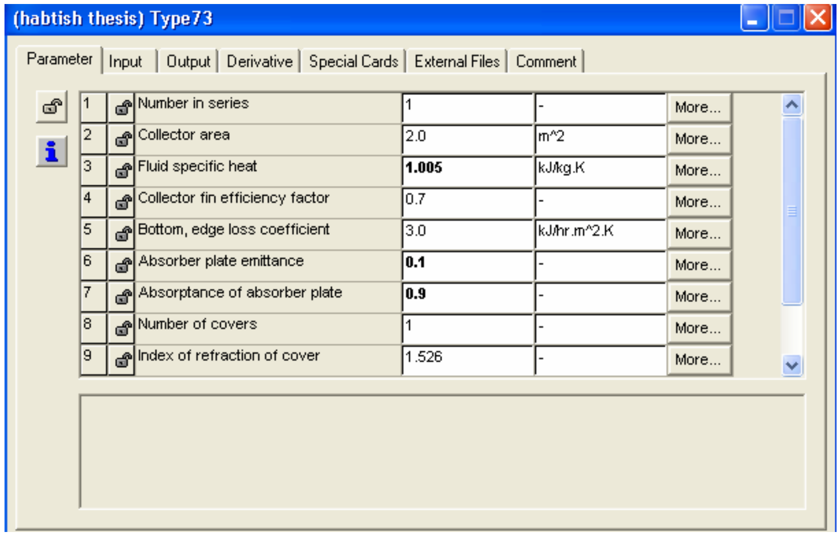

Figure 6-5: Parameters for the Collectors

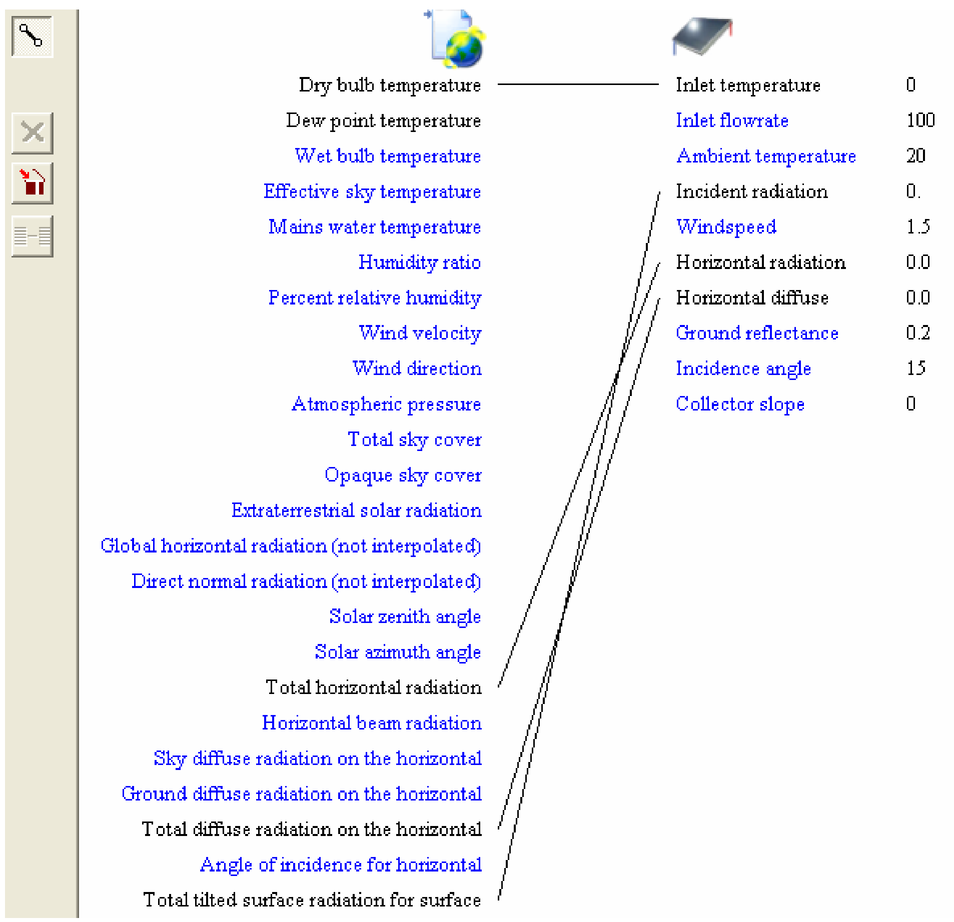

Figure 6-6: Connection of the Whether Data and Input of Collectors

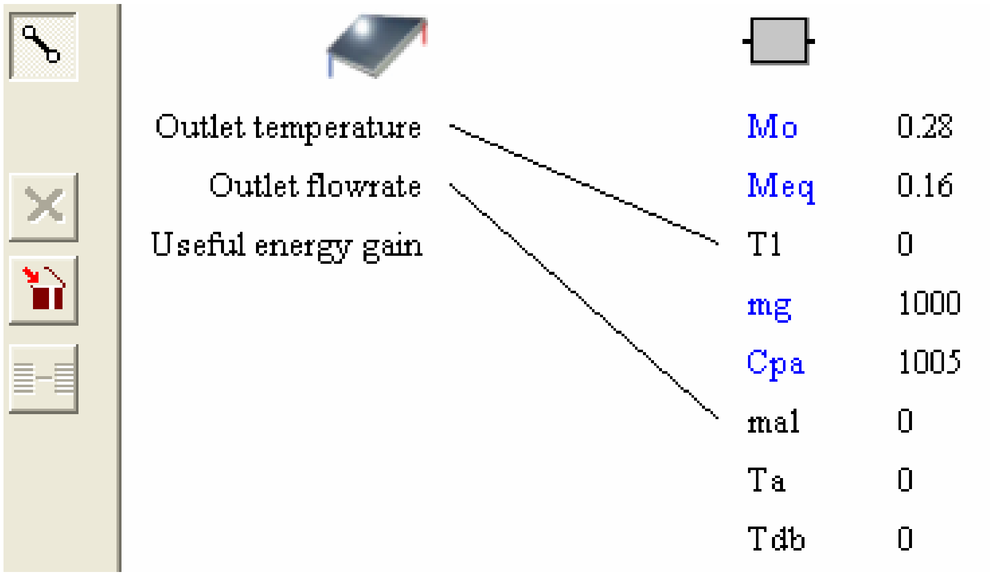

Figure 6-7: Connection of the Collectors Output and Input of the Drying Bed

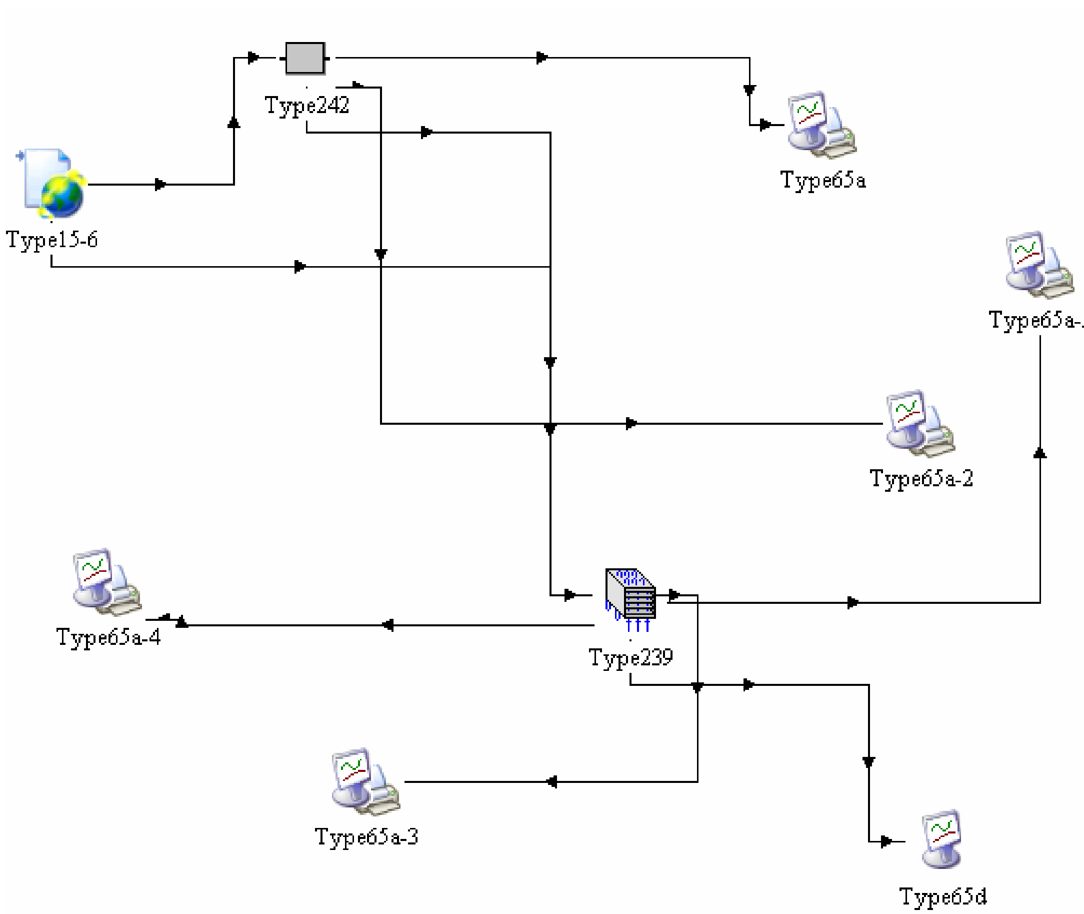

Figure 6-8: Constructing the Drying Project

Figure 6-9 shows the moisture content of cereals as a function of the drying time. As may be expected, bed 1, (the one placed nearer to the hot air), exhibits the most rapid drying.

These moisture contents indicate that the first bed reached the equilibrium moisture content at the middle of the first day. The advantages are the protection against direct sunshine, dust, and insects.

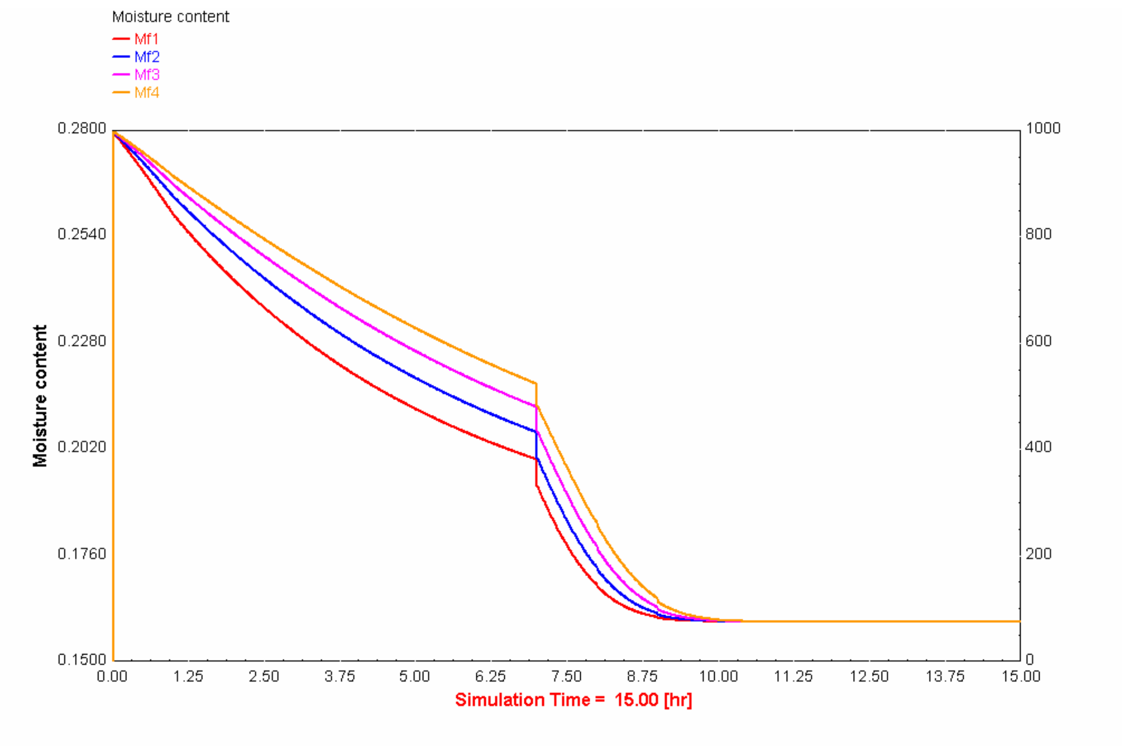

Figure 6-9: Moisture Content Curves for Barley in Solar Dryer

Figure 6-10 displays the variation of air temperature with vertical distance from the bottom of the drying chamber. The maximum temperature is found around 14:00 PM. A major drawback of the dryer is the uneven drying: As a result of the migration of the drying front, the materials at the entrance are dried, while at the exhaust are under-dried. This problem can be alleviated by rotating the drying beds. In such a rotating operation, the hot air from the collector is used to heat the product already in the latter stages of drying (falling rate period), while the unsaturated air is used to remove moisture from product in the upper beds.

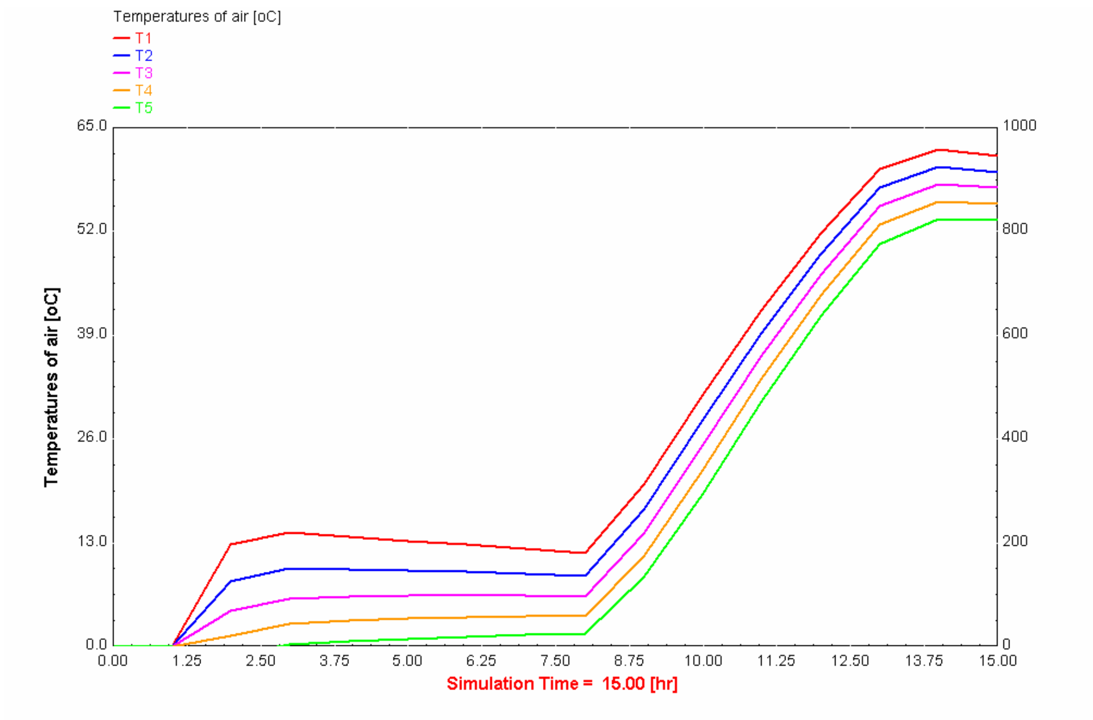

Figure 6-10: Temperature Distribution in the Vertical direction from the Bottom of the Drying Chamber

Figure 6-11 displays the variation of water removed from the cereals with vertical distance from the bottom of the drying chamber. As the Figure 6-11 shows the water vapor removed from the particle increases as the temperature increase up to the time where the air is saturated after this there is no vapor remove from the particle or it becomes constant after the saturation of the air.

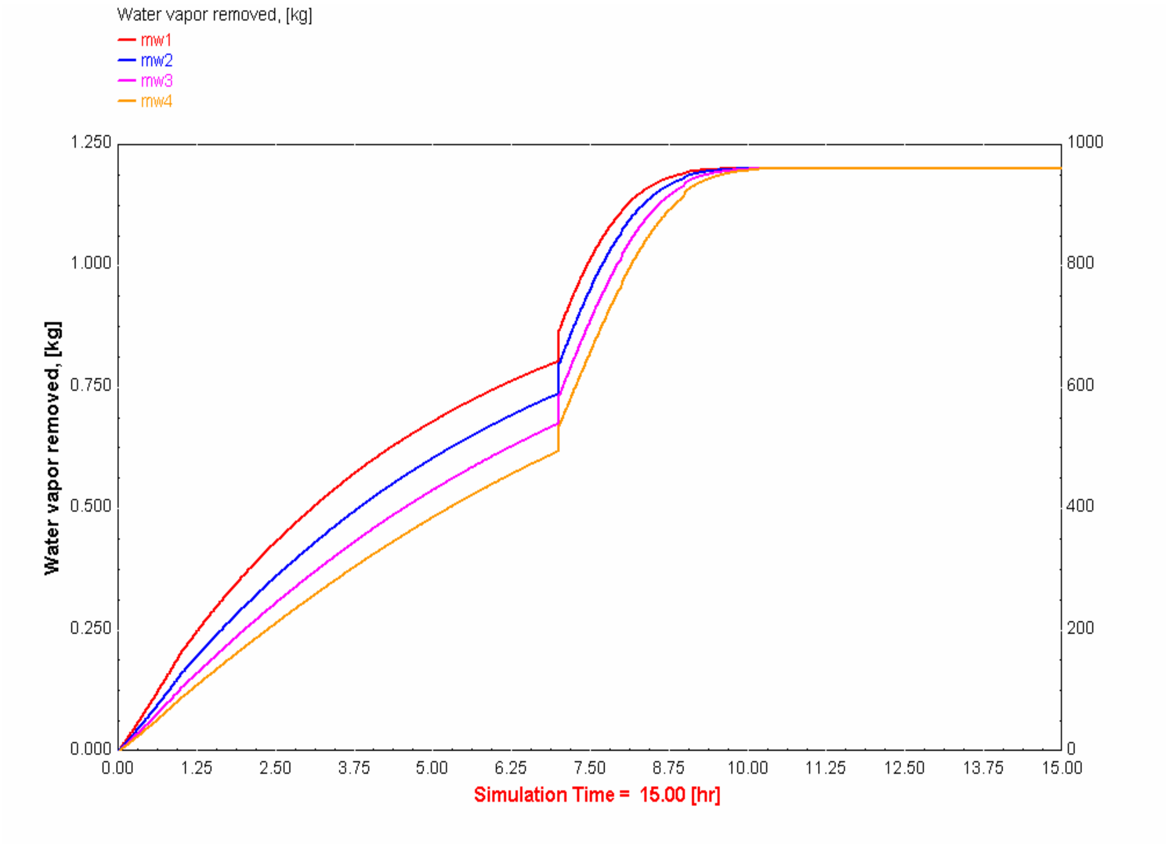

Figure 6-11: Water Removed from Cereals for the Four Drying Beds

Figure 6-12 and Figure 6-19 displays the variation of moisture content of the cereals and the temperature of the drying air with vertical distance from the bottom of the drying chamber. As shown in the Figure 6-12 the moisture content decreases as the temperature increase up to the time at which dry air temperature is saturated with moisture, after this the moisture content will be constant for the increase and decrease of the drying temperature, it does not depend on temperature that means.

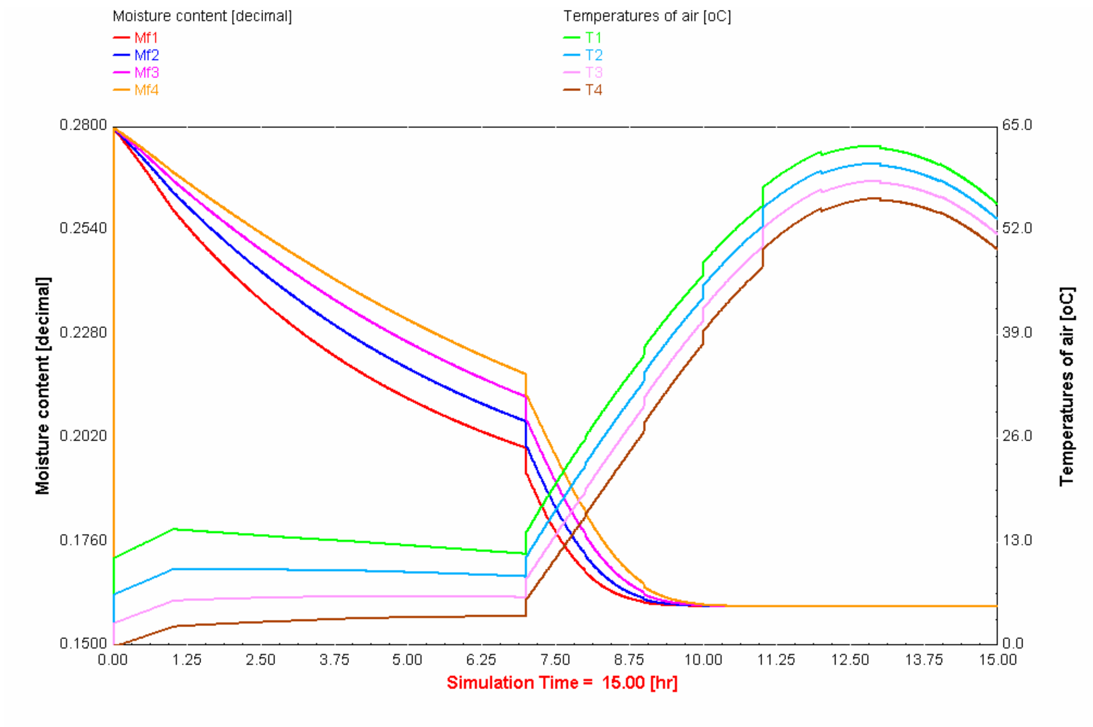

Figure 6-12: Moisture Content and Temperature of Dry Air for the Four Drying Beds

[Figure](#) 6-13 displays the variation of moisture content and water removed of the cereals with vertical distance from the bottom of the drying chamber.

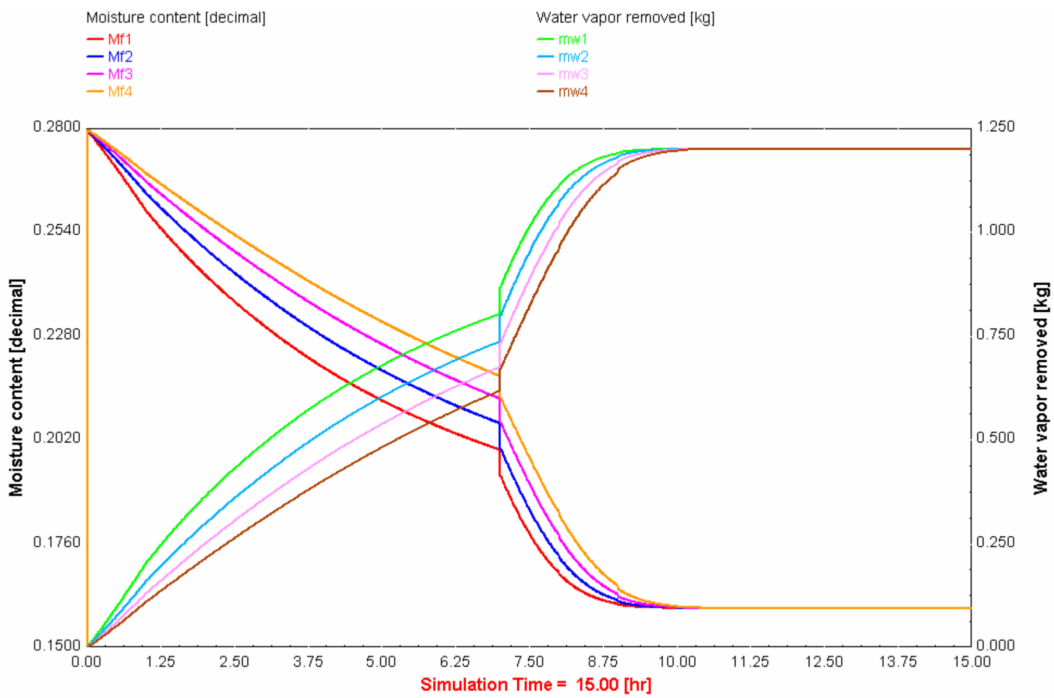

Figure 6-13: Water Removed and Moisture Content of Cereals for the Four Drying Beds

Figure 6-14 displays the variation of grain temperature with vertical distance from the bottom of the drying chamber. Ambient air temperature is included in the graph for comparison. The maximum temperature is found around 14:00 PM.

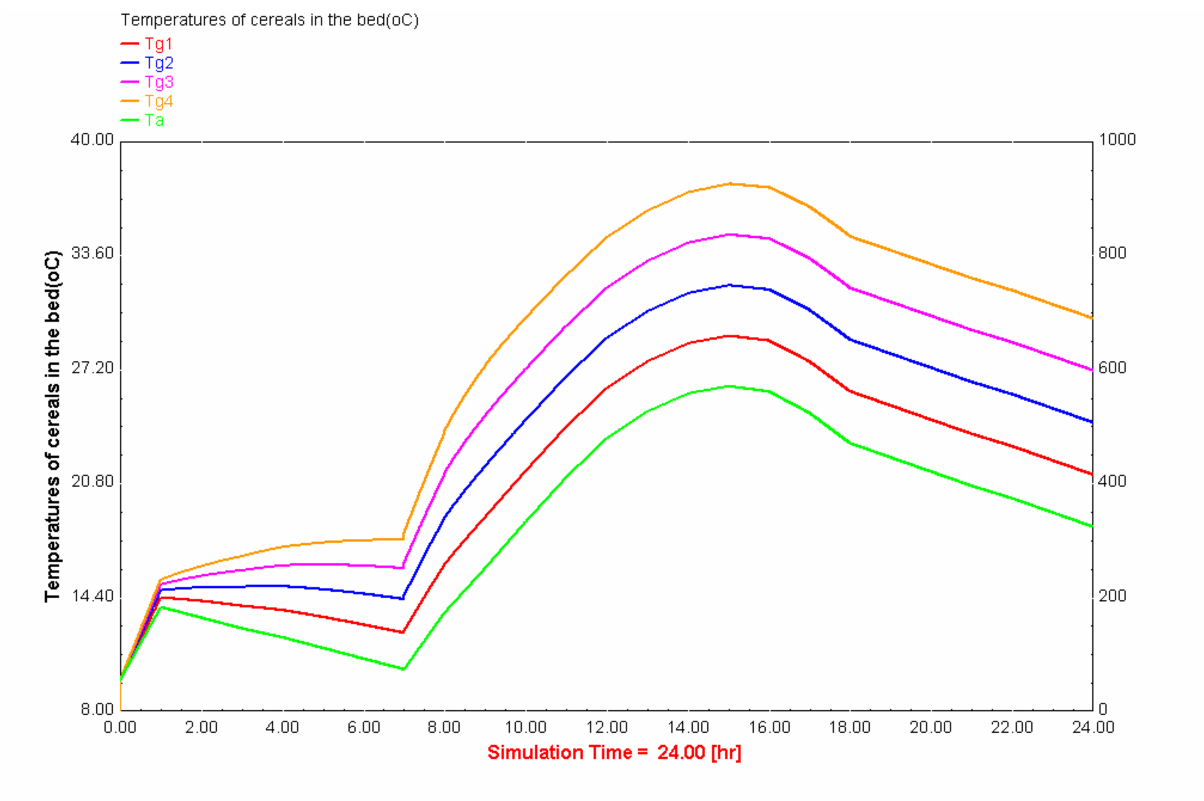

Figure 6-14: Temperature of Cereals for the Four Drying Beds

Figure 6-15 displays the variation of temperature of the drying air and latent heat of vaporization with vertical distance from the bottom of the drying chamber. Form the graph temperature and latent heat of vaporization are inversely proportional because as the temperature increases the energy need to vaporize is small.

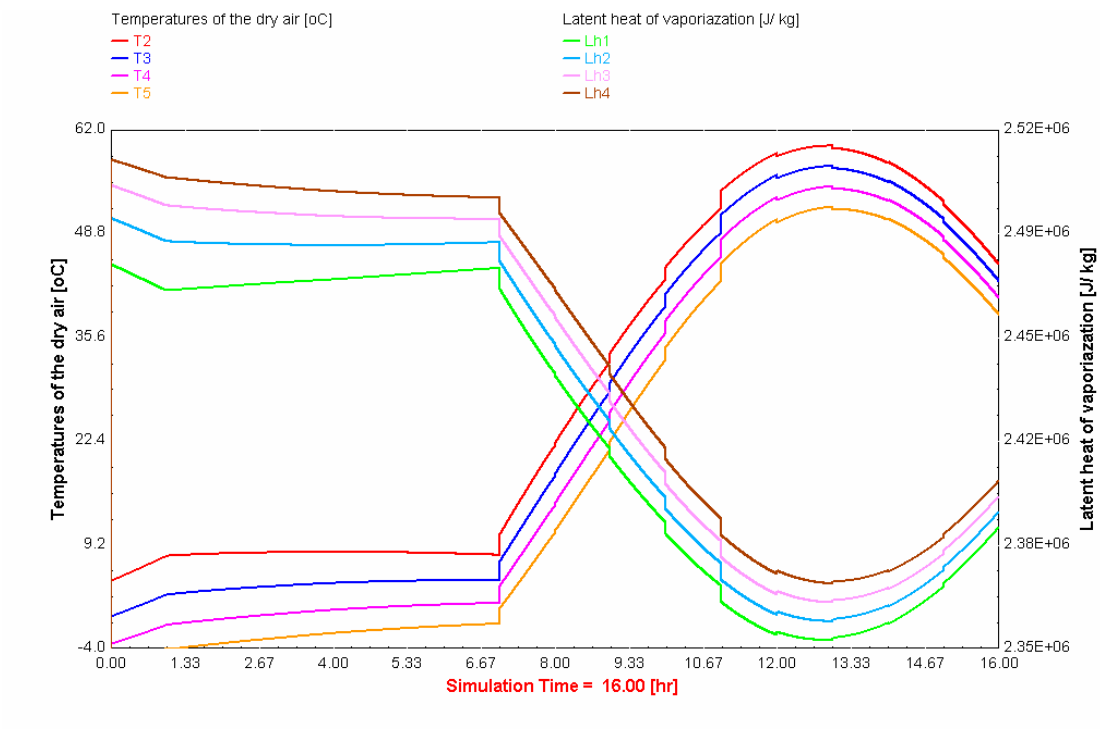

Figure 6-15: Latent Heat and Temperature of Dry Air for the Four Drying Beds

Figure 6-16 shows the relative humidity is affected by the air temperature. Heating the air decreases the relative humidity and respectively increases the capacity of the air to carry away moisture during a drying process. The extent to which this is achieved depends on the weather conditions, namely the absolute humidity and the temperature of the ambient air.

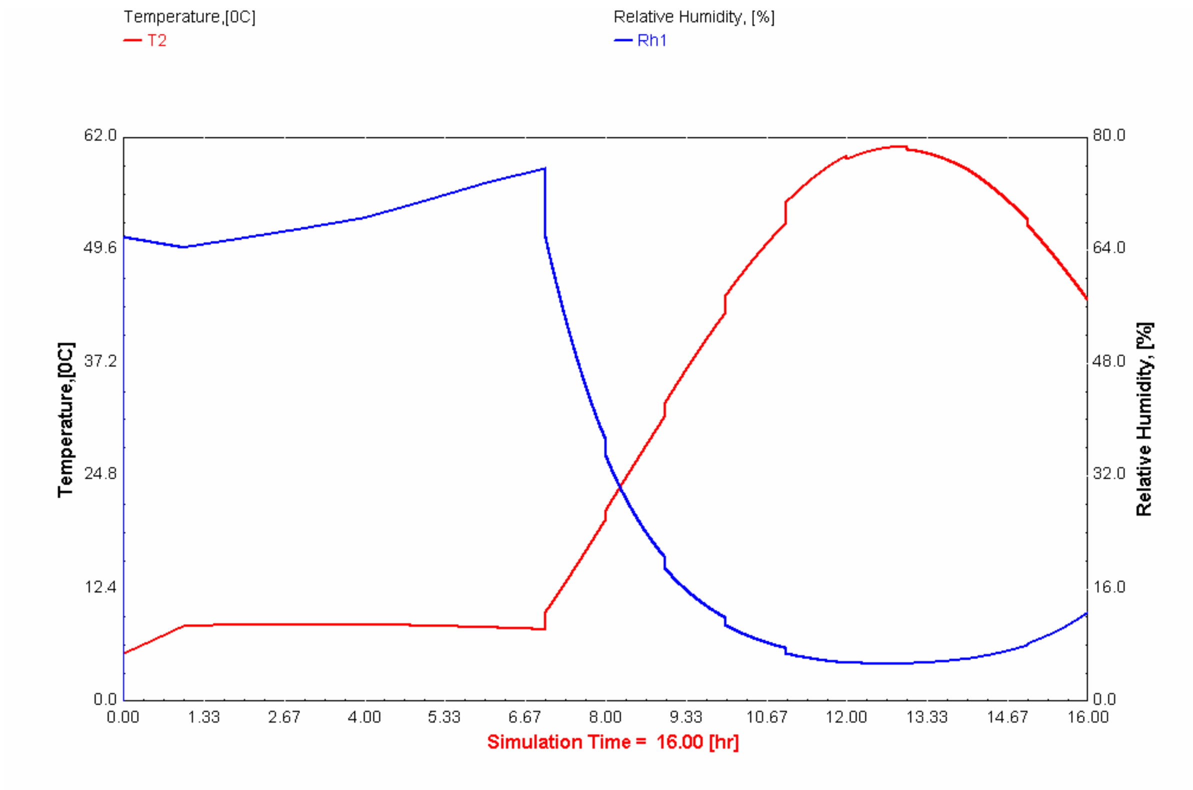

Figure 6-16: Relative Humidity and Temperature of Drying Air at the First Drying Bed

Figure 6-17 shows the drying rate of cereals as a function of the drying time. As seen from the curves in the figure, the drying rate for the first bed at the bottom of the drying chamber expectedly has the highest drying rate during the first 6 hours. However, as it gets dried its drying rate decreases. The drying rate of the barley on the second bed is larger than the first one after hours because the drying air absorbs less moisture from the first bed. Even though there was moisture loss during the night in all the beds but the drying rates were nearly zero this is because the moisture loss was the entire night. This effect is reflected in Figure 6-17.

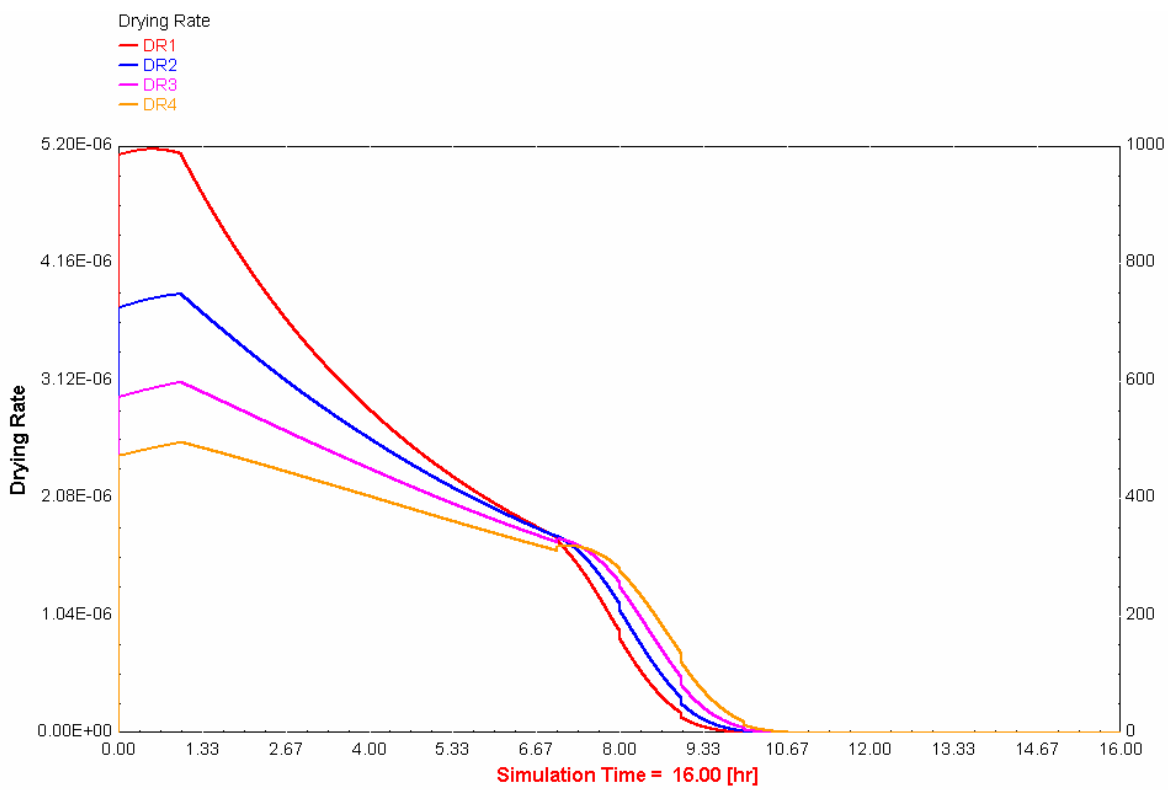

Figure 6-17: Drying rate curves plotted for Barley on a dry basis

During the initial stages of drying, the rate of moisture migration is sufficient to maintain the surface in a completely wet condition, Figure 6-18. Therefore, during this period, the rate of drying of the material is controlled by the rate of evaporation from the surface. This is controlled by the condition of air adjacent to the surface. Thus, during this period, the rate of drying is relatively constant as shown in figure 6-18, which is known as the constant rate period.

The point where the drying rate starts to decrease is known as the critical moisture content. Thereafter, the period of drying is known as the falling rate period. This is the period when the surface of the material is not wetted completely (by migration of moisture). The drying rate tends to zero when the rate of evaporation from the surface equals the rate of absorption of moisture by the material and is known as the equilibrium moisture content. Since the drying rate decreases to zero, Barley is a hygroscopic material.

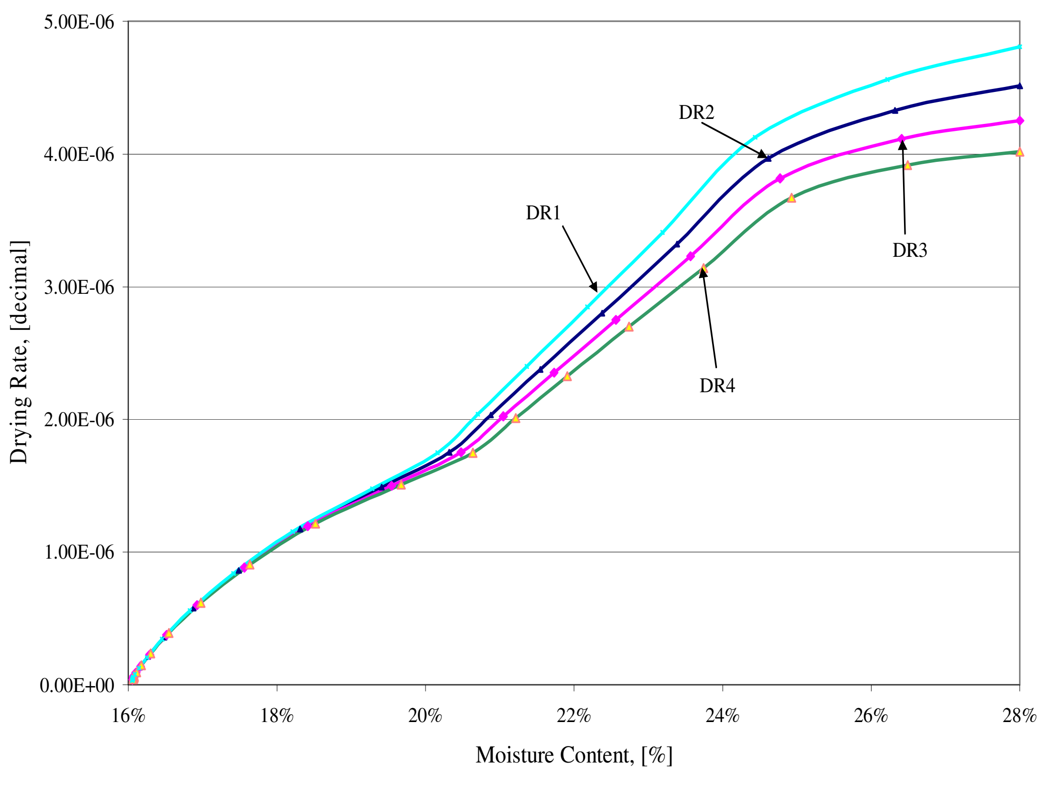

Figure 6-18: Drying rate curves

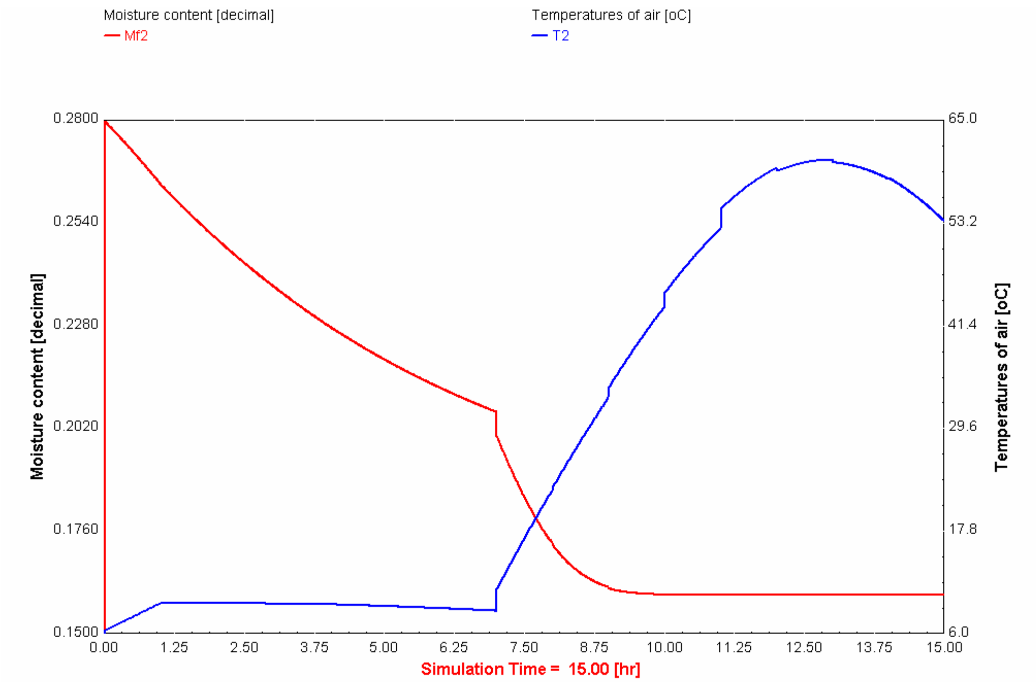

Figure 6-19: Moisture content and Temperature of Drying Air at the exit of First Bed

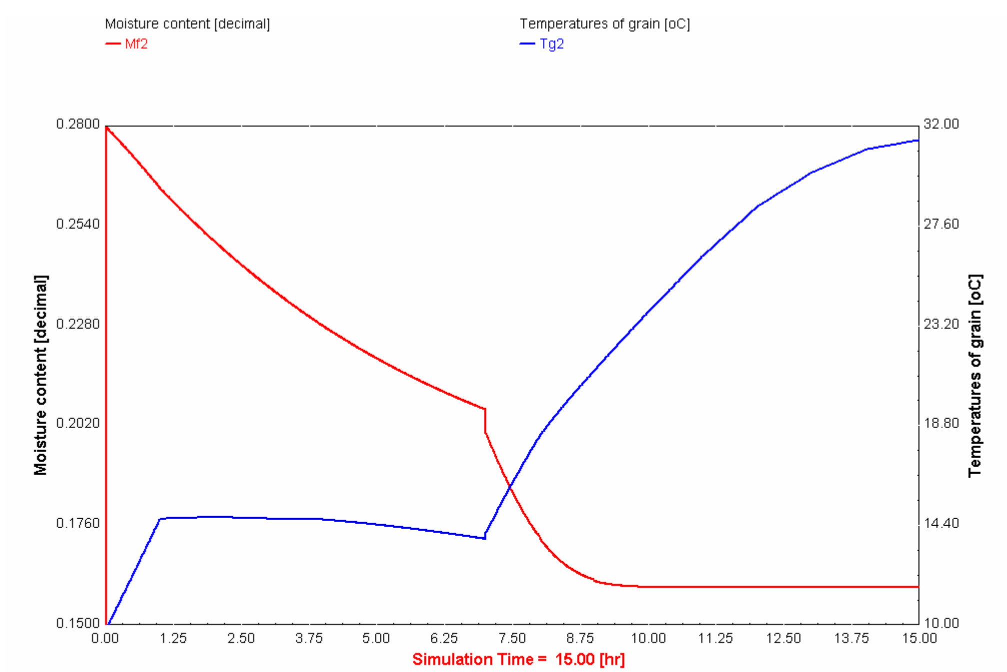

Figure 6-20: Moisture content and Temperature of grain at the exit of First Bed

Chapter 7

8.1 Conclusions and Recommendations for Future Work

8.1.1 Conclusion

1. Solar energy was utilized to dry cereal in the indirect natural convection type of solar dryer with $2m^2$ flat plate collector. It produced temperatures of 14-28^oC (from 8:30AM- 4:00 PM) higher than the ambient air temperature in a clear day. The final moisture content of the cereal of 0.1-0.12% which was observed after 13.5-14 sunny hours.

2. The drying time required by traditional open sun drying is reduced in natural convection dryer under the existing environmental conditions. Further more the drying material is protected from direct solar radiation, infestation by insects and contamination by dust. As a result, the product quality is high.

3. Since when the moisture content reaches equilibrium moisture, the drying rate is zero.

4. As drying air temperature and mass velocity flux increases moisture loss increases but as drying air relative humidity decreases moisture loss increases.

5. The initial moisture content of the local cereals ranges from 16 to 30% the final or the equilibrium moisture content of the dried cereal ranges from 10 to 12%.

6. As we go up from the bottom bed to upward, the drying rate decreases. This is because the inlet drying air temperature to the upper bed is lower than that of the lower chamber and also the drying air is relatively wet.

8.1.2 Recommendations

The following areas of interest can be looked to extend the research work on natural convection solar cereal dryers.

- Additional parametric studies can be done using TRNSYS which may include the counter flow with out a porous matrix for the collector in the solar cereal dryer.
- Performance study of indirect natural convection solar dryers using TRNSYS is possible by including the energy storage to the solar cereal dryer investigated here.
- Additional parametric studies can be done using psychometric chart in addition to the mathematical manipulation to compare both of it.
- As the drying air is exhausted to the surrounding so, one can study the recirculation of the drying air to improve the thermal efficiency of the drying chamber.
- The improvement of air distribution in the drying chamber can be studied for the performance improvement of the dryer.

Reference

1. A.M,Sayigh, *Solar Energy Engineering*, volume 2.

2. Abebayehu Assefa, *Thermal Analysis of Solar Dryers*, J.EAEA, Vol.15, 1998.

3. Aklilu Tesfamichael, *Experimental Analysis for Performance Evaluation of Solar Dryer*, MSc. Thesis, Department of Mechanical Engineering, Technology Faculty, AAU, 2004.

4. Akwasi Ayensu, *Dehydration of Food Crops Using Solar Dryer with Convective Heat Flow,* 2001.

5. Aruns, Mujumdar, *Drying'86*, Volume 1 and Volume 2.

6. B.K, Bala, J.L. WOODS, *Simulation of the Indirect Natural Convection Solar Drying of Rough Rice*, Vol.53.No.3, 1994.

7. B.M.Santos, M.R.Queiroz, *A Solar Collector Design Procedure for Crop Drying,* 2005.

8. Bala, B.K., Woods J.L., *Simulation of the Indirect Natural Convection Solar Drying of Rough Rice,* 1994.

9. C.Ratti and A.S.Mujumdal, *Solar Drying of Foods: Modeling and Numerical Simulation,* Vol-60, No-3/4, 1997

10. Carmen, Rosselic, *Simple Mathematical Model to Predict the Drying Rates of Potatoes,* 1992.

11. Curicd, *Rehydration Ratio of Fluid Bed-Dried Vegetables,* 2002.

12. Duffie, Beckman, *Solar Engineering of Thermal Processes*, second edition, 1991.

13. G.S.V.Raghavan, *Over View of New Techniques for Drying Biological Material With Emphasis on Energy Aspect,* 1998.

14. Graham,Thorpe, *Recirculation-a New Low Energy Method of Preserving Cereal Grains,* 2005.

15. Hassan Yousef,El-Lamush, *A Numerical and Experimental Study of a Photovoltaic Powered Solar Collector,* 1998.

16. Hideo,Inaba, *Heat and Mass Transfer Analysis of Fluidized Bed Grain Drying,*

17. J. A. Duffie and W. A. Beckman, *Solar Engineering of Thermal Processes*, J. Wiley and Sons, NY, 1991.

18. Lalit, R.Verma, *Drying of Agricultural Products and Grains,*

19. Mauri, Fortes, *Second Law Analysis of Drying: - Modeling and Simulation of Fluidized bed Grain Drying,* 2004.

20. Michael, J.Moran, *Fundamentals of Engineering Thermodynamics,*

21. Michael, W.Bassey, *Improving the Performance of Indirect Natural Convective Solar Dryers,"*

22. Milan,B.Stakic, *Numerical Study on Hygroscopic Capillary-Porous Material Drying in packed bed,*

23. Mingzhong Li, Stephen Duncan, *Dynamic Model of Batch Fluidized Bed Dryers,*

24. R.G.Morira, *Modeling of Drying Process of Foods,*

25. S.P.SukhatmeE, *Solar Energy Principles of Thermal Collection and Storage* volume 3.

26. Somchart, Soponoronnarot, *Solar Drying in Thailand,* 1995.

27. Sundarm, Gunasekarm, *Optimal Energy Management in Grain Drying,* volume 25, Issue1.

28. V.K. Srivastava,J.John, *Deep Bed Grain Drying Modeling,* 2001.